SUPPLEMENTO
AL VOLUME XVIII, SERIE X, DEL
NUOVO CIMENTO
A CURA DELLA SOCIETÀ ITALIANA DI FISICA

1960 — 4° Trimestre — N. 2

RENDICONTI

DEI LAVORI SCIENTIFICI

PRESENTATI ALLA

SEZIONE DI BIOFISICA

DEL

XLVI CONGRESSO NAZIONALE

DELLA

SOCIETÀ ITALIANA DI FISICA

NAPOLI, 4 OTTOBRE 1960

INDICE

G. Cortini – Parole introduttive . . . . . pag. 137

G. Montalenti – Brevi Parole . . . . . » 139

N. Rashevsky – Mathematical models and general mathematical principles in biology . . . . . » 140

V. Braitenberg and F. Lauria – Toward a mathematical description of the grey substance of nervous systems . . . . . » 149

M. Ageno – Some remarks on the shape of viruses . . . . . » 166

I. Archetti, D. Steve Bocciarelli and G. Toschi – Electron microscopic structure of a simian enteric virus . . . . . » 176

S. Aurisicchio, A. Celano and R. Rinzivillo – Molecular autoradiography performed by means of Ilford and Nikfi emulsions in gel form » 179

A. Celano, S. Aurisicchio, A. Coppo, P. Donini and F. Graziosi – Unusual biophysical properties of the temperate phage α . . . . . » 190

S. Aurisicchio, A. Chiozzotto, A. Coppo, P. Donini, C. Frontali and F. Graziosi – Physico-chemical and morphological aspects of temperate phage α particles . . . . . » 197

E. Calef – Deletion syngenotes and the problem of coding ratio. . . . . » 203

G. Tecce and G. Toschi – A study of ribosomes from a thermophilic microorganism . . . . . » 207

B. Babudieri and D. Steve Bocciarelli – Further research on the fine structure of leptospirae . . . . . » 212

A. Ascenzi, E. Bonucci and D. Steve Bocciarelli – Quantitative analysis of calcium in bone with a microradiographic method . . . . . » 216

G. E. Magni – The problem of evaluating the biological significance of sigmoidal X-ray inactivation curves in yeasts . . . . . » 221

G. Marin, F. Nuzzo e L. De Carli – Analisi di alcuni fattori sperimentali che influenzano le curve di sopravvivenza ai raggi X di cellule umane coltivate in vitro . . . . . » 227

A. Vescia, E. Boeri e S. Traniello – Impiego delle radiazioni ultraviolette per lo studio dei gruppi attivi degli enzimi . . . . . » 237

1122

SUPPLEMENO AL VOLUME XVIII, SERIE X
DEL NUOVO CIMENTO

N. 2, 1960
4° Trimestre

Parole introduttive

DI

G. CORTINI

In un gruppo di amici, l'altro giorno, è stata espressa l'opinione che si dovesse dare solennità a questa particolare sessione del Congresso della Società Italiana di Fisica, nella quale per la prima volta i fisici italiani — in sede di Congresso nazionale — riconoscono — direi « ufficialmente » — l'importanza straordinaria della biofisica come ramo originale e affascinante della ricerca scientifica di punta, e la inseriscono tra le attività di riconosciuto interesse per i fisici.

La proposta è sembrata troppo giusta, ed è stato chiesto al Presidente della Società, prof. G. POLVANI, di intervenire e pronunziare un breve discorso di apertura. Il prof. G. POLVANI ha con molto favore acconsentito a dare il suo patronato a questa iniziativa per la quale ha formulato i voti di miglior successo.

Purtroppo, però, le nuove e ancor più alte responsabilità del prof. G. POLVANI, quale presidente del Consiglio Nazionale della Ricerche, lo hanno obbligato a lasciare Napoli oggi, e pertanto tocca a me, quale Segretario generale del Congresso, di parlare in sua vece.

Nel porgere il benvenuto e il caldo ringraziamento nostro ai colleghi biofisici, biologi e medici, oltrechè naturalmente fisici, che hanno voluto partecipare a questa sessione del Congresso, devo allora, anzitutto pregarli di scusare il carattere direi quasi estemporaneo di questo nostro breve incontro.

Il tempo che si è avuto per organizzare questa sessione di Biofisica, è stato infatti brevissimo; l'iniziativa è sorta da uno scambio di idee che il mio amico e collega E. R. CAIANIELLO ed io stesso avemmo con diversi Colleghi, fisici e non fisici, poche settimane fa.

Sapevamo di dover quasi improvvisare, ma ci è parso ugualmente opportuno organizzare questo primo incontro, anche se non potevamo in alcun modo aspirare alla perfezione, anzichè rimandare tale riunione a un'imprecisata data futura.

Lungi è quindi da noi la convinzione che l'incontro di oggi possa costituire una rassegna esauriente, o anche una rappresentazione sintetica dell'attività italiana nel campo della biofisica. Pensiamo però che l'incontro tra fisici e biofisici che avviene oggi possa avere interessanti risultati sia per i biofisici che per i fisici. Infatti, l'entusiasmo con cui i primi hanno accolto il nostro pur così tardivo invito è ampia prova del loro desiderio di iniziare un colloquio con i secondi, molti dei quali da qualche tempo si stanno occupando attivamente di ricerche di carattere biofisico.

In aggiunta agli illustri colleghi presenti, diversi altri che a causa dei loro impegni non sono potuti intervenire, hanno tuttavia espresso la loro viva adesione a questa iniziativa e i loro voti perchè essa segni l'inizio di uno scambio sempre più vivo tra le nostre scienze: cito in particolare il prof. E. Amaldi, di Roma, presidente dell'Istituto Nazionale di Fisica Nucleare, il prof. G. Toraldo di Francia di Firenze e il prof. G. Moruzzi di Pisa.

Confesso ora che Caianiello ed io siamo stati spinti a questa iniziativa oltre che dai motivi di carattere generale che ho appena accennato, anche da un vivo interesse personale: infatti a Napoli vi sono parecchi colleghi e ricercatori che si occupano attivamente di questioni di carattere biofisico oppure hanno espresso vivo interesse e volontà di collaborare a sforzi in questo senso. Tra questi posso nominare ben cinque professori della Facoltà di Scienze: E. R. Caianiello, B. De Lerma, A. Liquori, G. Montalenti e me stesso. Ci addolora assai che il prof. Montalenti sia per lasciare la nostra Facoltà, ma ci conforta il fatto che l'Istituto da lui creato è in piena fioritura e dotato di personale altamente qualificato, la cui preziosa collaborazione aumenterà certo le probabilità di riuscita di un eventuale piano comune di ricerche in tal campo. Del resto, la nostra Facoltà, chiedendo l'inserzione — per la prima volta, credo in Italia — della biofisica tra le materie complementari del corso di laurea in fisica ha compiuto un passo che molto ci incoraggia in tal senso.

Queste ragioni spingono dunque il mio collega Caianiello e me stesso ad offrire, oltre che i nostri voti augurali, la assicurazione precisa che saremo lietissimi di impegnarci al meglio delle nostre possibilità e capacità a sostegno di ogni iniziativa che gli amici biofisici vorranno prendere, affinchè le loro ricerche vengano a coordinarsi in una organizzazione quale già si è realizzata nel campo della fisica. Sono certo che tutti i fisici presenti si associano a questo nostro augurio e sono particolarmente felice che — come ho già detto — l'illustre Presidente della Società Italiana di Fisica abbia voluto dare il suo patronato a questa iniziativa.

SUPPLEMENTO AL VOLUME XVIII, SERIE X
DEL NUOVO CIMENTO

N. 2, 1960
4° Trimestre

Brevi Parole

DI

G. MONTALENTI

Desidero ringraziare, a nome dei biologi qui convenuti, i colleghi fisici per avere organizzato nel loro Congresso questa sezione dedicata alla Biofisica. In questa occasione mi sembra utile ricordare che la collaborazione tra la fisica e la biologia — in particolare la genetica — in Italia data da tempi ormai antichi. Quando il gruppo di E. Fermi era in piena attività a Roma, negli stessi anni in cui TIMOFIEFF, ZIMMER e DELBRÜCK elaboravano la teoria fisica della mutazione e quel modello del gene che hanno avuto tanta importanza nella storia della genetica, i contatti fra i fisici ed i biologi a Roma erano frequenti e gli scambi di idee risultavano molto utili; fra i fisici, F. RASETTI era particolarmente interessato alla biologia e competente in problemi biologici e più volte fu chiamato a risolvere i dubbi dei biologi su problemi di biofisica. In seguito i professori di fisica dimostrarono sempre il proprio interessamento per la genetica, e in più di una occasione ebbero a sostenere e ad appoggiare i programmi dei genetisti: programmi di lavoro, o di organizzazione.

Desidero anche ricordare che recentemente i colleghi fisici della Facoltà di Scienze di Napoli hanno proposto la introduzione dell'insegnamento della biofisica per il loro corso di laurea.

Sono certo di interpretare i sentimenti di tutti i biologi qui convenuti, nell'esprimere ancora una volta gratitudine ai colleghi fisici, e nell'augurare che l'introduzione di una seduta dedicata alla biofisica in questo Congresso non rappresenti un evento isolato, bensì l'inizio di una consuetudine. Dai contatti che qui possono stabilirsi trarrà certo molto vantaggio questa recente disciplina, la biofisica, che potrà sempre meglio definire il proprio ambito e i propri scopi.

SUPPLEMENTO AL VOLUME XVIII, SERIE X
DEL NUOVO CIMENTO

N. 2, 1960
4° Trimestre

Mathematical Models and General Mathematical Principles in Biology.

N. RASHEVSKY

Committee on Mathematical Biology, The University of Chicago - Chicago, Ill.

The purpose of my address is to give a short survey of mathematical biology, principally as developed in the United States. Limitation of time makes this survey of necessity very incomplete.

1. – Mathematical biology, or as it is sometimes called, mathematical biophysics, stands to experimental biology in the same relation as mathematical physics to experimental physics. The mathematical biologist establishes some hypothesis about the mechanism of different biological phenomena and develops, on the basis of this hypothesis, mathematical theories. Like in physics, the criterion for the goodness or usefulness of a theory is its ability to explain *quantitatively* experimental facts and to predict the outcome of new experiments.

In this type of research the mathematical biologist is essentially building physico-mathematical models of different biological phenomena. This procedure is familiar to the theoretical physicist, who develops models of the atom, of the solid bodies, etc. In physics, however, such models are based on some general principles, such as the laws of Newton, the principles of thermodynamics, or the principles of quantum mechanics. The biological models which we shall discuss to-day are on the other hand based on general physical principles, rather than on biological ones. In the second part of this paper we shall mention attempts to formulate general mathematical principles of a biological nature.

Before we proceed further we must dwell for a while on the terminology used. As defined above, mathematical biology does not include such sciences as biometry or biostatistics. Yet those important sciences deal also with applications of mathematics to biology. Biometry and biostatistics are, however, not directly concerned with the development of mathematical theories of various

biological phenomena. They deal with the statistical evaluation of observational and experimental facts. Biometry and biostatistics form an important bridge between experimental biology and mathematical or theoretical biology. The formers supply to the latter the necessary facts in a quantitative form. As all terminologies, the one adopted here is to a large degree arbitrary.

Another remark which must be made now concerns mathematical genetics. The well developed mathematical theories in genetics, associated with the distinguished names of J. B. S. HALDANE, L. HOGBEN, SEWALL WRIGHT, and others, fall definitely, according to our definition, into the domain of mathematical biology. This branch of mathematical biology has been developed before the other branches, which we shall discuss to-day. Because of its specialization in the field of genetics, it was referred to as mathematical genetics. The terms « mathematical biology » and especially « mathematical biophysics » were coined about a quarter of a century ago to designate the type of theoretical studies which we shall discuss here. At that time mathematical genetics was already a well developed science. In view of the above we shall not include in our discussion problems of mathematical genetics.

Most of the work discussed here has been done in the Committee on Mathematical Biology, a department of the University of Chicago, which I began to organize 25 years ago. A large part of this research has been done by my former students and later by students of those students. In the last decade, however, a number of important investigations have been made in other American universities by persons not previously trained in Chicago. *The Bulletin of Mathematical Biophysics*, founded by me in 1939 and published under my Editorship by the University of Chicago Press, is the principal outlet for publications in this field.

One of the first problems which attracted my interest and the interest of my students was the problem of cell division. This is the basic process, through which life spreads on earth. A number of hypotheses of a qualitative nature have been made many times to explain cell division. A mathematical study of the consequences of those hypotheses showed that they were untenable quantitatively.

In trying to explain such a general phenomenon as cell division, it is natural to look for possible causes which are just as general. The presence of electric charges in all cells seemed to be such a general factor. Again, however, a mathematical study revealed that they cannot account quantitatively for all cases of cell division.

There is one phenomenon which is always present when life manifests itself. That is metabolism. Every living cell metabolizes a number of substances, which flow into it and out of it. Death is always accompanied by a cessation of metabolism. True enough, dormant spores do not metabolize, though they are alive. But until a spore is put into a milieu in which it begins

1127

to proliferate, there is also no way of telling whether it is dead or alive. A proliferation is always accompanied by metabolism. Thus metabolism is always present when and only when life *manifests* itself. It was therefore natural to look for a possible connection between metabolic processes and cell division.

The transport of metabolites into the cell and out of it, as well as *within* it, is in most cases effected by diffusion. Thus every living cell is the seat of complicated diffusion fields. The solvent offers a resistance to the flow of a diffusing substance. This is manifested in the finite value of the coefficient of diffusion. Hence, by the third law of Newton, every diffusing substance must exert a force on the solvent in the direction of diffusion flow. Therefore every living cell is the seat of a complicated field of forces, the so-called diffusion drag forces.

To investigate the possible effects of those forces upon the cell, we have to solve three distinct problems. First, for a cell of a given size and shape, we must solve the diffusion problem, to determine the diffusion fields. Second, we must calculate the fields of forces from the diffusion fields. Third, we must calculate the mechanical effects of those fields of forces upon the cell.

Each of the three problems offers in general very great mathematical difficulties and has not yet been solved exactly in its entirety. Exact solutions of very special cases were found which were of limited importance biologically. In 1938 I succeeded in developing a simple but general and very powerful approximate method for treating those problems. Great progress was then made, especially by H. D. LANDAHL. Here we can only mention the results.

In a spherical, or spheroid cell, the forces due to inflowing substances tend to stabilize the cell. The forces due to outflowing substances make the cell unstable when a certain critical size is reached and exceeded. The cell then begins to elongate, the length as a function of time being represented by an S-shaped curve, the equation of which can be derived. Eventually a constriction is formed at the equator, and the diameter of the constricted region decreases parabolically until the cell divides in two.

Such situations are actually observed in isolated cells, which can divide without being hampered by adjacent cells. In particular this picture is observed in the division of demembranated *Arbacia* eggs. After H. D. LANDAHL derived the equations for the elongation and constriction of cells during division, R. BUCHSBAUM and R. WILLIAMSON made quantitative experiments on some 50 *Arbacia* eggs, obtaining curves for each egg. All curves were found in excellent agreement with those previously calculated by LANDAHL.

The theory also permits to calculate the *average* critical size which a cell cannot exceed. It turns out to be about $3 \cdot 10^{-3}$ cm, which is actually the average size of most living cells.

As remarked above, it is the outflowing metabolites that contribute to the

1128

instability of the cell. In every cell there are many metabolites flowing in and many flowing out. Considering in a very crude manner the role of the most important metabolites, it can be shown that cells with a high glycolytic coefficient will be more apt to divide. This is in agreement with the well-known findings of WARBURG that cancer cells are characterized by an abnormally high glycolytic coefficient.

Another prediction of the theory, which is roughly verified, is that, in general, cell sizes should vary as the inverse cubic root of oxygen consumption.

In spite of all the above mentioned successes of the diffusion drag forces theory of cell division, it cannot be considered as a good theory. It fails completely to account for the complicated phenomena of mitosis in higher cells. Other factors besides diffusion drag forces must play an important role in cell division. They are likely to be found on the molecular level. Work in that direction has been and is being done.

We dealt more at length with the theory of cell division, in spite of its inadequacy, in order to give an idea of the general method of approach used by mathematical biophysicists. Now we shall mention much more briefly a few other examples. Even to enumerate completely here all the problems studied would take too much time.

As a by-product of the studies of diffusion fields, produced by various biochemical reactions, a theory of cell respiration was developed by me and LANDAHL. Landahl's equations predicted a relation between rate of oxygen consumption and oxygen tension. The equations were found in agreement with experimental data.

We have also shown that diffusion drag forces may result in the production of asymmetric structures within the cell, giving the latter a polarity. The polarity has the property of self-regulation and re-establishes itself when destroyed by external interference. Applications to embryological problems have been made.

Prof. LANDAHL developed a mathematical theory of various pharmacological phenomena, which leads to a number of practical suggestions. He also developed a theory of retention of particulate material in the respiratory tract, a work that has immediate practical applications in industries where workers are exposed to dusts and smokes.

Another set of biological phenomena that received considerable attention is the excitation and conduction in peripheral nerves. Real progress in this field began after the introduction in 1934 by me, and independently in 1935 by A. V. HILL, of the so-called two-factor theory of excitation. The theory assumes the existence of an excitatory and an inhibitory factor of unspecified nature. The approach is of a more formal nature than in the cases mentioned before. Hill's mathematical formulation was somewhat different from mine. F. OFFNER and G. YOUNG showed, however, the complete equivalence

of both theories. The names of A. HOUSEHOLDER, H. D. LANDAHL, and A. M. WEINBERG must be mentioned in connection with the work in this field.

The theory of nerve conduction is closely related to the theory of nerve excitation because conduction is due to the re-excitation by local bio-electric currents. The theory leads to functional equations.

Even a more challenging problem than the excitation in peripheral nerves is offered by the central nervous system (CNS). The development of the theory proceeded in the following way:

It was assumed that the complexity of the functions of the CNS is due to the well-known complexity of its *structure*. Therefore the simplest possible assumptions were made about the mode of interaction of a pair of neurons or neuroelements. These assumptions were embodied in a pair of ordinary linear differential equations. Then structures and arrangements of increasing degree of complexity were studied and the properties of such structures derived. It turned out that many of these theoretically studied structures possessed properties which not only qualitatively but also quantitatively were remarkably similar to a number of observed phenomena. Thus quantitative models of reaction times, of psycho-physical judgments, of learning, and conditioning were developed by LANDAHL. A theory of discrimination was successfully developed by A. S. HOUSEHOLDER. Three different theories of Gestalt perception were developed by myself, MCCULLOCH and PITTS, and J. T. CULBERTSON. A theory of discrimination of relations, of abstraction, of logical thinking, of rational problem solving, and of aesthetic perception was developed. Some predictions of the latter were subsequently verified experimentally. Thus some of the most perplexing and complicated phenomena of human behavior and of biopsychology became intelligible and amenable to mathematical analysis.

The basic equations postulated in the theory of the CNS are expressed in terms of differential equations. Therefore, except for the existence of threshold phenomena, which are explicitely introduced into the theory, the latter allows for *continuous* effects in transmission of excitation and inhibition. It is, however, known that actually the so-called « all-or-none » law holds for the CNS, which makes all phenomena in the latter basically of a discontinuous nature. In 1943 W. MCCULLOCH and W. PITTS showed that the appropriate mathematical apparatus for the representation of the discontinuous nature of the phenomena in the CNS is Boolean algebra. A curious paradox, however, emerged. The older, continuous theory led to an excellent quantitative description of a number of facts, as mentioned above. Yet it was based on obviously wrong postulates. On the other hand, the Boolean algebra method, while obviously more adequate, did not lead to a proper description of the above mentioned phenomena. The paradox is resolved in the following way. While the interaction of individual neurons is a discontinuous phenomenon, in actual psychophysiological experiments we deal not with a few but with a very large

1130

number of neurons. In such cases the average effect of a large number of discontinuous actions results in a quasi-continuous *macroscopic* effect. The situation is analogous to those found in physics. Thus the discontinuous impacts of individual molecules of a gas against the walls of a container result in a continuous pressure.

A probabilistic theory of neural networks, based on discontinuous interaction of individual neurons has been developed by A. RAPOPORT and his co-workers. As an important by-product of those studies it was found that the spread of excitation in *random* neural nets formally follows the same laws as the spread of epidemics or spread of rumors. Important applications were made for the latter case.

With this brief survey I must conclude the discussion of the mathematical models in biology. A number of other studies, such as mathematical theory of circulation, of blood-tissue exchanges, and many others cannot even be mentioned here.

2. – All the above discussed models are usually based, as already stated, on physical principles. A general principle in physics does not *as such* explain any particular phenomenon. It applies, however, to all phenomena. Thus the second law of Newton

$$m \frac{\mathrm{d}^2 x}{\mathrm{d}t^2} = F ,$$

as such cannot explain or describe any particular phenomenon. In order to apply it with predictive results we must have either an actual or a conceptual system, in which the masses and their positions, the forces, and initial conditions are prescribed. Then only does the law predict the future course of the system. But Newton's second law is used and is applicable in *every* situation of classical physics. Thus, when in the kinetic theory of gases we conceive of a gas as an aggregate of molecules, the laws of Newton are applied to study the properties of that aggregate.

Attempts have been made to formulate some general mathematical principles in biology. The only hitherto well established principles of a purely biological nature are the principles of genetics, formulated first in a somewhat crude form by MENDEL. For reasons, already mentioned, we shall omit their discussion. They are well known to workers in that field.

A general principle connected with the problem of organic form was tentatively formulated some 15 years ago. Briefly it may be explained as follows. Every organism performs a number of biological and sometimes purely mechanical functions. In general every function, such as metabolism, speed of locomotion, etc., can be quantitatively characterized by its intensity. If a set of

functions and their intensities are prescribed they may be performed by a number of structures of different design. The principle states that the designs of a biological system which are optimal with respect to economy of material and energy expenditure, are the ones which actually occur. But the design of a system determines its shape or form.

We cannot go here into any details of the application of this principle. All we can say is that, applied to a number of specific situations, it has led to results which agree with observations. Thus for quadruped mammals the principle leads to the conclusions that the width of the body should vary as the $\frac{3}{2}$ power of the length. This is verified within a wide range. Applied to the function of lungs, it predicts that the breathing frequency should vary, other conditions being equal, as the inverse cubic root of the mass of the animal, while the mass of the lungs should vary proportionally to the mass of the whole animal. This is again found to be approximately correct within the range from rat to horse. Applied to the arterial system, the principle leads to correct values for the size of aorta, number of total branchings of the arteries, average ratio of radii of branches at a bifurcation to the radius of the original artery (COHN), etc.

Another general principle deals with a very different aspect of biology. A paramecium, appropriately stimulated by food, moves towards that food, ingests it, digests it in its digestive vacuole, excretes the undigestible parts, absorbs and assimilates the digested material. Or it may move towards another paramecium and conjugate with it, thus performing an elementary sexual act.

A bird, at sight of an insect, will fly after it, swallow it, digest it, defecating the indigestible parts, and absorbing and assimilating the rest. A similar set of corresponding phenomena is found in any other organism.

We notice, nowever, that the mechanism of locomotion, digestion, etc., is quite different in a paramecium from that of a bird. The difference is both quantitative as to its intensity, and qualitative. Entirely different structures and mechanisms are involved in the different cases. Moreover, the mechanism of digestion of a higher animal is much more complicated than that of a lower one. It consists of a larger number of partial mechanisms. The same holds for the mechanism of sensation. To a simple sensitive spot of a paramecium corresponds a number of complicated organs, such as eyes, ears, nose, etc., in a higher animal. Also to the general indiscriminate sensitivity to a wide array of stimuli in a paramecium, there correspond the sensitivity to light, to sound, to smell, etc., in a higher animals.

But in spite of the difference of mechanisms involved in various biological functions, the *relations between corresponding functions* are the same in all organisms, as we have stated above.

This leads to a principle called that of biological epimorphism. The organism may be considered as a set of biological functions, which characterize it

1132

as such. The sets of biological functions of higher organisms contain more elements, than the sets of biological functions of lower ones. But an epimorphic (many-to-one) mapping exists between any two sets which correspond to two different organisms, such that certain basic relations are invariant with respect to that mapping.

The principle is formulated mathematically by postulating the properties of the mappings. Time does not permit me to go into details.

Once formulated mathematically, the principle enables us to make a number of deductions, which are both of theoretical and of potentially practical nature. Those deductions are formulated not in the form of analytical equations but rather as existential theorems. Thus one consequence is that in higher animals emotional disturbances may produce gastrointestinal disturbances. This is a well-known clinical fact. We may attempt to construct a model of the neural mechanism which produces it. This would not be difficult. But in order to become interested in such a model, we must have the phenomenon as given. Buth the phenomenon is by no means obvious. It might not have existed. The fact that we know empirically that it does exist, does not explain the reason for its existence. Its existence, can, however, be derived by means of the principle of biological epimorphism.

Another conclusion is that emotional disturbances may produce cardiovascular disturbances. This is another well-known fact. A still different conclusion is that there exist animals with glands the secretion of which are used for catching food. The spider-web is a classical example. The existence of antibiotics produced by micro-organisms is also a consequence of the principle. The antibiotics would have been predicted if mathematical biology would have been developed three decades earlier.

New powerful mathematical methods, such as the theory of natural equivalences of S. Eilenberg and S. MacLane, have been successfully applied by R. Rosen to problems of what is now called « relational biology ».

Whit this I must end my brief and inadequate survey.

3. – In conclusion I would like to say a few words about the training of mathematical biologists, responsible for the work which I mentioned. Those remarks may be of interest here because of the impeding program of developing research in that field in Italy.

Some 30-35 years ago there was a widespread opinion that important results could be achieved in the borderline between biology and physics by a co-operation between a physicist and a biologist, even though the physicist may not know any biology, and the biologist may not know any physics. I always, even then, maintained that this was not correct. Co-operation is a very useful thing. But each of the co-operating scientists must have *complete understanding* of *all* the aspects of the problem. Only then can each do

1133

creative work. Subsequent events corroborated my view. All the developments discussed to-day were made by men who are equally at home in the biological and in the physical sciences. To train such men the Committee on Mathematical Biology was established as a department of the University of Chicago. Students in the Committee receive Doctor's degree only after having taken approximately 14 *advanced* level courses in the biological sciences and an equal number of courses in the physical sciences. They take such courses as general biology, general physiology, human physiology, genetics, physiological genetics, embryology, biochemistry, etc. On the physical side they take calculus, differential equations, theory of functions, probability, integral equations, kinetic theory, thermodynamics, electrodynamics, quantum mechanics, etc. Our students are also required to take biological laboratory work, even though they are trained as theoreticians. In biology, like in physics, a useful theoretical work is possible only with a full understanding of experimental facts and methods. In addition an adequate research training is of course required.

This program of course requires much more time than do the programs in other non-clinical departments. The Committee on Mathematical Biology is still the only place where such a training is given *formally*, as a requirement for a Doctor's degree. *Informally*, however, students in many other universities follow that program, and, though they do not have an official degree in mathematical biology, they do excellent research in that field. Steps are now being taken in the United States to create officially in other universities departments similar to ours. A number of our former students are now working in other universities and in government research institutions.

Several universities have departments of biophysics, where a similar dual training is formally given. The emphasis is, however, on the experimental side. I can speak with full autority only on mathematical biology.

REFERENCE

N. RASHEVSKY: *Matematical Biophisics: Physico-matematical Foundation of Biology*. 3rd ed., vol. 2 (New York, 1960)

1134

SUPPLEMENTO AL VOLUME XVIII, SERIE X
DEI NUOVO CIMENTO

N. 2, 1960
4° Trimestre

Toward a Mathematical Description of the Grey Substance of Nervous Systems (*).

V. Braitenberg and F. Lauria

Sezione di Cibernetica, Scuola di Perfezionamento in Fisica Teorica e Nucleare - Napoli.

1. – Introduction.

A striking particularly of the biophysics of brains is that it deals with macroscopical organs, well accessible to structural and functional analysis, about which a great deal of information is collected in the literature but little—if any—satisfactory understanding of the central problems has been obtained. The search for better resolution in techniques developed recently, such as electron microscopy or electrical recording from single nerve cells has shown only too clearly that little can be gained by pushing the analysis to smaller orders of magnitude. The main question, how a brain does perform the remarkable functions which are often so difficult to imitate by machine is obviously related to the high degree of complexity of the structure of nerve cell aggregates (in the so-called grey substance) and to the equally high degree of functional organization which is apparent in them. This organized complexity poses novel problems to analysis. The divergent descriptions of the brains, ranging from introspective psychology to comparative neuroanatomy or the physiology of synapses would still be even without the hope of a common language, had it not been for recent attempts to formulate theories about the brain in a rigorous form which, potentially, embody all that can be said about brains. It is to these theories, as well as to some aspects of the brain which have not yet been built into the theories that we shall devote our attention here.

(*) Research reported in this document has been sponsored in part by the European Office of the A.R.D.C., United States Air Force.

1·1. *Logical theories.* – Among the facts which are best established through electrophysiological experiments one of the most obvious ones is the non linearity of the performance of neurons (by neurons, after CAJAL, we mean the cells of the nervous system when viewed as individual functional elements). Neurons will precipitate into a state of activity when a threshold of some afferent stimulation is reached, and this state will give rise to phenomena of conduction onto which further stimulation will have little influence. From this observation it is a small step to the picture of the neurons functioning as « all or none » elements capable of only two states: activity and resting state. And this in turn brings to mind binary algebra and, obviously, its best known application, Boolean logics. Some further simplifications such as the supposition of a unitary delay between the activity of one neuron and that of the succeeding one, and the assumption that threshold of neurons remain constant suffice to map binary logics onto nerve nets in a simple elegant way. This was done first by MCCULLOCH and PITTS [1] and has greatly influenced many subsequent attempts to formulate theories of the brain. There is no question at all that, if there are neurons functioning the way the neurophysiologists describe them, and if they are at all connected, they must be describable in the language of binary logics. The difficulty is rather one of quantity, since it is only too simple to show that MCCULLOCH and PITTS nerve nets must be enormously large if they are to do any non trivial specified task. Quantitative considerations force us to look for principles of economy in living brains, which are as yet quite impenetrable to our analysis but would be highly desirable to engineers. It is, we think, obvious that real nerve nets, wired to do specified sets of tasks, such as the tasks with which a living being is faced, embody all the economy that is needed. To find the wiring used in nature's economy is the problem of neuroanatomy.

1·2. *Statistical theories.*– If, instead of a well specified wiring, one prefers to see in living brains the nearly complete chaos of the connections of any element with a set of other elements for which nobody can give an accurate description, one is equally justified to do so, since whatever regular structure you may describe in a nervous system, the regularity never extends to the detailed specification of « which is connected to which ». Interindividual variations set a clear limit to the accuracy of generally valid anatomical or physiological descriptions. These are best expressed in averages and probabilities. Hence, the chaos in itself appeared to be such a general constituent of living brains, that it too, like the algebraic aspects, became the basis of theories. For a certain nerve net, defined by some simple probabilistic parameters of connection, one obtains easily some statistical regularities of performance, such as travelling waves of density of active elements, thresholds for the explosive crescendo or for a vanishing diminuendo of the average activity etc.

1136

These theories too present the double satisfaction that they are certainly true — at least provided that the abstraction used is realistic enough and that they are phrased in a well established mathematical language. But for them too, one can easily observe that they are insufficient compared with the actual performance of organisms. The hope underlying some « random » machines, that the unspecified structure may contain secrets useful in practical problems has largely disappointed the constructors (*). Random machines have been corrected by successive approximations in such a way as to contain ultimately a good deal of anatomy. This anatomy then gave useful results. We cannot escape the fact that what we can learn from living brains is largely organized structure.

1·3. *Psychological theories.* – A rather sound procedure in the study of the functions of the brain, *i.e.* of behaviour, or of the *psyche* is based on the complete neglect of the directly analysable aspects of the organ which we rightly or wrongly assert to be the carrier of these functions. This has been done for centuries by philosophers and by pure or applied introspective phychologists, the latter comprising practically everyone who uses conceptual models to understand and to communicate with his fellow men. It is conceivable that a rigorous analysis of « psyche », the abstract entity which stands for the behaviour of one individual person, when carried much farther than it has been done hitherto, with the aid of clever conceptual models, may lead to a complete system which would have to be ultimately isomorphic with the brain. As things stand now we may however exclude such attempts from the collection of rigorous theories mainly because an abstract language for psychology, necessary to make such theories independent from the historical accidents of linguistic categorization does not exist yet.

1·4. *Requirements for a realistic theory of the brain.* – If the emphasis is put on the explanation of the function of natural nervous systems, rather than on the construction of abstract brains, we should like to consider as completely as possible the established facts from physiology, anatomy and (behavioural) psychology. This proves unfortunately to be a superhuman undertaking at present, most likely because the organs (*e.g.* the *human* brain) from which these observations stem are of such inconceivable complexity, that the experimental picture which we obtain is very lacunary. We may get around this obstacle by limiting our theory in extent, in the sense that we consider only a very simple brain, or a rather homogeneous fragment of a more complex

(*) However, after this was written, A. Gamba [2] with his P.A.P.A. gave us a very convincing demonstration of the virtues of random connections in perceiving machines.

one. While the first alternative would seem equally desirable, we shall only pursue the second one here, concentrating our attention on two regular types of nerve nets occurring in vertebrate brains. It is however extremely important to realize that this limitation in extension may force upon us some perilous limitations of understanding, since no phenomenon occurring in a fragment of brain has *sense* unless it is understood in the language of input and output of the entire brain and of the return input through the feedback of the environment. Since this is a propedeutical study on the method rather than the foundation of a theory, we may get away with this simple cautionary remark.

The most important facts which should not be neglected even in a theory of a fragment of the brain are probably the following three. First, the already mentioned non linearity of the activity of neurons. Second, the facts connected with the geometrical arrangement of neurons of different sizes and shapes which will be discussed at some length. Thirdly, it is well known from all kinds of experimentation that effects from previous performances are carried over onto the performance of the future, but this « memory » is unfortunately not at all understood at the level of theories of neuron aggregates.

We shall not consider memory here, although probably theories of neuron aggregates which do not consider changes of the connections produced by the function itself (*i.e.* memory) cannot proceed beyond a rather elementary account. We refer the reader to the article of E. R. Caianiello [3] where a treatment of memory in equations describing the function of neurons is proposed. We may point out however that in a sense, memory enters our description when we consider the various complex ways of geometrical arrangement of neurons, which in their variation from place to place of the same brain and from species to species of the animal kingdom, bear obvious evidence of a process of selective evolution, best described as genetical memory in close analogy to the memory of individual experience. Through both processes regularities of the environment are inscribed into the structure of the brain in such a fashion as to insure the best and most economical performance. Whether this is done by the same principle (*e.g.* selection of preferential connections between neurons) in both instances, cannot be decided.

2. – Scheme of translation from physiological and anatomical data into a mathematical formalism.

2·1. *Abstract of the physiology of single neurons.* – Our account rests on the neuron theory insofar as we suppose that a stretch of functional history of a brain can be completely described by giving the discrete space time pattern of « firing » of its unitary components. Nothing happens, so the speak, between the lines. These unitary components we identify with the neurons of histology,

though it has been shown (BARRON and MATTHEWS) that in certain experimental conditions what appears histologically to be one neuron, may behave as an assembly of more than one elementary constituent which will not always fire together.

From a general biological point of view, neurons are cells, with a nucleus, a cell body and the corresponding limiting membranes. Their biological peculiarity is that they live without ever being replaced by daughter cells as long as the organism lives (in mammals, *e.g.*, the full set of neurons seems to be ready at birth). Neurons interest us in this connection insofar as they are cells strictly specialized for the conveyance and storage of information.

We may safely say that the actual carrier of signals in neurons is the neuronal membrane. Functionally, this membrane appears to be composed of two quite distinct parts: the membrane of type *a*), in which, impulses arise with a certain fixed amplitude, characteristic for each neuron, and are conducted without a diminution of their energy level (the « all or non » characteristics). This appears to be due to a chain reaction which consists in the sudden breakdown of a potential formed by the separation of ional charges across the membrane, and by the spread of this phenomenon to neighbouring points. The energy is stored in the membrane in the interval between one and the next signal. On the contrary, in the membrane of type *b*), the spread of similar phenomena occurs decrementally.

Morphologically, the most striking peculiarity of nerve cells is their radiate shape. Long, usually ramified processes emanate from the cell body. It is generally easy, on morphological grounds, to distinguish one of these processes, the so called *axon*, from the others, the *dendrites*.

It is basic for what follows, that this morphological distinction permits us to distinguish directly in histological preparations (Fig. 1) the two portions of the neuronal membrane described above, since the membrane of type (*a*) appears to be limited to the axon (« axonal membrane »), while the cell body

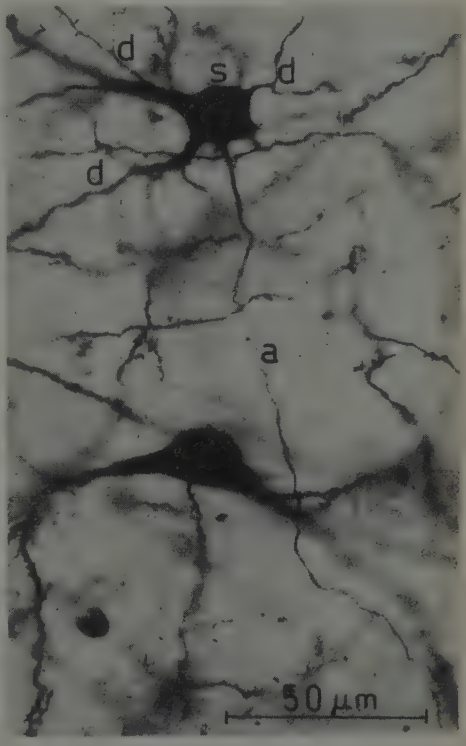

Fig. 1. – Microphotography of Golgi preparation. *s*: soma; *d*: dendrites; *a*: axon.

and the dendrites are covered by membrane of type (*b*) (« somatodendritic membrane »), conducting decrementally.

A *synapse* is the contact between two neurons, through which a signal (local depolarization of the membrane) in one neuron may produce a signal in another neuron. It is reasonable to assume from existing physiological evidence that synapses occur only between the membrane of type (*a*) of one neuron and the membrane of type (*b*) of the other and that the transmission of a signal happens exclusively from membrane (*a*) to membrane (*b*). This implies that the transmission of a signal *within* one neuron can only occur from the somatodendritic membrane to axonal membrane, and implies further, that the non-decremental conduction in the axon happens in one sense only, and is always triggered by decremental conduction in the somatodendritic membrane, provided that at the junction between the two portions of the membrane a certain *threshold* of amplitude is reached.

Thus we have assembled a set of physiological facts, which permit to reconstruct mentally the transmission of signals, or the transmission of « excitation » in connected neuron assemblies.

2·2. *Definition of excitation.* – From the physiological assumptions mentioned in the preceding paragraph, it follows, that a functional state of the brain is completely described by giving the spatial distribution of excitation in the neuron assembly. We may think then of our neurons as of a set of operators, distributed in a certain specified way, which operate on a pattern of distribution of excitation, the result of the operation being a new distribution of excitation, or a new state of the brain. Since our aim is at a quantitative description of these happenings, and since we do not suppose that binary algebra, assigning to each neuron at any one moment just the values 1 or 0 is a convenient language for real nerve nets, we need a quantitative appraisal of excitation.

2·3. – *Excitation* is the measure of the influence which neurons exert onto each other. It is well known from physiological experiments that in certain situations excitation is summated algebraically, which compells us to assume both positive and negative excitation, the latter being commonly called inhibition. In histological preparations, we have no method to distinguish synapses corresponding to positive excitation from those corresponding to inhibition. Therefore we must limit ourselves to define the absolute value of excitation, or in other words, the amount of functional connection of the neurons.

We define as the *unit of excitation E*, the amount of excitation produced by the contemporary activity of all axonal terminations which are present in 1 mm^3 of grey substance. (This definition is based on the assumption of a uniform density of terminal arborization in the cerebral cortex.)

1140

To establish the *amount of excitation e_T produced by the firing of individual neurons of type T*, we postulate that the excitation produced by a neuron is proportional to the volume of the whole neuron. Moreover we suppose the volume v_T of the so called perikaryon, *i.e.* the part of the neuron visible in Nissl preparations to be proportional to the volume of the whole neuron, for which assumption there is adequate histological support. We may write then

$$e_T = kv_T .$$

The value of k can be established as follows. By definition

$$\sum_T N_T e_T = E ,$$

where N_T is the number of neurons of type T. Since we have postulated that $e_T = kv_T$,

$$k \sum_T N_T v_T = E ,$$

which gives for k:

$$k = \frac{E}{\sum_T N_T v_T} .$$

The quantity

$$\frac{1}{\sum_T N_T v_T} ,$$

corresponds to what is called in neuroanatomy the « grey-cell coefficient of v. Economo ». We obtain the result that the amount of excitation produced by a neuron, expressed in units of excitation E, is equal to the volume of its perikaryon multiplied by the grey-cell coefficient of the piece of grey substance in which it is located. Values for the grey-cell coefficient of some regions, *e.g.* for different areas and layers of the cortex are available in the literature (HAUG [4], SHARIFF [5]).

2·4. *Abstraction from the histology.* – The conventional microscope, which has indeed yielded a great wealth of histological details on the nervous system, is however a somewhat inadequate instrument for purposes of immediate demonstration because of its thin focal plane, which allows one to view or to photograph only small fractions of a neuron at any one time. A very impressive view of neurons can be gained instead by using a stereoscopic microscope on Golgi preparations, in which a small number of individual neurons out of a large neuron population is stained thanks to some arbitrary selection performed by the nascent chromate-silver-precipitate used for the stain. One is

struck by the more or less dense clouds of ramified processes which constitute the neurons, clouds of different shapes and sizes, not unlike the clouds of foliage of trees when seen from far. If we mentally reconstruct the complete picture from such a view, multiplying the appearance of single neurons by their actual density in the tissue (which can be obtained through other histological techniques) we find that these cloudlike neurons vastly compenetrate each other, since the diameter of the « clouds » is in general by at least a factor 10 larger than the average distance of the neurons. Actual calculation shows for many regions intersections of any one cloud with $1\,000 \div 10\,000$ other clouds.

If we look more closely, we observe that these clouds are of two kinds. The first kind is given by the distribution of all the dendrites of a neuron, the second kind by the distribution of the « terminal arborizations » of the axon of a neuron. The clouds of the two kinds, pertaining to one neuron, are connected by the axon proper. Thus we have a histological tripartition of the neuron into dendritic cloud (including the cell body), axon, and cloud of terminal arborization, which according to our physiological premises acquires immediate functional significance. In fact the dendritic cloud represents the region in which a neuron can receive excitation; the cloud of terminal arborizations represents the region in which a neuron can excite other neurons, while the axon is the channel through which effects from one region are carried to the other region.

In different species of animals, in different region of one brain, and even for different neuron types of one and the same region the shapes and sizes of the clouds of dendritic and of axonal ramifications vary greatly. A great deal of this variation has been described in a burst of neuroanatomical activity during the last two decades of the last century and the first decade of our own; following the discovery of Golgi's invaluable chromate-silver method. Later on Golgi studies became rare, in spite of the fact that only a small fraction of the existing nerve nets had been described in sufficient detail: most likely because no theory had emerged (except Cajal's stupendous general intuition of the « neuron theory ») to lend life to the descriptions. In recent years, cybernetics has proceeded to ask questions for which an answer could only be obtained by means of the old histological techniques, and the unsurpassed Golgi method was re-exhumed to be used steadily in several laboratories including our own. For a survey of the very astonishing variations of neuron shapes and sizes we refer the reader to the work of CAJAL [6], for recent attempts to relate physiological findings with the histological picture see SHOLL [7], BRAITENBERG [8].

2·5. *Abstraction of a neuron model.* – Clouds of dendrites and clouds of axonal terminations, as described in the preceding paragraph, are more than

just a convenient image, a shorthand expression, to describe the complex arborization of cell processes. Indeed, if we notice that the fibers carrying sensory input to the brain, distribute their excitation in clouds of terminal arborization, and that at the other end the output of the whole brain (in each motor fiber) is derived from some sort of average over a large dendritic field, we may suspect that it would be redundant to carry analysis farther than to the consideration of the functional states of the total afferent and efferent fields of each neuron. Our abstraction therefore reduces to this: for each neuron we consider the simplest geometrical shape which outlines the dendritic arborizations, and which we call « *dendritic field* »; the simplest geometrical shape which outlines all the axonal terminations and which we call « *axonal field* » and finally an arrow, which symbolizes their connection by means of an axon.

A few more assumptions suffice to complete our scheme of translation. First, we suppose that excitation is produced uniformly in the whole axonal field. Second, we suppose that what counts to make a neuron fire, is the average density of excitation within its dendritic field. Finally, we have to make some assumption about the threshold of neurons with respect to excitations derived from other neurons, about which there is no experimental evidence. Again, we may suppose that the threshold is higher for larger neurons, and make it simply proportional to the volume of the dendritic fields. Therefore, if the threshold is expressed in terms of density of excitation, we can also say that it is the same for all neurons. We ignore the absolute value for the threshold, though in some special cases, it is easy to fix a lower bound, below which a neuron assembly would go into a generalized discharge, and an upper bound, beyond which all activity in a neuron assembly would soon be extinguished.

Knowing the outlines of the dendritic and axonal fields of all the neurons of a particular neuron assembly, as well as their relative positions and therefore the intersections between these different fields, we have a method which allows us to predict the further evolution of the states of excitation given any initial state.

We are consciously ignoring many subtleties of neurophysiology, which could easily be built in to our model, such as threshold variations due to past activity of the neuron itself, frequency responses to different intensities of excitation, etc. Our emphasis is on the geometrical aspects. It is our conviction that in such a simple translation from histology to function, provided the method is kept constant, differences of structure in different regions of the brain will reflect themselves in differences of the functional scheme which will be obtained, and that these will throw some light onto hitherto obscure problems.

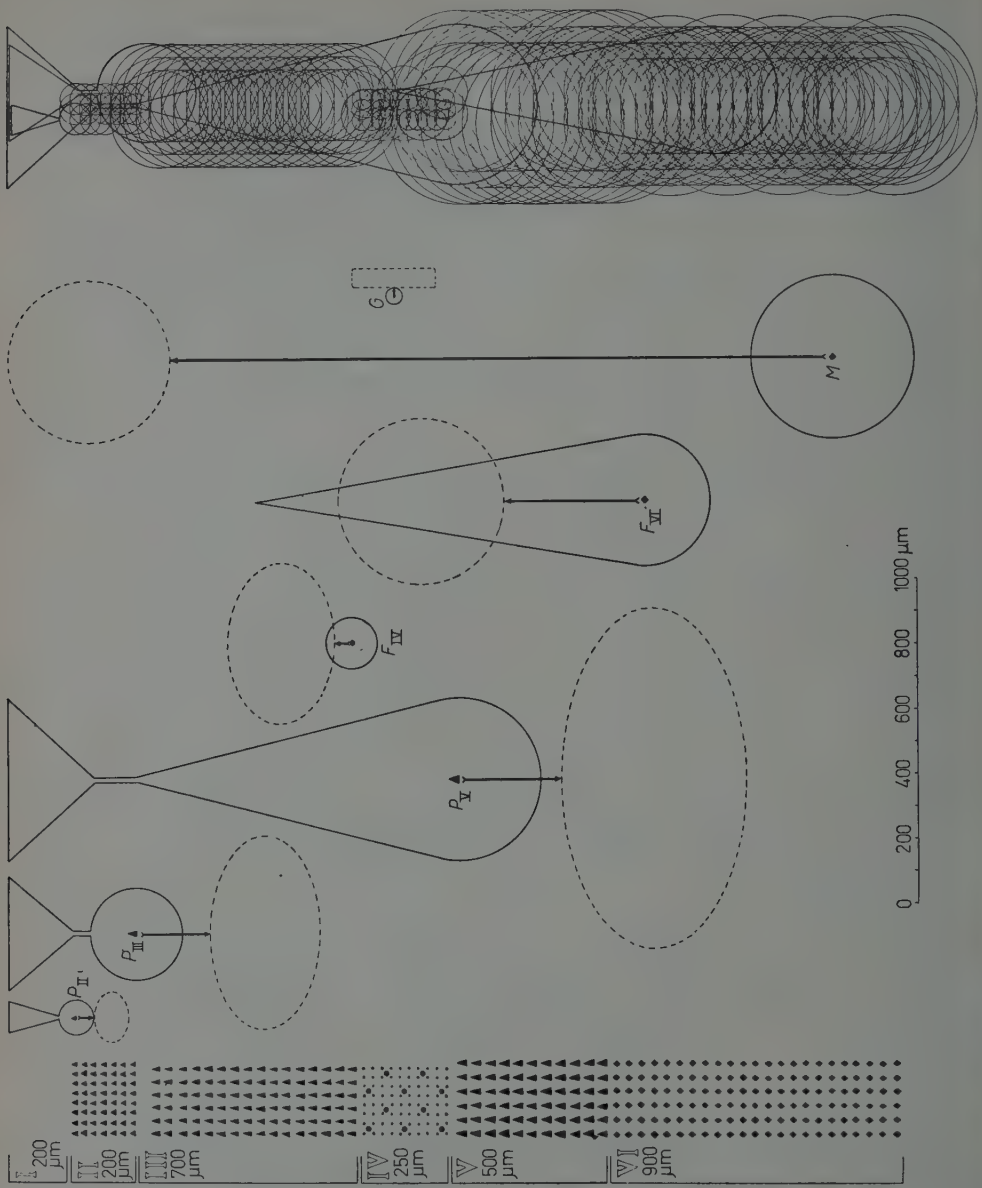

Fig. 2. - Abstraction of the histology of the undifferentiated human cerebral cortex. To the left, the distribution of neuron cell bodies (as they appear in Nissl preparations) in different layers of the cortex is represented diagrammatically. The numbering of the layers corresponds to conventional descriptions. In our abstraction, the cell bodies are arranged in the vertices of a cubic lattice, whose sides are so chosen (for each layer) as to represent the real cell density. Seven neuron types are represented. For each we draw the outline of the cell body (triangle, circle or diamond) which allows

3. – Examples.

In this section we shall mention briefly two examples of typical nerve nets of vertebrate brains, to which we have applied our scheme of translation from the histology into « wiring diagrams ». In the first, the cerebral cortex of man, the result obtained is of such complexity, that it can only be considered as preparatory for a future separate mathematical study. On the contrary, in the second example, the cortex of the small brain, or cerebellum, the translation proves valuable in itself, since it leads to immediate insights into the particular function of this portion of vertebrate brains, which had not been obtained by any other method.

3·1. *Undifferentiated human cerebral cortex.* – Though certainly no isolated portion of the brain contains all the secrets of intelligent behaviour, the cerebral cortex, which becomes more and more preponderant with respect to the rest of the nervous system as one ascends the vertebrate scale, and reaches its maximum development in man, is certainly the strongest candidate to being nature's most refined « thinking machine ». This agrees with the observation that isolated lesions of the brain in man will produce the most evident effects on intelligence, speech, recognition, etc., when they are localized in the cerebral cortex. Again, in the cortex we may distinguish specialized *sensory* and *motor* regions, in which the outside world is somehow mapped onto the cortex, from the *undifferentiated* cortex, in which no such clearcut projection occurs. It is from the latter type of cortex, which admittedly is not of completely uniform structure in all places, that we have abstracted our data.

---

one to recognize its distribution in the laminar arrangement to the left, the outline of its dendritic field (solid lines), the outline of its axonal field (broken lines) and an arrow representing the connecting axon. The types are: P_{II} pyramidal cell of the second layer, P_{III} pyramidal cell of the third layer, P_{V} pyramidal cell of the fifth layer, F_{IV} large granular cell of the fourth layer (upper feedback neuron), F_{VI} cell with ascending axon of the sixth layer (lower feedback neuron), M « Martinotti cell » and G small granular cell of the fourth layer. All the outlines of this drawing should be interpreted as sections through solids of revolution around a vertical axis contained in the plane of the drawing. Axons leaving the cortex (which are offshoots of the axons of P_{II}, P_{III} and P_{V}) and axons entering the cortex are not represented. To the right, the dendritic fields of three neighbouring cells of each row (some of them drawn as circles instead of the more complicated figures) are shown, to demonstrate the vast overlap of these neuronal fields. The overlap would be considerably more impressive, if the axonal fields, as well as all the neurons with cell bodies lying behind and in front of the plane of the drawing were considered.

Our version of cortical « architectonics » (the minute description of local variations of cortical structure, as practised in some laboratories around the turn of the century) though checked on our own histological preparations, is based mainly on descriptions and illustrations in CAJAL [6], on descriptions, cell counts and illustrations in HAMMARBERG [9], a rare book which under an unfortunate title hides some excellent quantitative data on cell-architectonics, on photographs in BAILEY and VON BONIN [10]. Our objective was to produce a model which was quantitatively defined in every detail. In order to achieve this, measurements are frequently given with a precision which is not warranted by the available data. This is not necessarily dangerous, since the most obvious features of the structural differentiation of various neuron types, of their distribution in different layers, etc., which are retained in our abstraction, are most likely to reflect the most essential specifications of the genetic blueprint of the cortex. Thus our model, though abstract, is essentially realistic.

The cortex is a thin layer of grey substance in which a number of neurons of the order of magnitude 10^{10} are connected together. The cortex is divided in two symmetrical halfs (right and left hemisphere). The total surface is about 2 500 cm^2, the thickness about 2.5 mm. The structure is isotropic in the plane of maximal extension of the cortex, while along the thickness a definite stratification occurs. At any point of the (undifferentiated) cerebral cortex fibers enter the cortex and fibers leave the cortex. Some of these external fibers connect different points of the same cortex, others connect the cortex with other structures of the nervous system.

Our abstraction of the cortex is laid down in the diagram (Fig. 2) and in the accompanying table. The following procedure was used. Seven neuron *types* where defined according to their most marked morphological distinctions. The number of types abstracted by other authors may be larger or smaller, depending on the criteria used, which is not surprising, since any such classification relies on somewhat physiognomical definitions. However, most neuron types described in the literature can be identified with some of our types, which were chosen in such a way as to represent the most marked and easily recognizable variations of neuron shape. In a similar arbitrary fashions different *layers* of the cortical thickness were defined. The distribution of neuron types in different layers was then studied. No precise statistical data are available on this point and our drawing may be more schematic than is necessary; however, though *e.g.* granular cells occur also outside of the IV layer, for the vast majority of neurons of a certain type a typical localization is easily recognized.

The cell density (of neurons of any type) in different layers is available in HAMMARBERG [9]. The distribution is not as regular as represented in our diagram, in which the cell bodies are drawn in the vertices of a square

1146

TABLE I. – *Some numerical values corresponding to the abstraction represented in Fig. 2.*

Type	No. and thickness of the layer	Diameter of the soma	Dimensions of « dendritic field »	Dimensions of the « axonal field »	Density
P_{II}	II, 200 μm	10 μm	cone in the first layer: $h = 200$ μm, $r = 50$ μm; sphere: $r = 50$ μm	semiaxes of the ellipse: $a = 75$ μm, $b = 50$ μm; $z = z_0 + 250$ μm	40000/mm³ ~1 every 30 μm
P_{III}	III, 700 μm	20 μm	cone in the first layer: $h = 200$ μm, $r = 150$ μm; inferior cone and half sphere: $h = z_0 - 200$ μm, $r = 150$ μm	semiaxes of the ellipse: $a = 300$ μm, $b = 150$ μm; $z = z_0 + 400$ μm	15000/mm³ ~1 every 40 μm
G	VI, 250 μm	8 μm	sphere: $r = 25$ μm	cylinder $z = 1225 + \mu$m: $h = 250$ μm, $r = 25$ μm	45000/mm³ ~1 every 30 μm
F_{IV}	IV, 250 μm	10 μm	sphere: $r = 75$ μm	semiaxes of the ellipse: $a = 250$ μm, $b = 150$ μm; $z = z_0 - 200$ μm	45000/mm³ ~1 every 60 μm
P_V	V, 500 μm	25 μm	cone in the first layer: $h = 200$ μm, $r = 250$ μm; inferior cone and half sphere: $h = z_0 - 200$ μm, $r = 250$ μm	semiaxes of the ellipse: $a = 500$ μm, $b = 250$ μm; $z = z_0 + 650$ μm	12000/mm³ ~1 every 43 μm
F_{VI}	VI, 900 μm	15 μm	cone and half sphere: $h = 1000$ μm, $r = 200$ μm	sphere: $r = 250$ μm; $z = z_0 - 550$ μm	16000/mm³ ~1 every 40 μm
M	VI, 900 μm	15 μm	sphere: $r = 250$ μm	sphere: $r = 250$ μm; $z = 250$ μm	16000/mm³ ~1 every 83 μm

z_0: distance of the cell body from the surface of the cortex; z: distance of the center of the axonal fields from the surface of the cortex. The other abbreviations are self explanatory. The values given for the various measurements are approximations to about ± 20 %.

TABLE II. – At the intersection of a row h with a column k (each representing one of the neuron t
amount of excitation transmitted by a neuron of type k to a neuron of type h; the range of position
while z and z_0 are the vertical co-ordinates of the neurons k and h, respectively, as given in Tab
the right of the table give the values for afferent fibers, of which we consider only those of cor

$h \downarrow$ \ $k \rightarrow$	P_{II}	P_{III}	G	F_{IV}
P_{II}				
P_{III} 400 μm ⩽ z_0 < < 500 μm	$a_{hk}^{(0)} = 0{,}004$ $r \leqslant 170$ μm, 200 μm ⩽ $z \leqslant 400$ μm $N(k) = 726$			
P_{III} 500 μm ⩽ z_0 < < 800 μm	$a_{hk}^{(0)} = 0.004$ $r \leqslant 170$ μm, 200 μm ⩽ $z \leqslant 400$ μm $N(k) = 726$			
P_{III} 800 μm ⩽ z_0 ⩽ ⩽ 1100 μm		$a_{hk}^{(0)} = 0.000\,68$ $r \leqslant 350$ μm, $z_0 - 125$ μm ⩾ z ⩾ ⩾ $z_0 - 575$ μm $N(k) = 2595$	$a_{hk}^{(0)} = 0.001$ $r \leqslant 100$ μm, 1100 μm ⩽ $z \leqslant 1350$ μm $N(k) = 353$	$a_{hk}^{(0)} = 0.000\,8$ $r \leqslant 300$ μm, 1100 μm ⩽ $z \leqslant 135$ $N(k) = 318$
G		$a_{hk}^{(0)} \leqslant 0.000\,68$ $r \leqslant 250$ μm, $z_0 - 550$ μm ⩽ z ⩽ ⩽ $z_0 - 250$ μm $N(k) = 883$	$a_{hk}^{(0)} = 0.0329$ $r \leqslant 40$ μm, $r \leqslant 65$ μm, 1100 μm ⩽ $z \leqslant 1350$ μm $N(k) = 9$	$a_{hk}^{(0)} = 0.000\,8$ $r \leqslant 200$ μm, 1200 μm ⩽ $z \leqslant 135$ $N(k) = 84$
F_{IV}		$a_{hk}^{(0)} = 0.000\,68$ $r \leqslant 300$ μm, $z_0 - 600$ μm ⩽ z ⩽ ⩽ $z_0 - 200$ μm $N(k) = 1696$	$a_{hk}^{(0)} = 0.000\,2$ $r \leqslant 40$ μm, $r \leqslant 65$ μm, 1100 μm ⩽ $z \leqslant 1350$ μm $N(k) = 18$	$a_{hk}^{(0)} = 0.000\,8$ $r \leqslant 250$ μm, 1200 μm ⩽ $z \leqslant 135$ $N(k) = 132$
P_V		$a_{hk}^{(0)} = 0.000\,13$ $r \leqslant 300$ μm, 400 μm ⩽ $z \leqslant 700$ μm, $r \leqslant 400$ μm, 700 μm ⩽ $z \leqslant 1100$ μm $N(k) = 4287$	$a_{hk}^{(0)} = 0.000\,01$ $r = 150$ μm, 1100 μm ⩽ $z \leqslant 1350$ μm $N(k) = 795$	$a_{hk}^{(0)} = 0.000\,03$ $r \leqslant 325$ μm, 1100 μm ⩽ $z \leqslant 135$ $N(k) = 373$
F_{VI}				
M				

ribed and labelled accordingly) this table shows: the coupling coefficient $a_{hk}^{(0)}$ which stands for the ons k which impinge on a neuron h, where r is the distance in the horizontal plane of the cortex number of neurons of type k, $N(k)$, which impinge on one neuron of type h. The two columns to n and distinguish two types, stemming from P_{III} neurons and P_V neurons, respectively.

P_V	F_{VI}	M	Afferents type P_{III}	Afferents type P_V
		$a_{hk}^{(0)}=0.0025$ $r\leqslant 290\ \mu m$, $1850\ \mu m\leqslant z\leqslant 2750\ \mu m$ $N(k)=380$		
		$a_{hk}^{(0)}=0.0025$ $r\leqslant 350\ \mu m$, $1850\ \mu m\leqslant z\leqslant 2750\ \mu m$ $N(k)=559$		
		$a_{hk}^{(0)}=0.0025$ $r\leqslant 350\ \mu m$, $1850\ \mu m\leqslant z\leqslant 2750\ \mu m$ $N(k)=559$	$a_{hk}^{(0)}=0.00068$ $r\leqslant 400\ \mu m$ $N(k)=5275$	$a_{hk}^{(0)}=0.00087$ $r\leqslant 400\ \mu m$ $N(k)=3014$
		$a_{hk}^{(0)}=0.0025$ $r\leqslant 350\ \mu m$, $1850\ \mu m\leqslant z\leqslant 2750\ \mu m$ $N(k)=559$	$a_{hk}^{(0)}=0.00068$ $r\leqslant 400\ \mu m$ $N(k)=5275$	$a_{hk}^{(0)}=0.00087$ $r\leqslant 400\ \mu m$ $N(k)=3014$
	$a_{hk}^{(0)}=0.0016$ $r\leqslant 200\ \mu m$, $1850\ \mu m\leqslant z\leqslant 1950\ \mu m$ $N(k)=201$		$a_{hk}^{(0)}=0.00068$ $r\leqslant 350\ \mu m$ $N(k)=4035$	$a_{hk}^{(0)}=0.00087$ $r\leqslant 350\ \mu m$ $N(k)=2304$
	$a_{hk}^{(0)}=0.0016$ $r\leqslant 250\ \mu m$, $1850\ \mu m\leqslant z\leqslant 2000\ \mu m$ $N(k)=471$		$a_{hk}^{(0)}=0.00068$ $r\leqslant 350\ \mu m$ $N(k)=4035$	$a_{hk}^{(0)}=0.00087$ $r\leqslant 350\ \mu m$ $N(k)=2304$
	$a_{hk}^{(0)}=0.0016$ $r\leqslant 350\ \mu m$, $z_0+300\ \mu m\leqslant z\leqslant$ $\leqslant z_0+800$ $N(k)=3072$	$a_{hk}^{(0)}=0.0025$ $r\leqslant 400\ \mu m$, $1850\ \mu m\leqslant z\leqslant 2750\ \mu m$ $N(k)=723$	$a_{hk}^{(0)}=0.00068$ $r\leqslant 400\ \mu m$ $N(k)=5275$	$a_{hk}^{(0)}=0.00087$ $r\leqslant 400\ \mu m$ $N(k)=3014$
0.00075 50 μm, μm $\leqslant z\leqslant$ 1850 μm =3817	$a_{hk}^{(0)}=0.00142$ $r\leqslant 200\ \mu m$, $z_0-200\ \mu m\leqslant z\leqslant$ $\leqslant z_0+400$ $N(k)=1206$			
0.00087 00 μm, 300 μm $\leqslant z\leqslant$ z_0-400 μm =3769	$a_{hk}^{(0)}=0.0016$ $r\leqslant 300\ \mu m$, $z_0\leqslant z\leqslant z_0+800$ $N(k)=804$			

lattice where the side of each mesh represents the average distance of the cell bodies in that layer of the cortex.

3·2. *Cerebellar cortex.* – This example has been more extensively treated elsewhere (BRAITENBERG and ONESTO [11]; BRAITENBERG [8], and shall be reported here in summary. Like the cerebral cortex, the cortex of the cerebellum is a stratified sheet of grey substance in which neurons of different types are connected together; unlike the former, the connections in the plane of the sheet of the cerebellar cortex are however anisotropic: two entirely different ways of connection are apparent along two rectangular co-ordinates of the sheet. Like in the cerebral cortex, in the cortex of the cerebellum too, every small fraction receives input axons and emits output axons. The situation is somewhat simpler than in the preceding example, since the classification of the neurons on morphological grounds presents no difficulties: two main neuron types and a few more secondary ones (not present in all species of animals who have a cerebellum) are neatly distinct both in their shape and in their position. The translation from the histology into wiring diagrams by means of our abstract neuron model, *i.e.* considering only the regions in which the various neurons can receive excitation and the regions in which they can excite other neurons, leads among other things to one important functional relation. For any one output axon, hundreds of input axons entering the structure along a line parallel to one of the two main rectangular co-ordinates of the sheet are equivalent except for varying delays interposed between input and output. The delays are proportional to the distance between the point of input and the point of output. Thus the whole structure becomes understandable as a delay line and, considering its connections with the rest of the nervous system, as a clock useful for the timing of successions of impulses in various functional contexts.

APPENDIX

A table of coupling coefficients for cortical neurons is relegated to this appendix, since it is based on some simplifications of the morphological evidence which go beyond the simplifications implicit in the method outlined in the preceding paper. Thus *e.g.*, in order to facilitate calculations, all dendritic and axonal fields were considered to be composed of cylinders, whose radius and height were chosen so as to give a first approximation of the volumes of the original geometrical bodies outlined in Fig. 2 and Table I.

Coupling coefficients $a_{hk}^{(0)}$ were calculated for Caianiello's [3] neuronic equation:

$$u_h(t+\tau) = 1\Big[\sum_{k,r} a_{hk}^{(r)} u_k(t - r\tau) - \mathcal{S}_h\Big] .$$

The function $1[x]$ is defined as

$$1[x] = \begin{cases} 0\,, & x \leqslant 0\,, \\ 1\,, & x > 0\,, \end{cases}$$

$u_h(t)$ is equal to 0 or 1 in any interval $\{M\tau, (m+1)\tau\}$ (τ is a suitable unit of time) and represents the behaviour of a neuron h. S_h is the threshold of the same neuron. $a_{hk}^{(r)}$ $(h \neq k)$ is the coupling coefficient which describes the transfer of excitation from the neuron k to the neuron h, the index r being introduced to describe the decay of excitation, while $a_{hh}^{(r)}$ expresses the variations of the threshold during the absolute and relative refractory time. We pose

$$a_{hk}^{(0)} = \frac{V_i e}{V_d V_a}\,,$$

where V_d is the volume of the dendritic field of neuron h, V_a the volume of the axonal field of neuron k, V_i the volume of the intersection between the dendritic field of h and the axonal field of k, e is the quantity of excitation produced by the neuron k. V_i we fixed at half the maximum of the value allowed by the histological geometry for all the pairs of neurons h and k having any intersection at all.

REFERENCES

[1] W. S. McCulloch and W. Pitts: *Bull. Math. Biophys.*, **5**, 115 (1943).

[2] A. Gamba: *Proc. IRE*, **49**, 349 (1961).

[3] E. R. Caianiello: *Journ. of Theor. Biology*, **2** (in print).

[4] H. Haug: *Journ. Comp. Neurol.*, **104**, 473 (1956).

[5] G. A. Shariff: *Journ. Comp. Neurol.*, **98**, 381 (1953).

[6] S. Ramon y Cajal: *Histologie du Système Nerveux de l'homme et des vertébrés*. 1911 (Madrid, 1952).

[7] D. A. Sholl: *The Organization of the Cerebral Cortex* (London, 1956).

[8] V. Braitenberg: *Funktionelle Deutung von Strukturen in der grauen Substanz des Nervensystems*, in *Die Naturwissenschaften* (in print).

[9] G. Hammarberg: *Studien über Klinik und Pathologie der Idiotie nebst Untersuchungen über die normale Anatomie der Hirnrinde* (Uppsala, 1895).

[10] P. Bailey and G. von Bonin: *The Isocortex of Man* (Urbana, 1951).

[11] V. Braitenberg and N. Onesto: *The cerebellar cortex as a timing organ*, in *Atti del Congresso di Medicina Cibernetica* (Napoli, 1960).

SUPPLEMENTO AL VOLUME XVIII, SERIE X
DEL NUOVO CIMENTO

N. 2, 1960
4° Trimestre

Some Remarks on the Shape of Viruses.

M. AGENO

Istituto Superiore di Sanità - Roma

1. – Five years have passed since F. H. C. CRICK and J. D. WATSON [1, 2] published their first considerations on the shape of viruses. Since then a great deal of new experimental data has accumulated and, at present, the shapes of many viruses are sufficiently well known. It would seem, therefore, that it is time to try to face the problem again on better defined and partly new foundations. It is necessary to warn that what follows concerns only those viruses, generally of small size, which have a specific shape.

On the basis of the results then known, CRICK and WATSON thought they could state that virus particles are always either small rods or spheres and that the particles of the same virus are all identical. Since then, this second conclusion has been confirmed repeatedly both as a result of direct observation with the electron microscope and, above all, by the fact that the particles of a virus often tend to aggregate into regular lattices of crystal type (Fig. 1). Their first conclusion, on the contrary, is undoubtedly contradicted by the data. The « spheres » of CRICK and WATSON (as they, however, alredy suspected) were shown to be polyhedrons and (what is important) each face of the polyhedron is, so to say, paved with a regular array of a relatively high number of protein molecules: this can clearly be seen in high resolution electron micrographs [3, 4].

All the considerations by which CRICK and WATSON tried to justify the shapes they considered cannot therefore be accepted, now. From the mathematical point of view, in fact, the problem no longer consists in the subdivision into equal parts of a given closed surface and in the demonstration that, in the case of the sphere for example, this is possible in a limited number of ways. The question is, on the contrary, to demonstrate that only some polyhedric shapes are possible for the virus particles and the principle of the demonstration cannot be exclusively geometrical, but can be found only in the physical features of virus structure.

2. – We shall begin by summarizing briefly the most important of these characteristic features.

The electron microscope confirms substantially the structural pattern proposed by CRICK and WATSON. A virus particle appears to be made up of a central nucleus, essentially consisting of nucleic acid, and of an outer coat, sheath or membrane formed by protein molecules. Staining with uranyl acetate evidences the distribution of the nucleic acid [5] (Fig. 2) and, by means of the freeze drying technique, it is possible to see these two components, nucleus and outer coat, at the same time; the nucleus appears to repeat on a smaller scale the shape of the particle [5] (Fig. 3). One can observe some shells, stripped of their nucleic acid content, which still maintain substantially the outer shape of the particle [6] (Fig. 4, 5).

Furthermore, as we have already mentioned, the high resolution photographs also show that the protein coat is made up of sub-units of roundish shape, probably molecules, tightly packed and forming a monolayer (Fig. 6). The outer shape of the whole virus particle is that of a plane-face polyhedron, which can be regular (*e.g.* an icosahedron). Each face, however, is covered with a great number of tightly gathered protein sub-units, so that the image one obtains reminds one of a blackberry.

There are two striking facts. The first is that, if preparations are made with great care, so that the viruses are not deformed, one does not observe roundish particles: it seems, really, that for viruses of small size these shapes are due only to artefacts. In particular, one never sees spheres which should, however, be strongly favoured by surface tension.

The second fact is the extraordinary uniformity, within the limits of our power of observation, which the particles of the same virus present. Simple as viruses may be, they are still organisms, but there is no trace of that biological variability which is always to be seen in the sizes and in the shapes of all organisms, even if only slightly more complex than these.

A theory on the shape of viruses should allow to explain not only *the exclusive presence of certain polyhedric shapes*, but also *the extreme uniformity of the absolute dimensions*.

3. – First of all we ask whether among the categories of natural objects already known some exist in which these biological objects of polyhedric shape may be included for structural analogy.

We know of two kinds of entities of geometrically defined shape: crystals and molecules. We shall see, therefore, if viruses may be included in one of these categories.

A crystal is, in fact, (as well as a virus) a polyhedric solid figure limited by plane faces. There are, however, some fundamental differences between viruses and crystals. What characterizes a crystal is, as is well known, only the value

of the dihedral angles. Two real crystals of the same kind may differ very much from each other with respect to shape, volume, and the extension of their faces. The dihedral angles remaining constant, the faces can be arbitrarily parallely transferred. We can synthetize this, saying that a crystal is a system which has many degrees of freedom: it can grow or become smaller in directions perpendicular to each face, without ceasing to remain a crystal of that particular kind.

A virus particle, on the contrary, is a system in which all the degrees of freedom are frozen. Not only are the dihedral angles fixed, but the general shape, the volume, the extension of the faces are also fixed. Such a particle can be (from the geometrical point of view) made up only in one way and cannot become larger or smaller without loosing its specific individuality.

Furthermore, if we consider the elements of symmetry, either present or possible in both cases, we find other fundamental dissimilarities. For example, a crystal cannot present to macroscopic observation a quinary axis of symmetry (because the plane cannot be divided in regular pentagons). To the contrary, in viruses quinary axes are frequent: the adenoviruses, for instance, have the shape of a regular icosahedron which is not a possible shape in common crystallography [3-5].

The foregoing considerations are, as it seems, sufficient to conclude that virus particles do not have a crystallographic structure in the current meaning of the word. They cannot, in fact, be composed of identical sub-units which are obtained from each other through parallel transfer.

On the other hand, what we know to day about virus structure allows to exclude that each particle consists of a single molecule. As we have already mentioned, it consists of an organized aggregate of (a relatively small number of) molecules, *i.e.* a very simple organism, but nevertheless an organism.

Excluding that virus particles can be classified either among crystals or among molecules, we are forced to conclude that they form a particular category of natural polyhedric shaped solid figures and that up to the present we have no model by which the uniformity and the specificity of their shape can be justified.

4. – We can get, however, a certain number of suggestions that can help to make a model with which at least the chief features among those observed can be explained. These suggestions especially come from the electron microscopic works.

As we have already observed, the nucleic acid of the virus and the protein coat that covers it appear to have the same shape. Undoubtedly, all the characters of the virus including its shape and size find their ultimate justification in the molecular structure of the specific nucleic acid. Nevertheless, we may ask whether, from the point of mechanical rigidity, the stability of

1164

the shape of the virus particle is due to the nucleus or to the outer coat. In other words: we distinguish two components and see them of the same shape, one inside the other. The simplest hypotheses we can propose are the following: either the nucleus is rigid and has its own geometrically defined shape and the protein sub-units of the coat are attached to it and cover it like the tiles of a wall, or the protein shell is rigid and has its own geometrically defined shape, while the nucleus forms a yielding mass which, like a very viscous liquid, fits into the protein container.

Of course, many other less simple hypotheses are also possible and the second of the two mentioned above does not detract at all from the nucleus its orienting function in the fabrication of the particle; the synthesis of the specific protein molecules of the shell is in fact to be induced by nucleic acid.

It seems that there is some experimental evidence supporting the second hypothesis. The electron micrographs show, occasionally, a damaged virus particle in which the protein coat is broken in a point. From that point the nuclear substance is seen to come out, as a small mass without a definite shape, just like a very viscous liquid (Fig. 7). When nucleic acid is expelled artificially from the phages it has an analogous appearance [6] (Fig. 8).

By means of negative staining with phosphotungstic acid one can easily observe the protein coats totally or partially stripped of their contents [6] (Fig. 9, 10): they maintain practically unaltered the shape of the entire virus. In addition, analytical ultracentrifugation shows, by the schlieren technique, a defined peak apparently due to these ghosts: therefore, they all seem to have the same mass, smaller however than the mass of the whole virus particle [6].

Viceversa, it seems that virus particles which have at least partially lost their protein coat while retaining to a certain extent their original shape have never been observed.

We, therefore, think it reasonable to admit, at least as a working hypothesis, that from the mechanical point of view it is the protein coat that assures to the virus particle its own characteristic shape.

5. – We shall therefore draw our attention to the protein coat. As we have already mentioned, it consists of roundish shaped sub-units, apparently all identical, disposed in a unique monolayer and tightly packed.

In the conditions of closest packing, all the protein particles, except those placed on the vertices of the polyhedron, touch six other particles. It is clear that some bonds must exist between the contiguous particles and that these bonds (that allow the shell to maintain its shape even when stripped of its contents) must be stronger than those which bind each protein particle to the nucleic acid.

It is certainly difficult, at present, to understand what exactly is the building up mechanism, around the previous nuclear substance, of the protein coat, with its specific shape and size. It seems reasonable to exclude that the protein molecules are synthetized « in loco », if for no other reason keeping in mind the phenomenon called phenotypic mixing [7-10], which shows how the specific proteins can unite with a nuclear substance of a virus particle genetically different from that which has determined their specificity.

It may be supposed that, on the whole outer surface of the nuclear substance, there are a great number of points where a protein molecule can attach: in a first phase, the specific protein would be attached, therefore, to the condensed nucleic acid, as to a sticky surface, forming a closest packed monolayer. Only in a second phase, strong bonds between adjacent sub-units would be established. This would explain why the shell results mechanically more rigid and stable than its content. This hypothesis would also explain the observations of KELLENBERGER *et al.* [11], according to which the virus particles already formed are dissolved, if lysis of the host cell is made to occur immediately after their formation, while they are not altered if lysis is allowed to take place after a sufficient time.

Very little can be said concerning the nature of the forces existing between protein sub-units and between these and the nucleus. It is, however, certain that the forces among protein sub-units are of very short range as compared with their dimensions. It seems, therefore, possible to admit that the protein sub-units, as single molecules, behave as small rigid bodies which can set up a bond among themselves only when they effectively come in contact. The maximum binding energy and, consequently, the maximum rigidity of the coat will be obtained when the number of bonds among the protein particles is maximum, *i.e.* when the arrangement of such a particle in the monolayer is that of the closest packing. Finally, the coat should, generally, form a completely closed container.

Summarising what has been said, it seems that the protein coat of a virus particle may be thought of as a monolayer of molecule units having the following properties:

a) each units behaves as a rigid particle;

b) adjacent units are directly in contact and their arrangement in the monolayer is that of the closest packing;

c) the monolayer forms a closed container.

6. – *It is easily seen that the foregoing three conditions are by themselves sufficient to give a very severe restriction to the possible shapes for a virus particle. Only some categories of geometrically well defined shapes are possibile* and even for these the volumes, so to say, are quantized.

1158

Furthermore, it is clear that it is possible to develop a real systematic crystallography of the closed monolayers, obtaining a category of objects with geometrical properties similar to those which have been observed in the viruses.

Of course it is not possible, at present, to state that this is the precise mechanism responsible for the shape of viruses. It is necessary to put in evidence that there is not enough experimental material in support of this hypothesis. We, therefore, present it as a basis for discussion: only a systematic and broad investigation will allow to show if the shapes, which occur in nature, are indeed those foreseen by the crystallography of the monolayers.

In what follows, we shall not develop a real systematics, the exposition of which will be reported elsewhere, but we shall limit ourselves to justifying the foregoing considerations, giving some simple examples.

We begin by simplifying drastically our problem supposing the protein particles to be all identical and perfectly spherical. Later it will perhaps be possible to try to put aside these limiting hypotheses, introducing, for example, two or more kinds of particles of different shape. One must say however that the more complicated the situation is, the more difficult it is to satisfy the conditions of contact and closure: to the limit, these cannot be satisfied except in extremely particular cases and then a systematics is no longer possible.

Let us suppose that we place a number of identical spherical beads on a convex surface. The maximum number of spheres which a given sphere can come in contact with is six. This can take place either on a plane or on a cylindrical surface . If the surface is doubly curved, for example spherical (with a radius greater than that of the beads) it is not possible to place a bead upon it, in contact with six more. Now, a plane or cylindrical surface, does not satisfy the conditions of closure. It is, therefore, necessary that at least occasionally a bead be surrounded by a number N of other beads, N being smaller than six: only under these conditions can a closed monolayer be formed. But in this case, the point of the monolayer where $N < 6$ is a singular point: it is the vertex of a polyhedron.

This explains why small spherical (or more generally roundish) viruses have never been observed, while *a priori* we would expect this shape, strongly favoured by surface tension, to be the most frequent.

Monolayers present three fundamental types of vertices: those with $N = 5$, those with $N = 4$, and a third type derived from the case $N = 3$. In fact, in the case $N = 3$ the bead that should be on the vertex is absent. The other three, in contact with each other, would isolate it completely, preventing it from establishing a bond with the nucleus.

Let us consider for example the case $N = 5$ and suppose that the five beads in contact with the one in the center are placed on the vertices of a regular pentagon. What one obtains in this case is the vertex of a regular icosahedron which can be completed by putting along each edge any number n of

beads ($n = 2, 3, ...$). Let us calculate the total number of beads on the whole monolayer. There are 12 beads on the 12 vertices of the icosahedron. Then, on each of the 30 edges there are $(n-2)$ beads which do not fall on the vertices and on each of the 20 triangular faces there are $\frac{1}{2}(n-2)(n-3)$ beads that do not fall either on the vertices or on the edges. On the whole, to form the icosahedral monolayer such as the one we consider here

$$(1) \qquad \tfrac{1}{2}(n-2)(n-3)\cdot 20 + (n-2)\cdot 30 + 12 = 10(n-1)^2 + 2$$

beads are therefore necessary.

It could easily be seen that the regular icosahedron is, among the possible shapes, the closest to the spherical shape. It is, therefore, the most favoured by surface tension, and this explains how it is so frequent in spite of its complexity.

Another possible shape, belonging to a category of monolayers different from the previous one, is the orthogonal hexagonal prism. This shape also corresponds to $N = 5$, but the five beads in contact with the one which is on the vertex, do not form a regular pentagon. The two bases of the prism are equiangular, but not necessarily equilateral hexagons. Let us consider the case in which along each edge of the bases there is a row of beads in contact with each other. Let us now calculate the total number of beads that are required to form a monolayer.

Let n_1, n_2, n_3 be the numbers of beads along the three unequal edges of a base. The perimeter of the bases is made up of

$$(2) \qquad 2(n_1 + n_2 + n_3) - 6$$

beads and on each hexagonal base they add up to

$$(3) \qquad n_1 n_2 + n_2 n_3 + n_3 n_1 - n_1 - n_2 - n_3 + 1 .$$

On the lateral surface of the prism, the beads are placed on planes parallel to the bases. There are, however, two kinds of planes, those having a bead on each lateral edge, like the bases, and intermediate planes having no bead on the lateral edges. If n_4 is the number of beads (not in contact) on each lateral edge, the number of beads that cover the surface of the prism and do not belong to the bases is $(2n_4 - 1)$ times the number of beads along the perimeter of a base. Therefore, the total number of the small spheres forming the monolayer is given by the expression:

$$(4) \qquad 2(n_1 n_2 + n_2 n_3 + n_3 n_1 - n_1 - n_2 - n_3 + 1) + 2(n_1 + n_2 + n_3 - 3)(2n_4 - 1) .$$

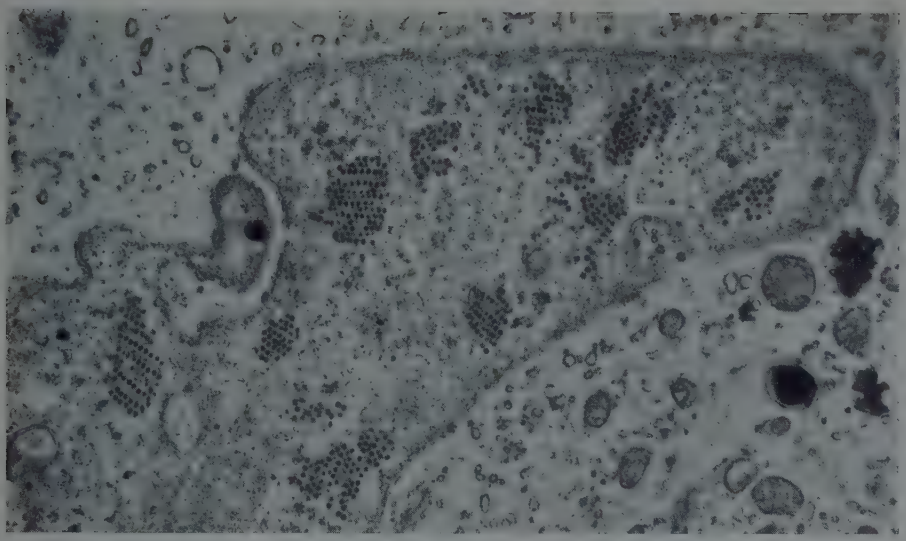

Fig. 1. – Enteric simian virus grown on cultures of monkey kidney cells. Ultra-thin section (Electron photograph by Archetti, Bocciarelli and Toschi, Istituto Superiore di Sanità, Roma). Several orderly arranged groups of virus particles are seen inside the nucleus of a cell. The periodicity in the optical density of the particles is related to the angle that the plane of the section forms with the reticular planes.

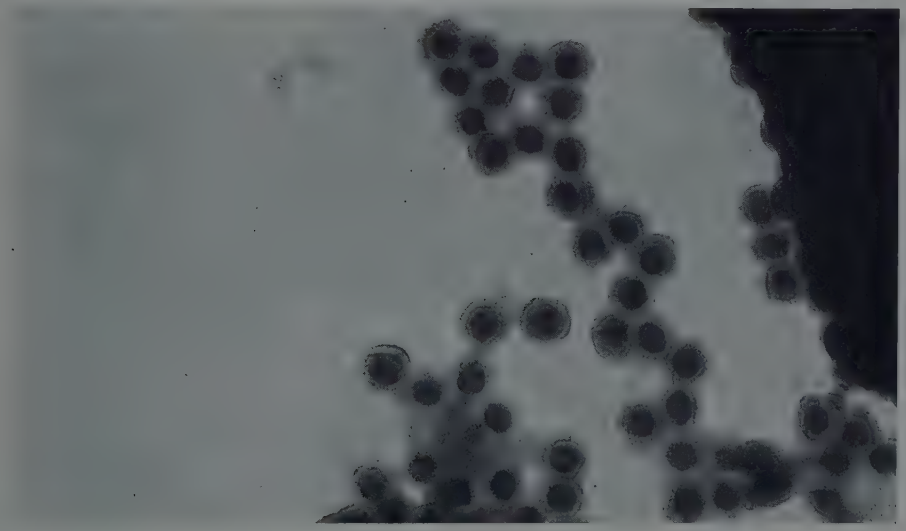

Fig. 2. – Enteric simian virus grown on cultures of monkey kidney cells. Staining with uranyl acetate (Electron photograph by Archetti, Bocciarelli and Toschi, Istituto Superiore di Sanità, Roma). The nucleus, more strongly stained, and the protein coat are clearly visible.

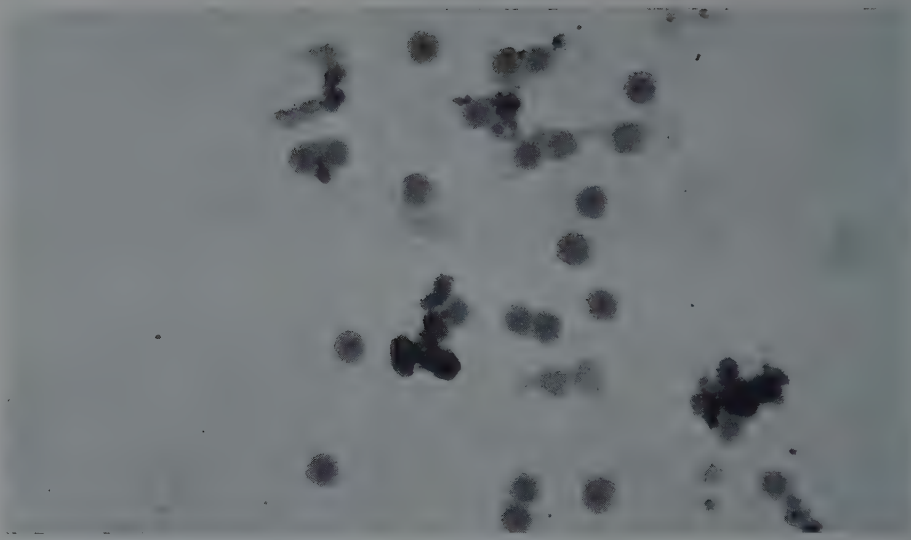

Fig. 3. – Enteric simian virus grown on cultures of monkey kidney cells. Freeze-drying technique. (Electron photograph by Archetti, Bocciarelli and Toschi, Istituto Superiore di Sanità, Roma). The hexagonal shape of the icosahedron is clearly visible both in the coat and in the nucleus.

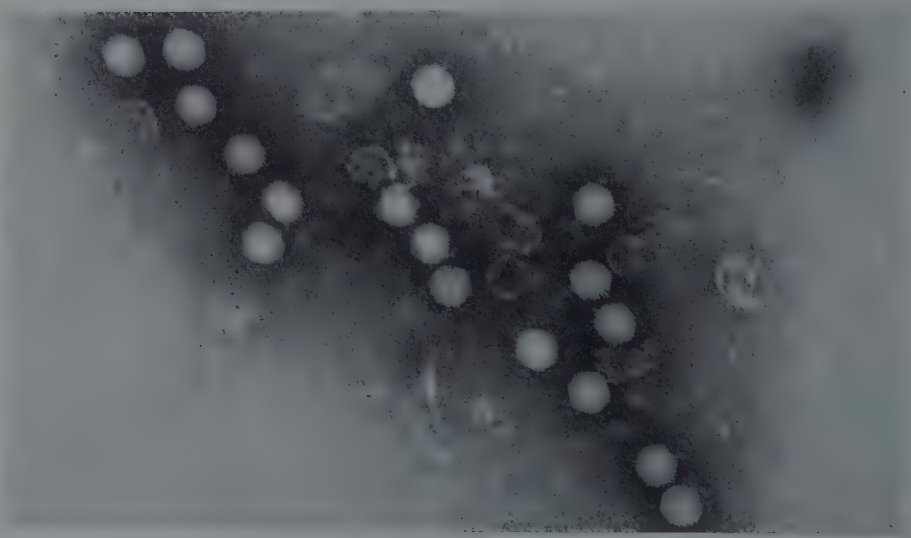

Fig. 4. – Enteric simian virus grown on cultures of monkey kidney cells. Negative staining with phosphotungstic acid (Electron photograph by Archetti, Bocciarelli and Toschi, Istituto Superiore di Sanità, Roma). Several hexagonal shaped particles and some ghosts of the same shape are visible.

Fig. 5. – Temperate phage α active on *B. megatherium*. Negative staining with phosphotungstic acid. (Electron photograph by Aurisicchio, A. Chiozzotto, Coppo, Donini, Frontali and Graziosi, Istituto Superiore di Sanità and Institute of Microbiology of the University of Rome). Here also a great amount of particles and some ghosts of the same hexagonal shape can be seen.

Fig. 6. – Enteric simian virus grown on cultures of monkey kidney cells. Negative staining with phosphotungstic acid (Electron photograph by Archetti, Bocciarelli and Toschi, Istituto Superiore di Sanità, Roma). The protein units of the coat with hexagonal symmetry can be seen.

If the hexagon of the base is regular ($n_1 = n_2 = n_3 = n$) the expression is reduced to

$$2(3n^2 - 3n + 1) + 6(n - 1)(2n_4 - 1) . \tag{5}$$

It can be noted that the beads placed on the lateral surface of the hexagonal prism, here considered, appear to be arranged like in a spiral. This corresponds to what has been observed in some plant viruses having a rodlike shape with hexagonal section [12, 13].

Another shape, compatible with the foregoing conditions, is the orthogonal pentagonal prism, terminating with two pentagonal pyramids. On the contrary, the hexagonal bipyramid is not a permitted shape. From this point of view, it would be interesting to examine more in detail the shapes of the even numbered phages of the *T* series, which, on the basis of incomplete evidence, are generally believed to have the shape of a hexagonal prism terminating with two hexagonal pyramids [14].

7. – One of the most important consequences of the foregoing considerations concerns the size that a monolayer of a given shape can assume. As we have already mentioned, the volume which a monolayer encloses is always quantized.

Let us consider, for instance, the case of a virus of icosahedral shape. Since the size of the specific protein molecules is fixed, a complete series is actually possible of icosahedrons of increasing sizes. The icosahedrons of the same series differ from each other in the number n of protein sub-units along the edge of the polyhedron. The volume at the disposal of the nucleic acid varies, in this series, approximately with $(n - 2)^3$. Therefore, while n increases, the volume which the nucleic acid can occupy, as far as the protein coat is concerned, are proportional to the numbers

$$1 , \quad 8 , \quad 27 , \quad 64 , \quad 125 , \quad \ldots .$$

Not only is the volume quantized, but the differences between each volume and the following one are remarkable.

This explains how the particles of a given virus are all strictly identical. In fact, one must not forget that the mass of the nucleic acid is also a discrete variable. The nucleus of the virus particle will be generally made up either of a single molecule or, at most, of a very small number of molecules.

Let V_n be the volume enclosed by the outer shell, having n protein particles on each edge, u the volume of a molecule of nucleic acid and r the number of the molecules of nucleic acid for each virus particle; we shall have then

$$V_n \simeq ru . \tag{6}$$

However, even if we admit that this relation cannot be interpretated too strictly, since n and r are certainly very small numbers and V_n, as has already been said, varies very strongly when n increases by one, there will be in general, at most, a single pair of values $\bar{n}$ and $\bar{r}$ for which the relation is sufficiently satisfied. It is clear then that all the particles of the same virus will be of identical size and that there will be no trace of the variability that is observed in more complex organisms.

On the other hand, it should be noted that one can not exclude that (6) can be satisfied equally well by two different pairs of values for n and r. Then we should see virus particles of two different sizes mixed together. At first, we might be induced to think that we are dealing with two different viruses. Only a careful check of the identity of the biological characters of the two types could lead us to conclude that we are dealing with one kind of virus type.

We are finally confronted by a question of fundamental character. If the ideas developed here have any relation to reality, why are all the viruses not of the same shape? Why aren't they all of icosahedral shape, for example, which, as has already been mentioned, is certainly much favoured by surface tension?

It is certainly not possible, at present, to give a satisfactory answer to this question. Probably, there are several causes influencing the choice of the shape. First of all, relation (6) might have no solution for the icosahedral shape and might have one, for example, for the hexagonal prismatic shape. Secondly, it is possible to suppose that the spatial orientation of the bonds that can be established among the contiguous specific protein particles must be limited in some manner. This would clearly have a direct influence on the choice of the shape.

Even if these limitations should not exist, it seems, however, improbable that the same virus assume two distinguished shapes: one of them will always be more favoured than the other by surface tension.

In conclusion, the model proposed here is based essentially on the hypothesis that it is the protein coat which determines, from the geometrical and mechanical points of view, the shapes *a priori* possible for the particles of a virus, while the volume of the nucleus, the orientation of the possible bonds among the contiguous protein particles, and surface tension would define the choice of the specific shape.

* * *

I wish to thank very much Prof. Franco Graziosi for the long and interesting discussions on this subject and for his advice and suggestions and for having put at my disposal his electron micrographs.

I also thank very much, for this last reason, Prof. Archetti, Prof. Steve Bocciarelli and Dr. Toschi.

REFERENCES

[1] F. H. C. Crick and J. D. Watson: *Nature*, **177**, 473 (1956).
[2] F. H. C. Crick and J. D. Watson: *The Nature of Viruses* Ciba Fondation Symposium (London, 1957).
[3] R. W. Horne, S. Brenner, A. P. Waterson and P. Wildy: *Journ. Mol. Biol.*, **1**, 84 (1959).
[4] I. Archetti, D. Steve Bocciarelli and G. Toschi: this issue p. 176 and *Virology* (to be published).
[5] I. Archetti, D. Steve Bocciarelli and G. Toschi: *European Regional Conference on Electron Microscopy Delft*, 1960, *Acta* (to be published).
[6] S. Aurisicchio, A. Chiozzotto, A. Coppo, P. Donini, C. Frontali and F. Graziosi: this issue p. 179.
[7] M. Delbruck and W. T. Bailey: *Cold Spring Harb. Symp. Quant. Biol.*, **11**, 33 (1946).
[8] A. Novick and L. Szilard: *Science*, **113**, 34 (1951).
[9] G. Streisinger: *Virology*, **2**, 388 (1956).
[10] S. Brenner: *Virology*, **3**, 560 (1957).
[11] E. Kellenberger, J. Séchaud and A. Ryter: *Virology*, **8**, 478 (1959).
[12] R. C. Williams: *Bioch. Bioph. Acta*, **8**, 227 (1952).
[13] R. E. F. Mattews, R. W. Horne and E. M. Green: *Nature*, **178**, 135 (1956).
[14] T. F. Anderson, C. Rappaport and N. A. Muscatine: *Le Bacteriophage*, Premier Colloque International (Royaumont, 1952), p. 5.

SUPPLEMENTO AL VOLUME XVIII, SERIE X
DEL NUOVO CIMENTO

N. 2, 1960
4° Trimestre

Electron Microscopic Structure of a Simian Enteric Virus.

I. ARCHETTI, D. STEVE BOCCIARELLI and G. TOSCHI

Istituto Superiore di Sanità - Roma

The development and the structure of a simian enteric virus (SV39) belonging to the family of adenoviruses, which had been isolated by ARCHETTI, has been studied with the electron microscope. The development of the virus was studied on sections of cultivated monkey kidney cells, and the free viruses were observed after purification with freon-heptane [1] and high speed centrifugation. Further purification was used when preparing the virus for freeze-drying or for staining with uranyl-acetate; it consisted of treatment with deoxycholate followed by centrifugation in a density gradient and chromatography on DEAE-cellulose.

The results on the relation of virus to the host cell will be reported elsewhere; this article concerns the structure of the virus itself. This can be better observed on free viruses than on sections of infected cells, on account of the higher resolution that is obtained when working with a thinner specimen.

Nevertheless it is useful to include Fig. 1, to give some information about the aspect that the virus has in the sections. This shows the appearance of clusters of virus in the nucleus of an infected cell; the particles have a crystal-like array, similar to that observed by MORGAN and his colleagues [2] with viruses of the RI-APC group. The formation of these crystal patterns is not simultaneous with the appearance of virus in the cell, but they are easily found in later stages of the infection, when the nuclear matrix begins to rarefy and dissolve. When, still later, the nuclear membrane begins to fragment and the nucleus to disrupt, the ordered clusters disgregate, showing that the forces acting between virus particles to form these ordered structures must be very weak.

The particles do not show here a sharp geometrical form, but a hexagonal profile can be recognized and it is possible to see that, in the ordered clusters viral particles exhibit a characteristic orientation.

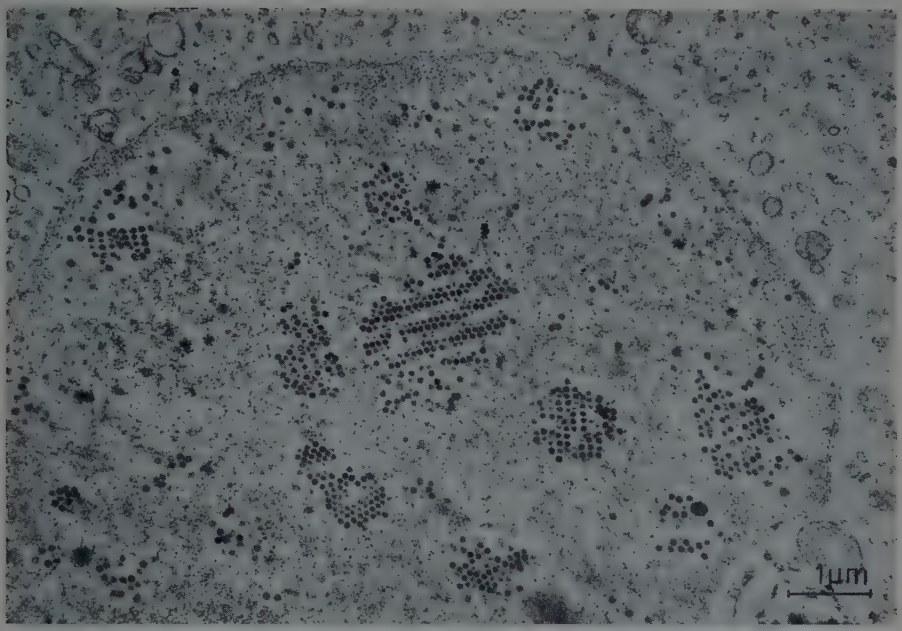

Fig. 1. – Crystal-like arrangement of virus in the nucleus of an infected cell.

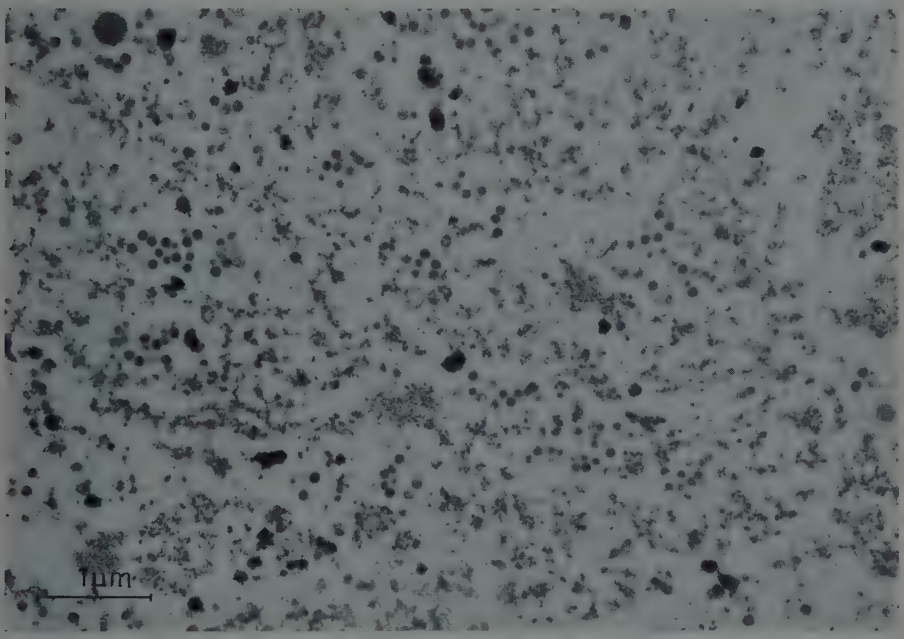

Fig. 2. – Clusters of virus in the nucleus of a cell: two types of virus are seen: the dense and the transparent ones.

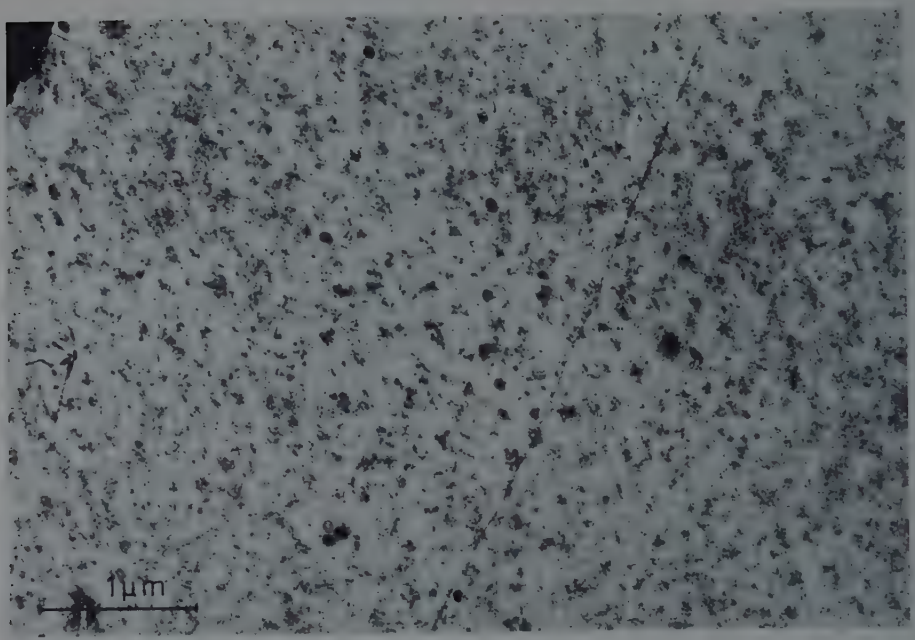

Fig. 3. – Nucleus of a cell fixed a few hours after infection.

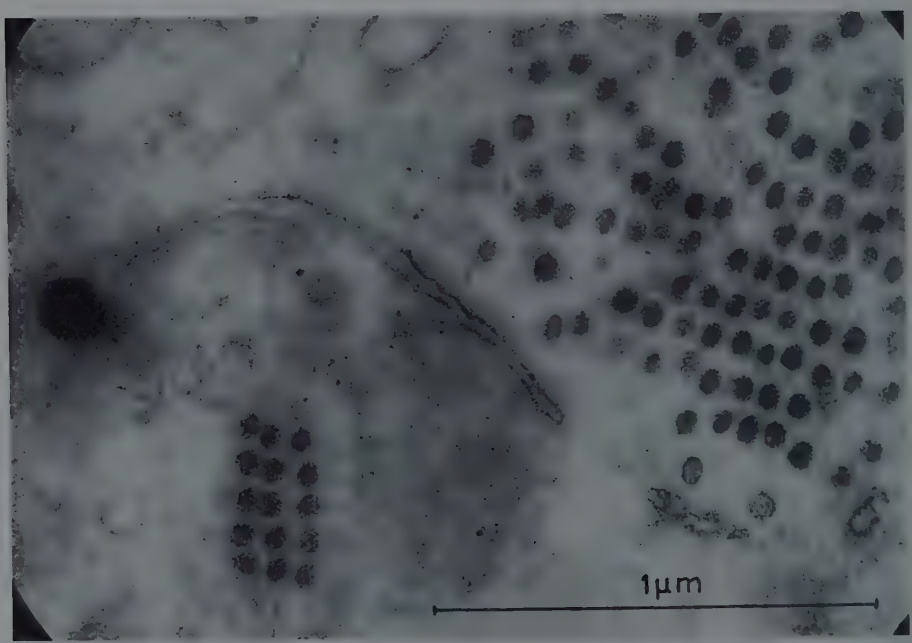

Fig. 4. – Section of an infected cell at high magnification: viruses are seen in and outside the nucleus.

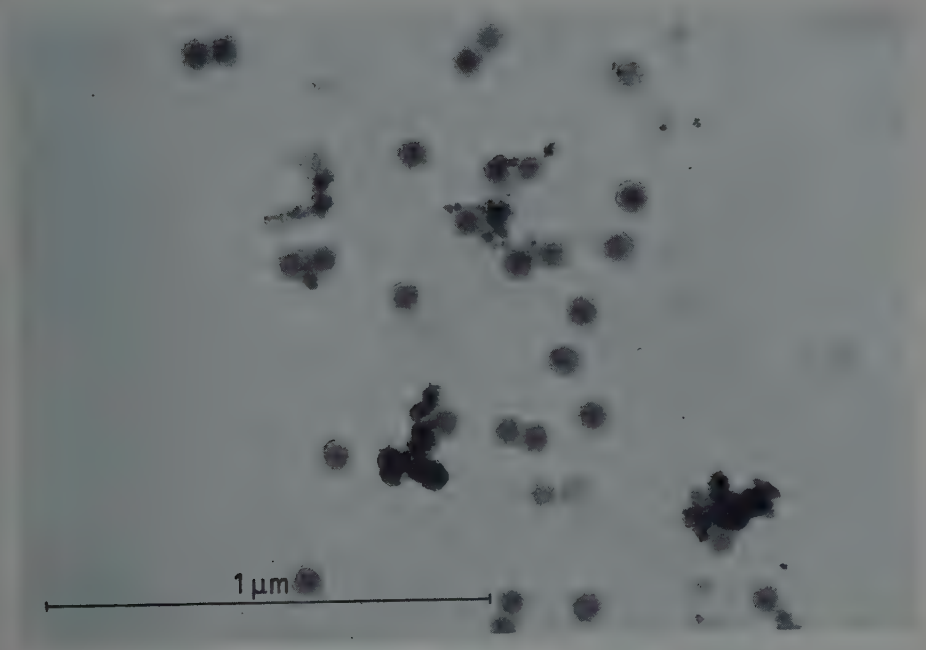

Fig. 5. – Virus particles prepared with freeze-drying method, deposited on a carbon film.

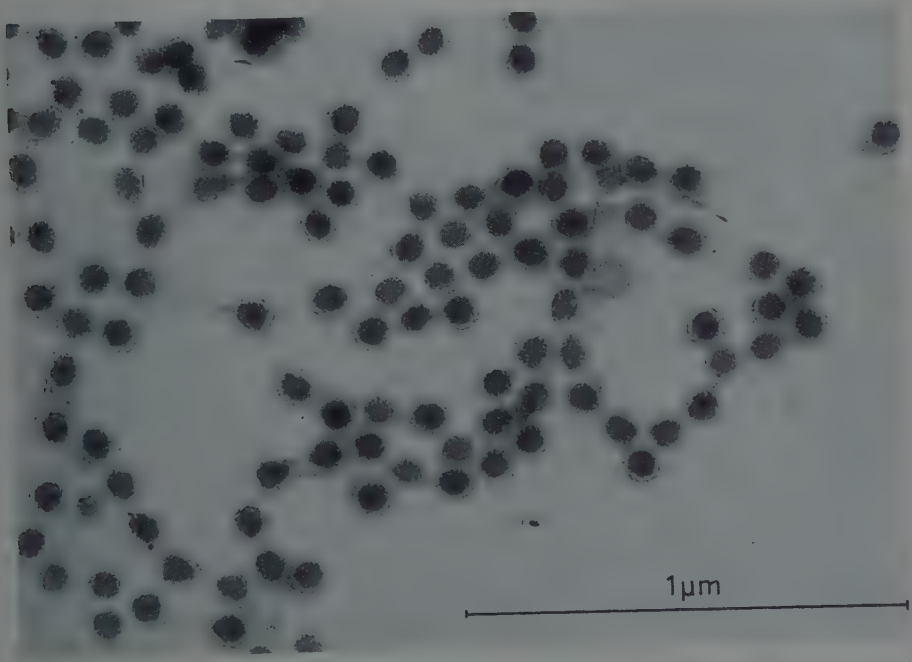

Fig. 6. – Virus particles stained with uranyl-acetate and deposited on carbon film.

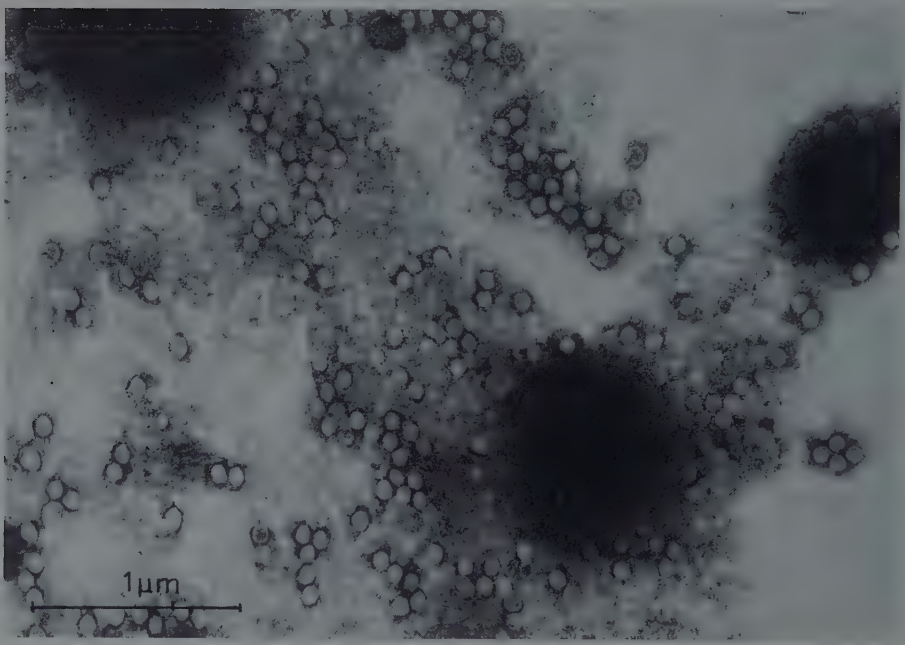

Fig. 7. – Virus particles in potassium phosphotungstate.

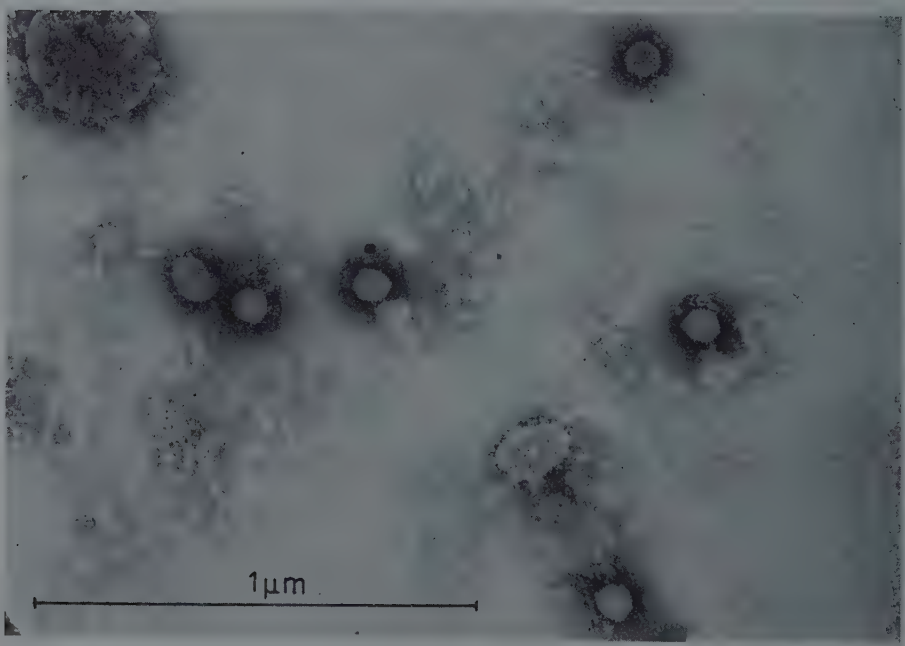

Fig. 8. – Virus particles in potassium phosphotungstate.

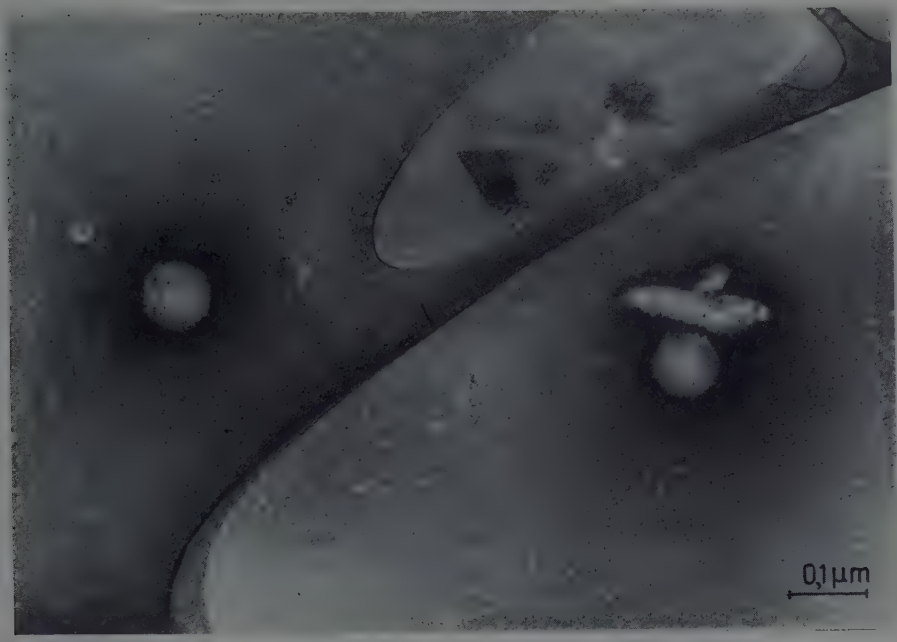

Fig. 9. – Virus particles in potassium phosphotungstate.

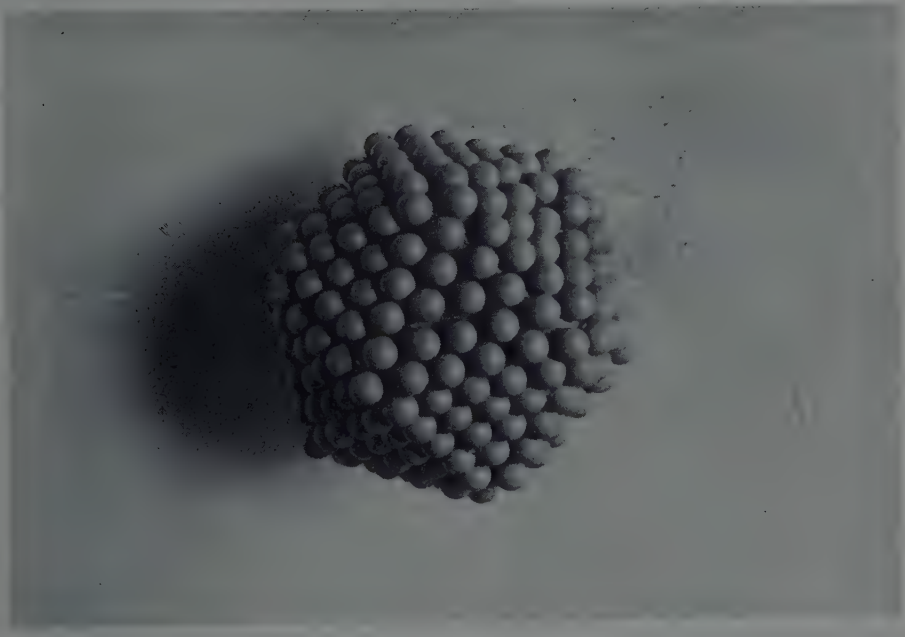

Fig. 10. – A tentative model of the virus.

The particles appear to consist of at least two different types (Fig. 2); the majority of them are uniformly dense, whilst a few are transparent, with or without a small central body with no definite structure and no constant opacity. The appearance of sections of cells fixed a few hours after infection suggests that these transparent viruses are incomplete particles which are just forming from the nuclear matrix (Fig. 3).

Sections observed at higher magnification do not give more information, as the thickness of the section (at least (200÷300) Å) prohibits good resolution. The specimen shown in Fig. 4 was stained with uranyl-acetate and phosphotungstic acid to emphasize the contrast. In spite of the fact that the particles are poorly defined, their polygonal shape is apparent. A far better resolution is reached on particles deposited on a carbon film about 50 Å thick, as in Fig. 5, and observed after freeze-drying without fixation or staining.

Using comparatively low voltage at the electron microscope (60 kV) and preparing virus with the freeze-drying method, which avoids the deformation presented by particles dried on a film, it is possible to see, not only the polygonal profile of the particle, but also an internal core which is denser than the outer part. The diameter of the internal core is about half that of the outer shell. The external diameter is about 750 Å.

Fig. 6 shows virus particles fixed with osmium tetroxide, stained with uranyl-acetate, suspended in water, and deposited on the carbon film. In this case the particles dry on the supporting film and adhere strongly to it, and become flattened. Although they are markedly distorted, it is easy to recognize the hexagonal profile of the internal core, which is heavily stained, and the outer shell which appears thinner than in Fig. 5.

Provided that uranyl-acetate is a selective stain for nucleic acid, the internal core contains for the most part nucleic acid. The particles show a granular surface. The best method for observing the details of this surface is the negative staining method [3], using potassium phosphotungstate. In Fig. 7 it is evident that the structure of the virus particles is not uniform: some of them are apparently complete, others seem to be partially disrupted and still others appear as empty shells. The complete particles show a clear sub-unit structure (Fig. 8). In accordance with sections, the incomplete particles could be the youngest ones.

With a higher resolution, it is possible to decide that the complete virus has a polyhedral form, which probably is an icosahedron, as HORNE and his colleagues found in adenoviruses [4], and its surface is covered with granules disposed in a reasonably regular fashion. If the internal core is made up of nucleic acid, it is probable that the outer coat is made up of protein molecules. These molecules appear globular and are (50÷60) Å in diameter.

In Fig. 9 a pair of highly magnified, negatively stained particles show that the coat structure seems to have a six-fold symmetry. The arrangement of

the sub-units, as it appears in the pictures, is not sufficiently well defined to make possible a definite reconstruction of the surface pattern. The sub-units seem to be not on the edges of the icosahedron, but adjacent to them, five along each edge. A tentative model built according to the above specification is shown in Fig. 10.

From these first observations it may be concluded that SV39 virus has an internal core, probably of nucleic acid, and an outer shell consisting of globular molecules. The external diameter of the virus particle is from 700 to 800 Å, the internal core is about 400 Å and the sub-units (50÷60) Å.

The internal core and the outer shell have a polyhedral shape, which is almost certainly a regular icosahedron. The disposition of the sub-units on the external coat seems to differ from that found by Horne *et al.* in a human adenovirus [4].

These observations will be extended in order to be able to decide on the arrangement of the sub-units.

* * *

It is a pleasure to acknowledge the capable technical assistance of A. Chiozzotto, F. Piccirilli, N. Tomassini and F. Valente.

REFERENCES

[1] A. C. Gessler, C. E. Bender and M. C. Parkinson: *Trans. N. Y. Acad. Sci.*, **18**, 701 (1958).
[2] C. Morgan, C. Howe, H. M. Rose and D. H. Moore: *Journ. Bioph. Bioch. Cyt.*, **2**, 351 (1956).
[3] S. Brenner and R. W. Horne: *Bioch. Bioph. Acta*, **34**, 103 (1959).
[4] R. W. Horne, S. Brenner, A. P. Waterson and P. Wildy: *Journ. Mol. Biol.*, **1**, 84 (1959).

SUPPLEMENTO AL VOLUME XVIII, SERIE X
DEL NUOVO CIMENTO

N. 2, 1960
4° Trimestre

Molecular Autoradiography Performed by Means of Ilford and Nikfi Emulsions in Gel Form.

S. AURISICCHIO

Istituto di Microbiologia dell'Università - Roma

A. CELANO and R. RINZIVILLO

Istituto di Fisica Superiore dell'Università - Napoli
Istituto Nazionale di Fisica Nucleare - Sottosezione di Napoli

1. – LEVINTHAL and THOMAS [1] in 1957 and later AURISICCHIO *et al.* [2], studied a number of properties of bacteriophages by means of the method known as « molecular autoradiography ».

This method consists of the following steps. The particles to be studied are prepared so that one element of them be marked with a known percentage of β-active atoms: it is necessary that any particle includes so many radioactive atoms as to emit in average several electrons in an exposure time not too long (exposure times between 5 and 100 days are suitable). A β-sensitive photoemulsion is prepared with a liquefied « gel », in which a suspension of the particles of interest has been included. After a convenient period of exposure the plate is processed. The emulsion is scanned looking for the « electron stars » (Fig. 1*a*) and for each star the number of prongs is counted: each star is associated with one of the particles which are the object of the experiment and each prong is produced by one electron. It is then easy to calculate, from the number of prongs, the original probable number of marked atoms in each particle and then to calculate the total number of atoms of that particular element in each particle. It is seen that—at least in principle—this method is a strong instrument for studying the structure of microscopic and submicroscopic particles and of their transformations, and that it is possible to apply it to biological materials (viruses, bacteria) as well as to chemical materials (macromolecules).

However, in practice the method is rather difficult to apply. Indeed the

β-tracks (electrons in the range of 1 MeV or less) are very difficult to observe, as they have minimum ionization and very high multiple scattering. Therefore, one may meet easily an emulsion which is suitable for studying minimum tracks of high energy (which are straight) and, at the same time, is not suitable for counting and following the β-tracks.

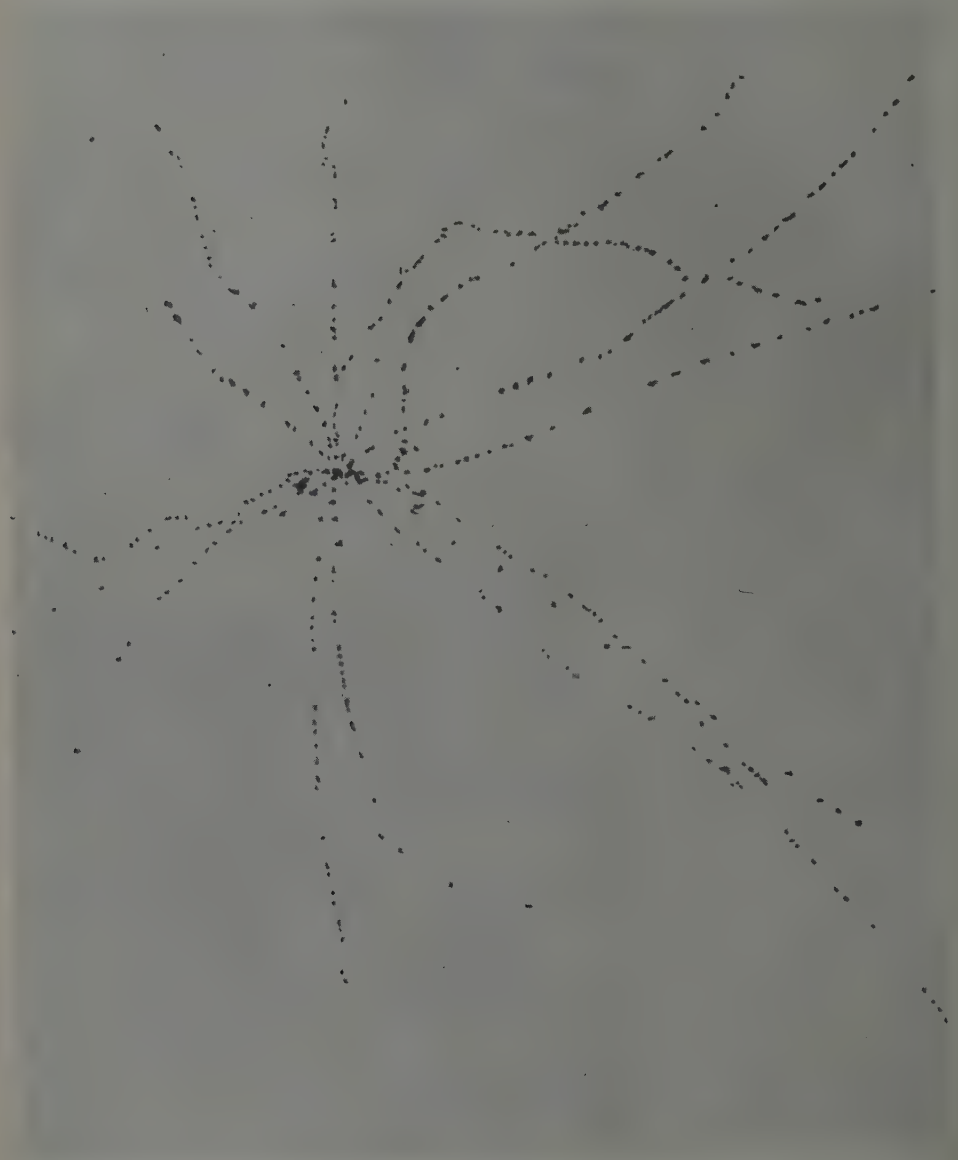

Fig. 1*a*.

1166

In conclusion, the emulsion is really « β-sensitive » only if it has excellent qualities with regards to the sensitivity and to the chemical background. In this paper we report about processing facilities and a processing method in which all the factors which are of importance in the several steps of the work (preparation of the plates from gel, exposure, developing and so on) are controlled as strictly as possible, in order to obtain the best possible results.

2. – If one wants to find the best possible conditions, many tries are necessary, any of which requires several days of work, with the inconvenience that only at the end of the processing one may receive some useful information. Therefore, it is very important that one—at least at the end of the process—be able to obtain quickly a quantitative measurement of the results. We employed two methods which we will call « of thorium stars » and « of blob counting ».

2·1. – The first method requires to mix to the liquid gel a given quantity of thorium salt (besides the suspension of phages); and to measure the mean number of electrons coming out from « thorium stars » with 4 and 5 α-prongs (Fig. 1*b*). As is described in Appendix I, a thorium star is associated with

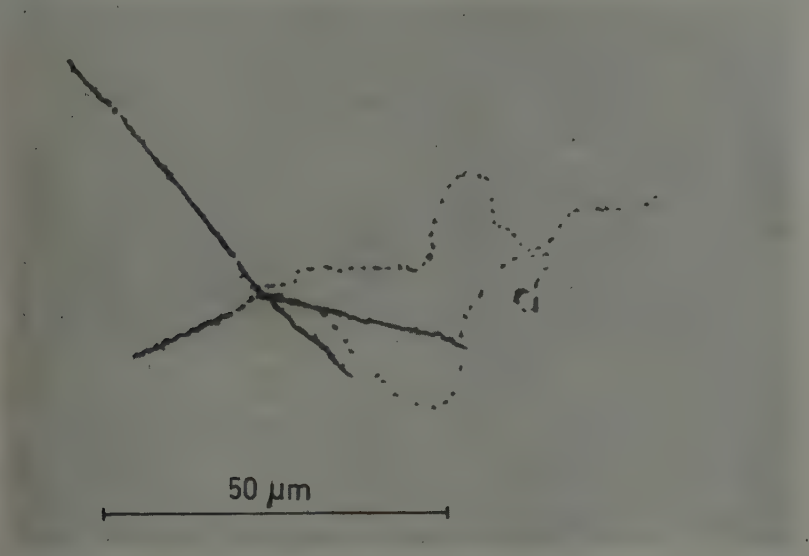

Fig. 1*b*.

the emission of 0 to 4 electrons (β-rays or conversion electrons). It is possible to calculate the expected mean number of the emitted electrons, once given the value of the exposure time.

After that, the ratio of experimental mean electron number to the expected one gives a direct measurement of the efficiency of the emulsion, considered as a β-ray detector. This measurement takes into account all of the involved factors, including the geometrical ones. For a number of plates we performed this efficiency measurements using at least 100 thorium stars.

The described method is the most direct and suitable one and has the advantage to give at the same time some indication about the uniformity of the dispersion of the studied particles inside the emulsion. It has however two weak points: it requires a rather long scanning work (otherwise the thorium background will be too heavy) and secondly it allows no direct comparison with the usual evaluations of the emulsion sensitivity. The last ones are based on the measurements of the blob density H along minimum tracks.

2·2. – As we worked with radiophosphorum (^{32}P) we tried to reach this aim by blob counting along the « fast » electrons (kinetic energy $E > E_0 = 0.5$ MeV) which are at the minimum of ionization and are rather numerous in the ^{32}P spectrum. For this it is necessary to select these fast tracks, by means of a method which must be quick and very efficient. In Appendix II a simple selecting rule is described, which is based on a rough measurement of the multiple scattering; it requires only some 10 min in order to find out

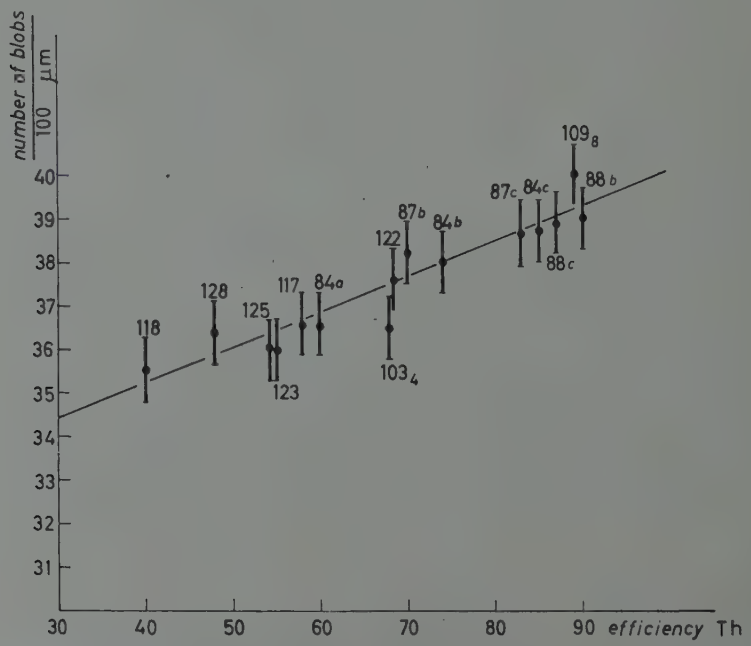

Fig. 2. – Experimental correlation on the efficiency measurements obtained with the thorium star method and the blob measurements.

a « good » track (for a normal exposure), and selects the good tracks with a probability $> 90\%$, for the ^{32}P spectrum. For every plate we performed 10 blob density measurements on 10 tracks which had been selected with this rule. The obtained values of H were consistent between them and showed no dependence on the depth in the emulsion for several plates. Fig. 2 shows the correlation between the direct efficiency measurements, obtained with the thorium star method, and the blob measurements. The reported errors are the statistical ones. The correlation is good.

3. – By means of the described methods we studied the influence of almost all of the factors which are of interest in the preparation and processing of the plates, looking for the best possible conditions. Most of the work was done with plates (or pellicles) 150 μm thick prepared from Ilford G-5 gel, but we worked also in very different conditions. During the preparation of the plates we took great care in order that the gel was always at low temperature (~ 5 °C), that it came in direct contact only with glass containers, that a time as short as possible elapsed before liquefying it by heating (at ~ 50 °C). A very small quantity (~ 0.1 cm^3) of liquid containing the phage suspension and the thorium salt was added just before heating and the mixing was obtained by rotating back and forth continuously, and for some time, the container, without stirring. Then the liquid gel was poured on a prepared Ilford glass which was placed on a horizontal glass surface and kept at a temperature of about 30 °C. This surface was included in a box containing the evaporator of a freezer. The box was closed and the first step of the drying was accomplished by means of the cold wall principle. When the plates were almost dry, they were kept in another box with an appropriate solution of sulphuric acid, until they reached equilibrium conditions at 5 °C and 40% humidity. Then each plate was closed in a small polythene bag and the latter was put in a box with copper walls 4 cm thick, in order to reduce the local radioactivity background. This box was kept at 5 °C during all the exposure time.

The processing was performed with the classical temperature method by DILWORTH *et al.* [3]. Details are given in Appendix III. We note here three points: 1) the pH of the developer was rather high (7.4); 2) no dilution was made at the beginning of the hot stage of development; 3) the latter was performed at a rather high temperature (~ 28 °C).

We note also that a considerable quantity of Ag ions (3 g for one liter of fixing solution) is necessary in order to prevent the corrosion of the developed grains.

4. – By means of these techniques we obtained plates with very high values of H. In the best plates we reached 40 blobs/100 μm with a background of

5.2 grains/1 000 μm^3. These figures are equivalent to those obtained with the best G-5 plates. A standard figure is 39 blobs/100 μm.

From Fig. 2, one can also see that the β-ray counting efficiency in a standard plate is high, so that this technique can be used with confidence. Indeed, it was successfully used in some experiments on bacteriophages [4].

5. – In the last time we had an opportunity of trying an amount of Nikfi emulsion kindly sent to us by Professor C. S. BOGOMOLOV through Professor H. G. DE CARVAHLO. We followed the same preparation technique described above. When drying the poured emulsion, a strong tendency was observed to detachment from the glass. We succeeded in preventing this inconvenience by pouring some mineral oil over the edges of the plates as soon as they became dry. The processing was performed by the methods suggested by OUVAROVA *et al.* [5]. We obtained excellent results: over 90% efficiency with negligible background.

6. – We are very glad to express our warmest thanks to G. CORTINI for his continuous help in performing this work, to H. G. DE CARVAHLO and to F. GRAZIOSI for many valuable discussions, to Mrs. F. SPERA-CATELLI for much laboratory and calculation work and to Miss A. DE SANTIS for microscope work. We are very indebted to Prof. C. S. BOGOMOLOV who kindly provided us with the Nikfi gel and to H. G. DE CARVAHLO who painfully transported it from Moscow to Naples. A great part of the processing facilities was put at our disposal by the Divisione Biologica of the Comitato Nazionale delle Ricerche Nucleari to which we express our deepest thanks.

APPENDIX I

The « thorium stars » method.

It is well known that the « thorium stars » take their origin from ^{228}Th (« radiothorium »), which is α-radioactive and gives a succession of unstable (α or β) nuclei with short mean lives [6]. In the processed emulsion the number of α and β tracks are seen, coming out (approximately) from a same center. The complete development of the radioactive chain gives 5 α-prong stars. But also 4 α-prong stars can come out from a chain which begins from ^{224}Ra or from a chain which stops at ^{212}Pb. These possibilities are illustrated in Fig. 3 which indicates the complete chain (Fig. 3*a*), a simplified version of it, in which the steps with very short mean lives are passed over and a branching of negligible probability is eliminated (Fig. 3*b*) and a sketch (Fig. 3*c*) of the three

possible types of stars, which can be classified giving the numbers of α and β prongs: $(4\alpha, 0\beta)$, $(4\alpha, 2\beta)$ and $(5\alpha, 2\beta)$. The probabilities of any other type (for reasonable exposure time) are negligible.

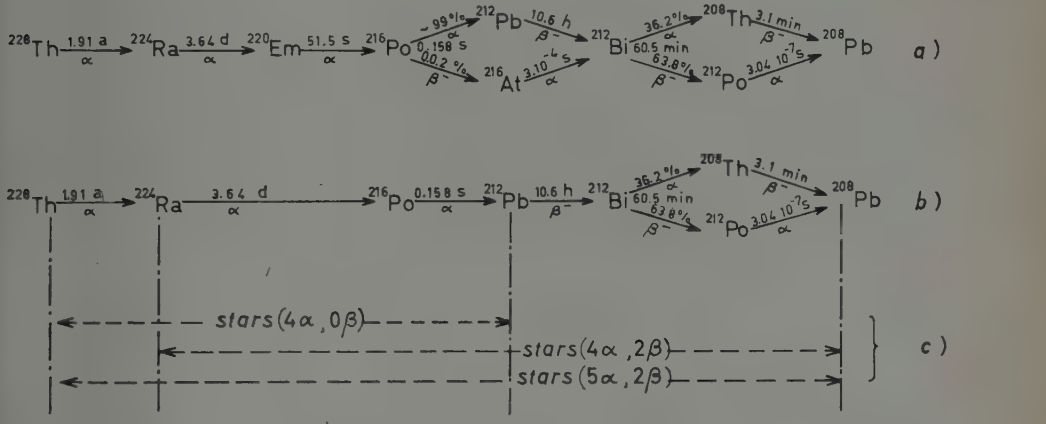

Fig. 3. – Radioactive chain of ^{228}Th.

Let now S_4^0, $S_4^2(t)$ and $S_5(t)$ be the numbers of $(4\alpha, 0\beta)$ stars $(4\alpha, 2\beta)$ stars and $(5\alpha, 2\beta)$ stars, respectively, after an exposure time t. We will put: $S_4 = S_4^0 + S_4^2$, and $S = S_4 + S_5$: Besides, let N_1 be the number of ^{228}Th atoms, and λ_1, λ_2, λ_3, respectively, the disintegration constants of ^{228}Th, ^{224}Ra and ^{212}Pb. We have (see Fig. 3) $\lambda_1 \ll \lambda_2$, λ_3 and $\lambda_1 t \ll 1$. Therefore, we can simplify the known formulae of the radioactive decay, and we get

$$(1) \qquad S_4^0 = \frac{N_1}{\lambda_3}\left[\lambda_1 + \frac{\lambda_1\lambda_3}{\lambda_2 - \lambda_3}\exp\left[-\lambda_2 t\right] - \frac{\lambda_1\lambda_2}{\lambda_2 - \lambda_3}\exp\left[-\lambda_3 t\right]\right],$$

$$(2) \qquad S_4^2 = \frac{N_1\lambda_1}{\lambda_2}\left[\frac{\lambda_2}{\lambda_3 - \lambda_2}\exp\left[-\lambda_3 t\right] - \frac{\lambda_3}{\lambda_3 - \lambda_2}\exp\left[-\lambda_2 t\right] + 1\right],$$

$$(3) \qquad S_5 = N_1\lambda_1\left[t - \frac{\lambda_2 + \lambda_3}{\lambda_2\lambda_3} + \frac{\lambda_3}{\lambda_2(\lambda_3 - \lambda_2)}\exp\left[-\lambda^2 t\right] - \frac{\lambda_2}{\lambda_3(\lambda_3 - \lambda_2)}\exp\left[-\lambda_3 t\right]\right].$$

The total number of 4 and 5 α-prong stars is therefore

$$(4) \qquad S(t) = N_1\lambda_1\left[t + \frac{1}{\lambda_3 - \lambda_2}\exp\left[-\lambda_3 t\right] - \exp\left[-\lambda_2 t\right]\right] \to N_1\lambda_1 t\,.$$

Eq. (4) is useful in order to determine the Th quantity to be introduced into the emulsion, once given the exposure time.

From eq. (1) to (3) one sees that the ratio $S_4^0/S_4^2 = \lambda_2/\lambda_3$ is constant, while the ratio S_4/S_5 is a decreasing function of the exposure time t.

Thus, we must only calculate the mean numbers $n_e(4)$ and $n_e(5)$ of electron

prongs coming out from the $(4\alpha, 0\beta) + (4\alpha, 2\beta)$ and from the $(5\alpha, 2\beta)$ stars, respectively, and then combine them in order to obtain the mean number of electrons from all the stars. The result

$$n_e(t) = n_e(4)\,\frac{S_4}{S_4 + S_5} + n_e(5)\,\frac{S_5}{S_4 + S_5}\,,$$

is obviously a function of t.

In order to calculate $n_e(4)$ and $n_e(5)$ we took into account the conversion electrons emitted (i) in the ^{228}Th decay to the excited state of 84 keV of ^{224}Ra (conversion coefficient $\alpha = 12$) [7]; (ii) in the disintegration ThC $\rightarrow$ ThC' which gives conversion electrons of 148 keV [8]; (iii) and in the double disintegration

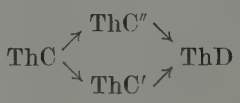

where in the 20% of ThC disintegrations we have conversion electrons of 25 keV.

We neglected Auger electrons which give $\sim$1% contributions [9].

In order to eliminate a rather high number of low energy conversion electron, not very well known, and not clearly seen in the confusion existing very near the center of the star, we put a cut-off at a range of 16 μm equivalent to $\sim$ 50 keV [10]. Of course, this gives a small loss of β-rays, which was roughly calculated, from the known spectra [11].

After that, one must combine, for every type of star, the probabilities of conversion electron emission with those of β-ray loss, so to obtain the probabilities that the total number of electron-prongs be any given number between 0 and 4 (a 5 electron event having negligible probability).

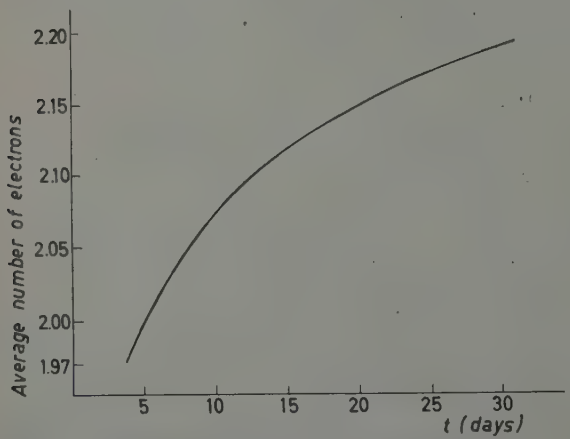

Fig. 4. – Average number of electrons deriving from thorium stars with 4 and 5 α-prongs.

We found $n_e(4) = 1.87$, $n_e(5) = 2.27$. For an exposure time $t \geqslant 5$ days, $n_e(t)$ varies from 1.97 to 2.20 (see Fig. 4).

As explained in the text the efficiency is obtained from the comparison of $n_e(t)$ with the experimental mean number of electron prongs (account being taken of the 16 μm cut-off).

APPENDIX II

The « blob counting » method.

The aim of this method is to get quickly a quantitative estimate of the quality of an emulsion. It consists of two stages: (i) a minimum track ($E > E_0 = 0.5$ MeV) is selected, and (ii) the blob density of the selected track is measured. The stage (ii) is performed by the known standard methods [12]. The stage (i) runs as follows. The plate is scanned looking for a track which appears to be promising (rather straight, with a small dip angle).

An eyepiece reticule having two scales crossing each other at right angles is then used to perform a rough scattering measurement. One of the scales determines the measurement cell: the extreme points of it are superposed to two points of the considered track. The deviation from a straight line *at the center of the cell* is then measured on the second scale. We use a cell length of 29 μm, while a division of the measurements scale is $d_0 = 0.77$ μm. We express the result of a measurement by means of the number n of divisions which gives an (excess) approximation of the observed direction. The stage is then moved so that a next section of the track is superposed to the measurement cell, a new measurement is made, and so on.

In order to select a track as a « good » one we require that

$$n_i \leqslant N_i\,, \qquad (i = 1, 2, \ldots, k)\,, \tag{1}$$

N_i being an established succession of k integral numbers, and n_i the results of k measurements made on successive cells.

Let us see how this method allows the selection of good tracks.

Once fixed the cell length, one can determine, for any given energy E the mean probable value $\bar{D}(E)$ of the deviation D (of an electron track) from a straight line, produced by the multiple scattering [13]. The distribution of the D's is approximately Gaussian (excluding the very large values of D). With this approximation, we can easily calculate, from $\bar{D}(E)$, the probability $p(E, D)\,\mathrm{d}D$ that the result of a given measurement falls in the interval $(D, \mathrm{d}D)$. Now, let $D_i = N_i d_0$ $(i = 1, 2, \ldots, k)$ be a fixed group of lengths, and put

$$P_i(E) = \int_0^{D_i} p(E, D)\,\mathrm{d}D\,, \qquad (i = 1, 2, \ldots, k)\,, \tag{2}$$

$$P_{1,2,\ldots k}(E) = P_1(E) \cdot P_2(E) \ldots P_k(E)\,. \tag{3}$$

Now, if we make a measurement on a random electron coming out from a nucleus, whose spectrum $F(E)$ is known, and if the obtained results satisfy eq. (1), then the probability that the so selected track be of energy $E < E_0$,

will be

$$\Pi_{1,2,\ldots k} = \frac{\int_0^{E_0} P_{1,2,\ldots k}(E) F(E)\,\mathrm{d}E}{\int_0^{\infty} P_{1,2,\ldots k}(E) F(E)\,\mathrm{d}E} .$$

Using the known [14] spectrum of ^{3}P, we calculated $\Pi_{1,2,\ldots k}$ for several possible groups of integral numbers $N_1, N_2, \ldots, N_k$. We found that a good compromise can be found between the two opposite requirements: quickness and efficiency. Two possible rules that we tried are: $k = 2$, $n_1 = n_2 = 1$, and $k = 3$, $n_1 = n_2 = n_3 = 1$. For ^{32}P we get

$$\Pi_{11} = .065 , \quad \Pi_{111} = .038 , \tag{4}$$

In practice the choice between these two rules is not very important. Indeed, after the selection, the blob density measurement is made along the track for a length of ~ 290 μm, in order to count ~ 100 blobs; if a strong scattering increase is found, the track is discarded, and with this added rule the selection becomes practically complete.

The experimental results are in agreement with eq. (4). No strong error is introduced by two opposite disturbing effects: (i) the preselection of « promising » tracks, and (ii) the energy loss between the origin of an electron and the measured section of its track. This last effect is small, due to the limited thickness of the emulsion layer.

Appendix III

Processing procedure.

A) *Composition of baths.*

Developing bath	Sodium sulphite	g	24
	Potassium bromide	g	0.8
	Amidol	g	4.5
	H_2O to	cm^3	1000
Stop bath	2% acetic acid solution		
Fixing bath	Hypo	g	400
	Silver chloride	g	4
	H_2O to	cm^3	1000

B) Procedure.

Wetting in distilled water	1 h at 5 °C
Developing bath, cold stage	1 h at 5 °C
Developing bath, hot stage	20 min at 28.5 °C (*)
Stop bath	1 h at 5 °C
Washing in distilled water	1½ h at 5 °C
Fixing bath	(15÷18) h at 12 °C
Washing in tap water	to elimination of hypo.

(*) This temperature can be slightly changed after proof processing of any new gel batch.

REFERENCES

[1] C. Levinthal and C. A. Thomas Jr.: *Biochem. et Biophys. Acta*, **23**, 453 (1957).
[2] S. Aurisicchio, G. Cortini, V. Emma and F. Graziosi: *Intern. Journ. Rad. Biology*, **1**, 86 (1959).
[3] C. Dilworth, G. Occhialini and G. P. S. Payne: *Nature*, **162**, 102 (1948).
[4] A. Celano, R. Rinzivillo, S. Aurisicchio, A. Coppo, F. Donini and F. Graziosi: *Unusual biophysical properties of the phage* (in this same issue).
[5] V. M. Ouranova, T. Krestovnikova, V. A. Myltseva and K. M. Romanovskaia: *Photographie corpusculaire*, vol. **2** (Montreal, 1959), p. 167.
[6] See *Rev. Mod. Phys.*, **30**, no. 2; two parts (1958).
[7] C. Victor, J. Teillac, P. Falk-Vairant and G. Bouissieres: *Journ. Phys. et Rad.*, **13**, 565 (1952).
[8] A. Flammersfeld: *Zeits. Phys.*, **114**, 227 (1959).
[9] I. Bergstrom: in *β- and γ-Ray Spectroscopy* (Amsterdam, 1955), cap. xx, p. 624.
[10] P. Demers: *Photographie: les emulsions nucléaires* (Montreal, 1955-58), p. 252
[11] K. Siegbahn and T. R. Gerholm: in *β- and γ-Ray Spectroscopy* (Amsterdam, 1955), p. 920.
[12] See for instance: M. Shapiro: *Handb. Phys.*, **45**, 342 (1958).
[13] See for instance: M. Shapiro: *Handb. Phys.*, **45**, 372 (1958).
[14] E. N. Jensen, R. T. Nichols, J. Clement and A. Phom: *Phys. Rev.*, **85**, 112 (1958)

SUPPLEMENTO AL VOLUME XVIII, SERIE X
DEL NUOVO CIMENTO

N. 2, 1960
4° Trimestre

Unusual Biophysical Properties of the Temperate Phage α (*).

A. Celano

Istituto Nazionale di Fisica Nucleare - Sottosezione di Napoli
Istituto di Fisica Superiore dell'Università - Napoli

S. Aurisicchio, A. Coppo, P. Donini and F. Graziosi

Istituto di Microbiologia dell'Università - Roma

Temperate bacteriophages penetrate into the host-cells but, instead of reproducing and causing lysis, they enter in a symbiotic relationship with the host and become a part of its genome. These lysogenic cells appear to be quite stable with respect to this new property and only rarely lose the phage genome and the memory of the foregoing infection. The latter phenommen, called curing, has not been well studied up to the present and its causes are unknown.

We have isolated in our laboratory a temperate bacteriophage, called phage α, which is active on *Bacillus megatherium* and presents curing to a great extent. An analysis of this phage system has enabled us to measure the curing rate which is about 10^{-2} at 35 °C and 10^{-3} at 18 °C per cell and per cell division. As the properties of this phage system seemed particularly interesting we have carried out further studies in the course of which we have encountered unexpected results which we reporte here.

X-ray inactivation of phage α was carried out with a Pickering apparatus operating at $2 \cdot 10^5$ V with an intensity 10 r/s. By means of adequate filters a practically monochromatic beam was obtained.

The inactivation curve for phage α given in Fig. 1 shows that the average lethal dose (e^{-1} survival) for this phage is $2.1 \cdot 10^4$ r. Fig. 1 also shows the inactivation curve corresponding to another phage active on *B. megatherium*

(*) This research is supported by a grant of the Comitato Nazionale per l'Energia Nucleare (lo Prof. F. Graziosi).

(phage BM) which is not correlated with α, has about the same size and presents an average lethal dose of $1.85 \cdot 10^5$ r. The difference in radiosensitivity is so striking as to seem a paradox. In fact, while it is known that bacteriophages present good correlation between radiosensitivity and size, in our case this correlation does not hold. The diameter of the spherical radiosensitive volume, calculated by means of Lea's empirical tables for high potential X-rays, is about 60 mμ for phage α; this value is greater than the actual physical dimensions of the virus (protein shell included) and is the largest radiosensitive diameter which has ever been found for a bacteriophage.

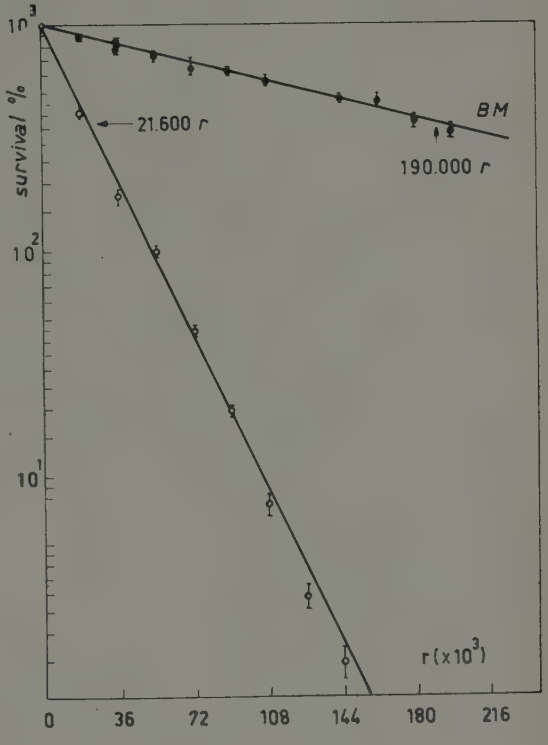

Fig. 1.

The above mentioned value differs greatly from the theoretical expectations which can be derived from Lea's empirical tables, if one considers the size of the virus as determined by means of the electron microscope and by means of the analytical centrifuge, and the percentage of DNA as determined chemically. In doing this, one must consider the fact that the radiosensitivity of bacteriophages is not due to all their chemical constituents but only to the DNA [1].

Fig. 2 shows the UV inactivation curves for phages α and BM. In these experiments UV rays of 2560 Å were used. Phage α turned out to be about twice as sensitive as BM; the behavior of this phage with respect to UV rays is therefore quite different than with X-rays.

The behaviour of phage α when treated with X and UV-rays is quite similar to that of phage ΦX 174, the smallest phage that has yet been found and which has been recently studied by TESSMANN [2]; taking into account its DNA content, ΦX 174 is about 10 times more sensitive to X-rays and 2÷3 times more sensitive to 2560 Å UV-rays than the other phages hitherto studied and has become an experimental material of great interest, since SINSHEIMER [3]

has shown that it contains a particular kind of DNA with a single stranded structure instead of the typical Watson and Crick structure [4].

Assuming that phage α also contains a DNA of unusual structure we have studied inactivation of this phage by assimilated ^{32}P. This effect is caused by the disintegrations of the ^{32}P atoms introduced into the phage DNA by means of synthetic culture media containing inorganic phosphates of high specific radioactivity [5]. It is possible to study accurately phage inactivation and to determine the lethal efficiency per disintegration and the possibility that it be influenced by physical and chemical factors.

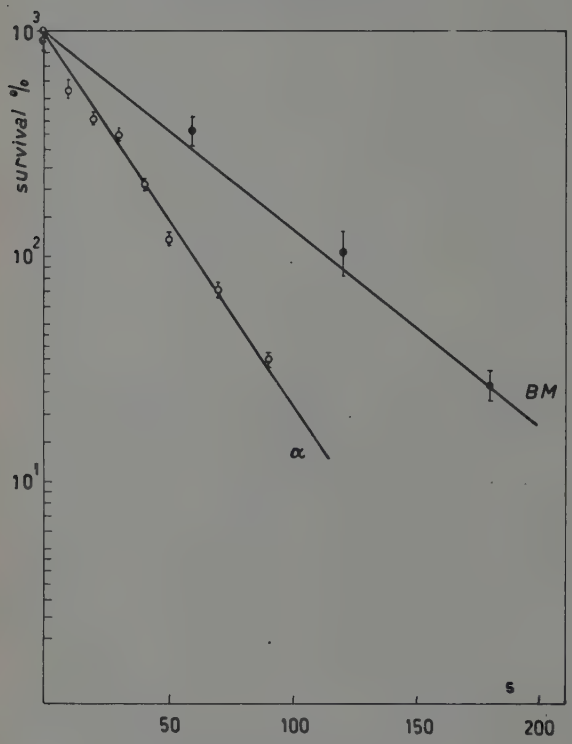

Fig. 2.

In this respect [6] we have already shown a temperature effect on the lethal efficiency due to assimilated ^{32}P in phage BM. Our findings are in agreement with the results of the experiments carried out by STENT *et al.* [7] on the T even phages.

The fact that a lethal efficiency of 0.1 has been found in bacteriophages can be explained by assuming that the depolymerization of DNA following the substitution of P atoms by S atoms can be at least partly prevented by the numerous hydrogen bonds which keep the two sister strands together. This hypothesis takes into account the structure of DNA and offers a good explanation for the temperature effect found by us and by STENT.

TESSMANN has shown that in ΦX 174 the lethal efficiency due to assimilated ^{32}P is 1 and that it does not depend upon temperature in accord with the fact that it contains a more simple DNA made up of a single nucleotide chain.

Fig. 3 shows the assimilated ^{32}P inactivation curve for phage α at 4 °C and — 79 °C. It is evident that in phage α the temperature effect is absent also; this fact shows up even more clearly if one examines the behavior of the other phages listed in Table I.

In Table II are given the data relative to three independent experiments carried out with great care and in which it is possible to observe a very slight temperature effect probably due to the natural instability of the phage suspensions at the temperature of the cold room.

In order to calculate the lethal efficiency of the assimilated ^{32}P disintegrations in the phage DNA it is necessary to know the inactivation rate of the phage, the specific radioactivity of the culture medium in which the virus has grown, the P content of the individual virus particles and the fraction of P which is contained

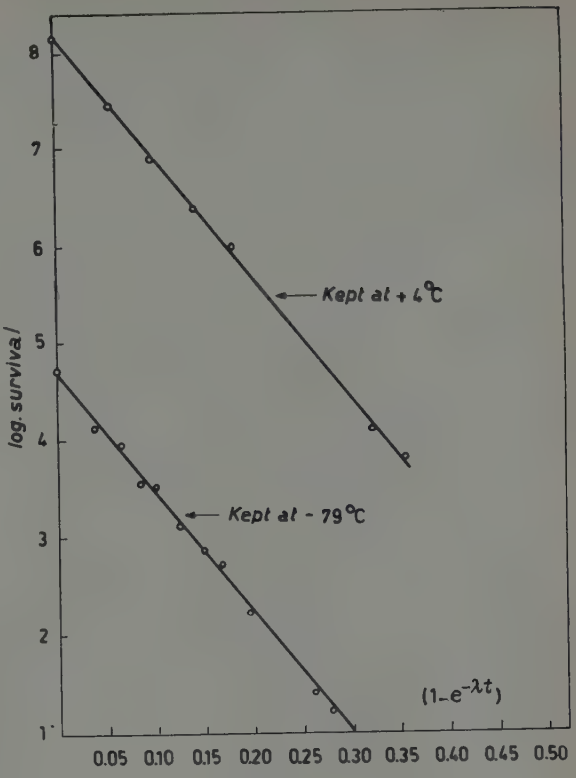

Fig. 3.

TABLE I.

Phage	Fraction of the inactivation rate constant at 4 °C for:		
	— 20 °C	— 79 °C	— 196 °C
T2	—	—	0.66
T5	0.68	—	0.55
T1	0.69	—	0.56
T3	—	—	0.52
T7	0.72	—	0.56
λ	0.71	—	0.54
HM	—	0.75	—

TABLE II.

Experim. no.	$K_{4\,°C}$	$K_{-79\,°C}$	$K_{-79\,°C/4\,°C}$
XVII	28.5	27.8	0.975
XIX	24.3	23.6	0.971
XX	32.5	31.4	0.966

in chemical constituents other than the DNA. One obtains the expression:

$$e = \frac{-\log S}{1.48 \cdot 10^{-6}\, a \cdot N \cdot A_0 \cdot (1 - \exp[-\lambda t])},$$

in which

e = lethal efficiency of the disintegrations,

S = percent survival of phage after t days;,

$1.48 \cdot 10^{-6}$ = factor which transforms A_0 into the ratio $^{32}P/^{31}P$,

A_0 = specific radioactivity in c/g,

N = number of P atoms per phage particle,

a = fraction of N not contained in DNA,

$(1 - \exp[-\lambda t])$ = fraction of ^{32}P atoms decaying in t days.

The value for A_0 is known an analysis of the total P contained in the culture medium and from measurements of the radioactivity. a is determined by means of paper chromatography of the phage hydrolysate and the comparison between the amounts of bases eluted from the spots with the total P content of the hydrolysate. N can be determined by making use of the autoradiographic technique [8, 9].

By means of these methods we have found for phage α the values of $1.35 \cdot 10^5$ for N and 0.75 for a (average of three experiments). The molecular weight of the DNA contained in phage α is therefore about $30 \cdot 10^6$ admitting that there is only one molecule per phage. A_0 was 78 and 90 c/g in the two independent experiments reported in Table III; this table gives the data pertaining to 281 phage β-stars distributed in 56 plates developed after various exposure times.

TABLE III.

Exper. no.	Plate no.	Exposure in d	Stars	$\bar{r}$	e
XVII	F 109	8	25	7.9	1.24
XVII	F 117	17	101	11.0	0.95
XX	F 122	6	53	7.1	0.93
XX	F 125	10	53	9.1	1.04
XX	F 133	20	49	12.2	1.31
					$\bar{e}_w = 1.07$

Note. – $\bar{r}$ = average number of rays; e = lathal efficiency in the expression (1); $\bar{e}_w$ = weighted average of the e values.

Table IV gives the distribution of the number of rays of β-stars found on a typical plate (plate 117); the distribution is remarkably homogeneous in accordance with the hypothesis that the amount of P per phage particle is constant.

TABLE IV.

Rays no.	Stars	
6	1	
7	4	
8	10	
9	7	
10	22	
11	16	Stars no. = 94
12	7	$\bar{r} = 11.51$
13	7	$\sigma = 12.70$
14	6	« Chi square » = 16.5
15	7	d.f. = 15
16	2	P. = 0.30
17	1	
18	0	
19	0	
20	0	
21	0	
22	1	
23	1	
24	1	
25	0	
26	0	
27	1	

Note. – The stars with less than five rays have been discarded and therefore the average must be suitably corrected.

As one can see from Table III the lethal efficiency of assimilated ^{32}P in the DNA of phage α is quite close to 1. This fact confirms that it is substantially similar to phage ΦX 174. This conclusion is not without consequences; it is necessary to admit that phage α contains a DNA with a different structure from that suggested by WATSON and CRICK and that it might have a DNA made up of a single nucleotide strand. This difference in structure could offer an explanation for the high curing rate of the cells lysogenic for α, if one keeps in mind that curing probably is the result of a faulty interaction between the DNA of the host cell and of the phage. This difference in structure could furthermore be the base of further experiments which would take in

account the fact that phage α, unlike ΦX 174, is a temperate phage and that it could therefore be particularly useful for a genetical analysis of the relationships existing between the phage and bacterial chromosome and more generally for an analysis of the mechanisms of DNA duplication.

REFERENCES

[1] H. T. Epstein: *Nature*, **171**, 394 (1953).
[2] I. Tessman: *Virology*, **7**, 263 (1959).
[3] R. L. Sinsheimer: *Journ. Mol. Biol.*, **1**, 43 (1959).
[4] J. D. Watson and F. H. C. Crick: *Nature*, **171**, 737 (1953).
[5] A. D. Hershey, N. D. Kamen, J. W. Kennedy and H. Gest: *Journ. Gen. Physiol.*, **34**, 305 (1951).
[6] C. Castagnoli and F. Graziosi: *Nature*, **174**, 599 (1954).
[7] G. S. Stent and C. R. Fuerst: *Journ. Gen. Physiol.*, **38**, 441 (1955).
[8] C. Levinthal and C. A. Thomas Jr.: *Biochem. Biophys. Acta*, **23**, 453 (1957).
[9] S. Aurisicchio, G. Cortini, V. Emma and F. Graziosi: *Int. Journ. Rad. Biology*, **1**, 86 (1959). See also S. Aurisicchio, A. Celano and R. Rinzivillo, in the present issue.

SUPPLEMENTO AL VOLUME XVIII, SERIE X
DEL NUOVO CIMENTO

N. 2, 1960
4° Trimestre

Physico-Chemical and Morphological Aspects of Temperate Phage α Particles (*).

S. Aurisicchio, A. Chiozzotto, A. Coppo, P. Donini
C. Frontali and F. Graziosi

Istituto Superiore di Sanità e Istituto di Microbiologia dell'Università - Roma

The temperate phage α like the coliphage ΦX 174 [1] contains a DNA with unusual properties, as shown by the high X-ray sensitivity, and the high lethal efficiency of assimilated ^{32}P. We have therefore undertaken research on both phage particles and purified DNA, in order to interpret in physico-chemical terms the results thus far obtained on a biological level, and to understand the structural basis for the unusual behaviour of this bacteriophage. We refer briefly some of the results obtained up to the present.

The thorough study of a great number of micrographs enables us to conclude that the head of phage α has a perfectly regular icosahedral form. Measurements made on about 100 randomly chosen particles, under strong magnification (Fig. 1) give a lenght of (30 ± 2) mμ for the edge; the tail appears as a stiff cylinder, 120 mμ long, enclosed in a delicate structure. The molecular weight of the whole particle is about $6 \cdot 10^7$ (taking into account all possible sources of error: absolute magnification, measurement error, etc.) if one assumes a density of 1.5. The molecular weight of the tail alone is about $1 \cdot 10^7$, assuming a density of 1.15 its composition being essentially proteic.

Studying phage suspensions with the analytic ultracentrifuge, one finds several components, which can be related to those observed under the electron microscope. Generally three peaks are present in the schlieren diagrams; their sedimentation constants are given in Table I. The fastest peak, corresponding to the most concentrated component, can be referred to the unaltered phage

(*) This research is supported by a generous grant of the Comitato Nazionale per l'Energia Nucleare (to Professor F. Graziosi).

particles, while the slowest can be ascribed to DNA, which is always present in phage suspensions which have undergone mechanical treatment. The intermediate peak may be due to the presence of ghosts, with or without tails, or to the presence of isolated tails.

TABLE I.

Material	s_1	s_2	s_3
Phage in NaCl 1%	400 ± 10	120 ± 5	20 ± 1
Phage in NaCl 1% + DNAase	470 ± 10	140 ± 5	7.3 ± 0.3

Sedimentation coefficients are expressed in Svedberg units.

This interpretation was confirmed by adding DNAase to the phage suspension; partially depolimerized DNA sediments more slowly, while the other peaks move faster because of the decrease in viscosity.

According to this interpretation we can obtain an estimate of the molecular weight of the phage particles, by comparing our data with those of PUTNAM [2], concerning phage T_2, ($s_{T_2} = 1050\,S$; $M_{T_2} = 250 \cdot 10^6$). Using the Mandelkern and Flory equation [3] and assuming that the two particles have similar hydrodynamic properties, one obtains $M = 7 \cdot 10^7$. (M indicates the molecular weight and s the sedimentation constant).

Phage particles and purified DNA have been subjected to chemical analysis. Purification of DNA was carried out by the method described by SINSHEIMER [1] for phage ΦX 174; we used also a cruder method, simpler than the one described by LONAN and SINSHEIMER for phage T_7 [4] and based on the treatment of phages with urea and lauril-sulphate, but avoiding the repeated precipitations in alcohol.

The composition in purine and pyrimidine bases of both phage particles and purified DNA has been studied by hydrolysis with formic acid, paper chromatography in isobutanol-HCl, quantitative elution of the spots, and spectrophotometric determination of eluates.

We have found that the DNA content is $(35 \pm 5)\%$ of the dry weight and that the ratio between the different bases are the same in purified DNA hydrolyzates as in phage particles. The data thus far obtained with the chemical analysis are collected in Table II.

The first thing to notice is that the DNA of phage α is richer in adenine and thymine ($A+T/G+C = 1.33$), but more important is fact the that A/T and G/C ratios are very near 1 (1.02 and 0.91).

Samples of phage DNA, purified with the two above mentioned methods were studied with the ultracentrifuge, performing a series of runs at different well known concentrations. For a sample of DNA purified with urea we ob-

Fig. 1.

tained values of s between 15 and 17 S, at a concentration $c = 0.15$ mg/ml, and between 26 and 28 S at $c = 0.02$ mg/ml. However the observed peaks are rather skew, showing that the preparation is not homogeneous. Further

TABLE II.

Material	A	T	G	C	A/T	G/C	A+T/G+C
Phage	1.65	1.78	1.15	1.26	0.93	0.91	1.42
Phage	3.83	3.89	2.44	2.97	0.98	0.82	1.43
Average	—	—	—	—	0.96	0.87	1.42
DNA (urea)	1.36	1.44	1.02	1.19	0.94	0.86	1.27
DNA (urea)	4.45	4.35	2.87	3.60	1.02	0.80	1.36
DNA (phenol)	2.28	1.79	1.62	1.60	1.27	1.01	1.25
DNA (phenol)	2.58	2.55	2.10	1.96	1.01	1.07	1.25
Average	—	—	—	—	1.06	0.94	1.28
Total average	—	—	—	—	1.02	0.91	1.33

A = adenine, T = thymine, G = guanine, C = cytosine. Experimental values are expressed in micromoles.

conclusive evidence that this DNA sample is denatured came from the observation that it is no longer sensitive to the action of DNAase: a run performed at the same concentration as above (0.15 mg/ml), in the presence of DNAase gave the same sedimentation coefficient (about 16 S).

To the contrary, DNA purified by the phenol method, and then treated with DNAase, depolimerizes to such an extent, that no peak can be observed. An indication of the homogeneity of the sample is given from the analysis of boundaries, performed with the method described by SCHACHMAN [5] (Fig. 2). Only one component is present, but there is a certain amount of polidispersity since for this substance diffusion should be negligible [5].

A series of runs performed at low concentrations of phenol purified DNA gave the results collected in Fig. 3. The value of s, extrapolated to zero concentration came out to be between 27 and 35 S. Such a value may be used in a rough calculation of the molecular weight, at least in two different ways:

a) Knowing the sedimentation constant and the intrinsic viscosity, assuming an hydrodynamical model for the molecules, and using the formulae calculated for this model (formulae of this kind have been derived by SHERAGA

and MANDELKERN [6] for rigid ellipsoids, and by MANDELKERN and FLORY [3] for flexible chains; as a matter of fact DNA molecules do not correspond perfectly to either model, but show an intermediate behaviour).

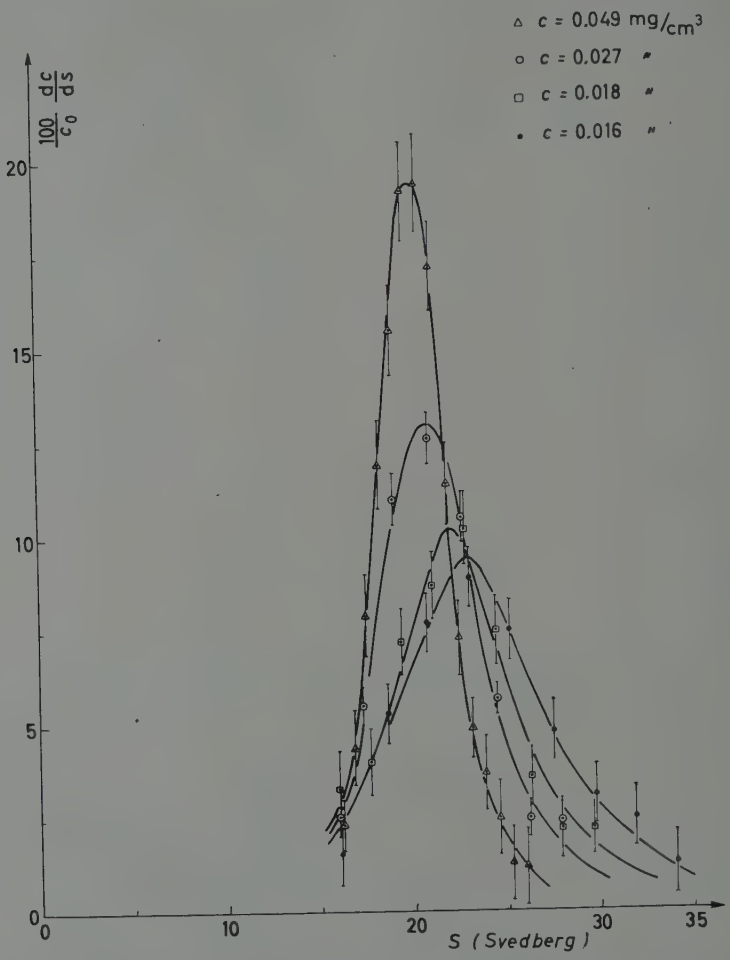

Fig. 2. – Effect of the concentration on the distribution curves for sedimentation coefficients. The error given is three times the standard error.

b) Using the empirical relation found by DOTY, MCGILL and RICE [7] between the sedimentation constant and the molecular weight for homologous samples of DNA, in the molecular weight range from $0.3 \cdot 10^6$ to $7 \cdot 10^6$.

At present we are in a position to give only an estimate of the molecular weight, assuming that Doty's empirical relation still holds somewhat outside

the range of molecular weight for which it was found. One obtains

$$M_{\mathrm{DNA}} = (s/0.063)^{1/0,37} = (19 \pm 6)\cdot 10^6 .$$

where the error is due entirely to the uncertainty on s.

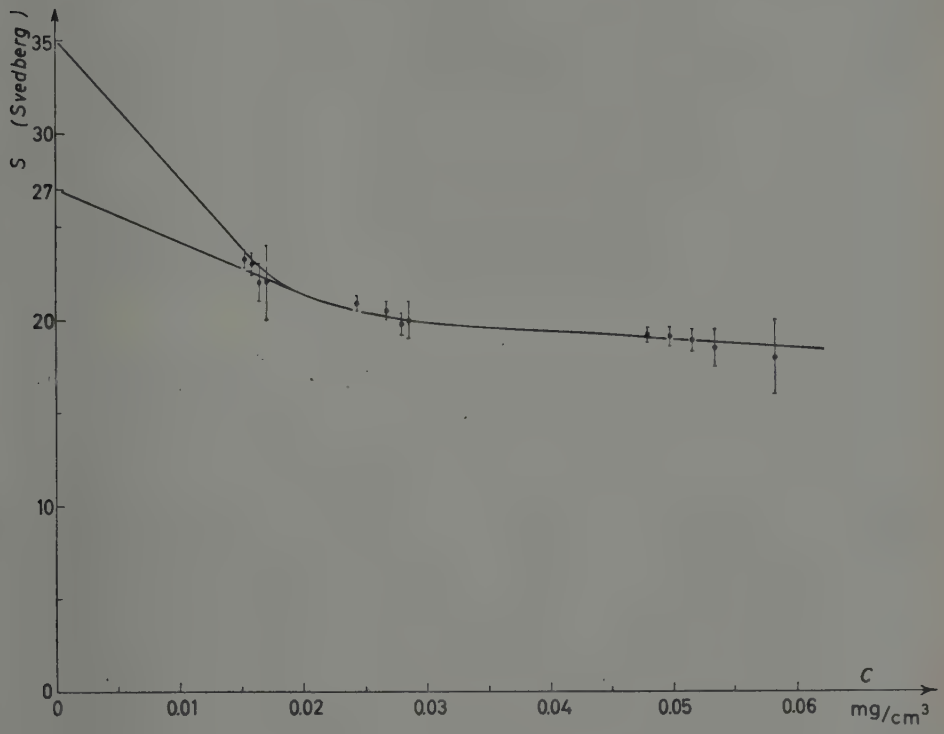

Fig. 3. – Dependence of sedimentation coefficient on concentration.

A comparison, in Table III, of the results obtained by means of different methods shows that phage α is likely to contain a single DNA molecule, of molecular weight about $3\cdot 10^7$. The decrease in the molecular weight, and the polidispersity observed by ultracentrifugation, may be explained by the de-

TABLE III.

Material	Method	M
Phage	Electron microscope	$6.2\cdot 10^7$
Phage	Ultracentrifugation (and comparison with T_2)	$6.6\cdot 10^7$
DNA	Ultracentrifugation	$1.9\cdot 10^7$
DNA	Autoradiography	$3.1\cdot 10^7$

1187

polimerization process, which DNA solutions undergo in handling. The DNA macromolecule present in phage α is, as we mentioned already, extremely sensitive to ionization produced by X-rays and to disintegrations of assimilated ^{32}P (letal efficiency $\simeq 1$), and could, therefore, contain a single nucleotide chain, in analogy with what has been observed for the DNA of phage ΦX 174.

However the value, close to 1, found for the ratios A/T and G/C, as well as the results of spectrophotometric tests, performed on the same DNA (lack of hyperchromic effect after treatment with formaldehyde, and steady absorbancy when temperature is shifted up to 80 °C [8]) suggest that this interpretation is too simple; there are at least two possible explanations:

1) Each phage particle contains a DNA molecule consisting of a single nucleotide chain; there are, however, two classes of particles present in the same amount in usual preparations, containing chains of complementary base composition. A sort of association between two complementary chains could take place during the purification process.

2) Each particle contains a molecule composed of two nucleotide chains having however a different structure from that proposed by WATSON and CRICK, and such as to give account of the high sensitivity to X-rays to assimilated ^{32}P.

The interest of further research on the biological, physical and chemical properties of phage α is evident. In fact, the discovery of phage ΦX 174 has led to new ideas on the possible structure of DNA and on its duplication mechanism, and the discovery of new types of viral particles could lead to more detailed and satisfying interpretations.

Biological and physico-chemical research is now in progress, in order to study the genetic structure of phage α, and to describe in a more detailed manner the shape and dimensions of its DNA macromolecules.

REFERENCES

[1] R. L. SINSHEIMER: *Journ. Mol. Biol.*, **1**, 37, 43 (1959).
[2] F. W. PUTNAM: *Journ. Biol. Chem.*, **190**, 61 (1951).
[3] L. MANDELKERN and P. J. FLORY: *Journ. Chem. Phys.*, **20**, 212 (1952).
[4] K. D. LUNAN and R. L. SINSHEIMER: *Virology*, **2**, 455 (1956).
[5] V. N. SCHUMAKER and H. K. SCHACHMAN: *Biochim. et Biophys. Acta*, **23**, 628 (1957).
[6] H. A. SHERAGA and L. MANDELKERN: *Journ. Am. Chem. Soc.*, **75**, 179 (1953).
[7] P. DOTY, B. B. MCGILL and S. A. RICE: *Proc. Nat. Acad. Sci.*, **44**, 432 (1958).
[8] G. TOSCHI *et al.*: work in progress.

SUPPLEMENTO AL VOLUME XVIII, SERIE X
DEL NUOVO CIMENTO

N. 2, 1960
4° Trimestre

Deletion Syngenotes and the Problem of Coding Ratio.

E. CALEF

Istituto di Genetica dell'Università - Pavia

1. – Introduction.

Lambda phage transduces in a specialized way [1]; it is able, in fact, to transfer only the genes controlling galactose metabolism. The transducing phage interacting with a bacterium gives a partial diploid called a syngenote. Syngenotes produce, upon U.V. induction, phage lysates (called HFT) which are composed of normal and transducing particles in a ratio close to one. The transducing particles differ in density from the normal non-transducing phage [2] genetically they are shown to be deficient for an interstitial segment of the phage genome [3, 4].

This system seems to afford unique possibility for an experimental approach to the coding problem.

Let us assume that it would be possible to produce a deletion in the exogenotic part of a given syngenote and that this deletion had the length of a functional unit (cistron); then the HFT lysate of the two syngenotes, the original and the deletion one, should show a difference in density measurable by cesium gradient centrifugation. Transforming this difference into terms of molecular weight we should obtain the molecular weight of a cistron.

This molecular weight can be compared with the molecular weight of the enzyme under control of the cistron.

Comparison of such weight to the molecular weight of the missing enzyme is of obvious interest for the problem of coding ratios.

The following report gives the preliminary results obtained in experiments using γ-rays on a syngenote with the aim of detecting a deletion in the region of galactose genetic determinants.

2. – Experiments and results.

A syngenote of the constitution represented in diagram 1 was used. The upper line represents the exogenotic or transduced portion, the lower gives the relevant section of the genotype of the original haploid gal⁻ bacterium.

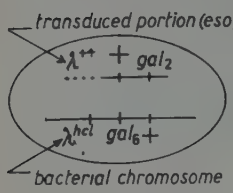

Diagram 1.

The symbols represent: λ^{++}, a Lambda phage of the reference type [5]; $\lambda^{h\,cl}$ a doubly marked prophage in the bacterial strain, a host range mutant (*h*), giving clear plaques (*cl*). Mutant genes for galactose are gal_2, a kinase deficient mutant, and gal_6, a transferase deficient mutant [6]; their position in the map with respect to Lambda is deduced from data previously published [7].

Diagram 2 gives the scheme of the experiment; on the left, the various kinds of bacteria derivable from the original syngenote are given. At the right are listed the various types of lysate obtainable.

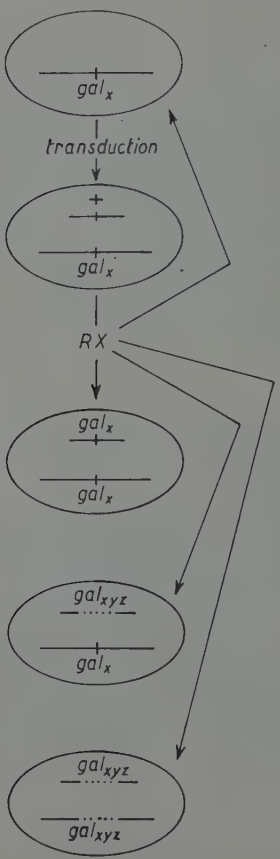

Bacteria and Their Phenotype	*Lysate Obtainable ob U. V. Induction*
Original gal_x mutant and gal_x haploid segretans	LFT gal_x
Heterogenote gal_{x^+}	HFT gal_{x^+}
Homogenote gal_x	HFT gal_x
Heterozygous deletion gal_x	HFT $gal_{xyz..}$ gal_x
Homozigous deletion $gal_{xyz..}$	HFT $gal_{xyz...}$

Diagram 2.

1190

In order to perform the density measurement, we need the lysate *E*, the densities of *E* and *B* shall be compared to obtain the desired information on cistron weight. Possibly lysate *D* can be used, but the difficulty involved in the determination of its genetic characteristics make this one less desirable.

The following is the method of characterizing lysate *E* and/or *D*.

Syngenotic bacteria with gal⁻ phenotype are singled out from a large majority of gal⁻ haploid syngenotes after irradiation treatment, by virtue of their ability to produce HFT lysate. This is performed by replica plating several hundred bacterial streaks on to a seeded lawn of a gal⁻ mutant, on EMB galactose plates. The mutant in question (U 34-2) belong to a complementation group different from that of the mutants contained in the syngenote.

The syngenotes, to be gal⁻, must be either homogenotes or deletions. In the latter case they can be homozygous and heterozygous. To distinguish and discard the homogenotes, lysates are prepared in the standard way, titrated and tested on a number of gal⁻ mutants. Homogenotes give a positive reaction with all but one of the gal mutants. The positive reaction will vary in intensity (as measured by papillae counting) according to the presence or absence of the cis-trans position effect.

Homozygous deletions will give negative results with more than one gene contiguous to the original mutant. Heterozygous deletions will give a reaction which can be distinguished from that of the homogenotes on a quantitative basis.

TABLE I. – *Test of the lysates from gal⁻ syngenotes.*

Lysate no.	Lysate titer	BACTERIAL TESTERS								
		U 112	U 135	U 186	U 190	U 201	U 212	U 162	U 33.6	U 34.2
2	10^6	—	—	—	—	—	—	—	+	—
8	10^8	15	+	18	—	+	—	+	+	+
10	10^6	5	15	18	—	—	+	+	+	+
21	10^6	—	20	7	—	—	—	8	+	+
14 B	10^8	—	10	13	—	8	11	—	+	+

Lysate from gal⁻ colonies derived from the heterogenote H 198/06 with the genetic constitution given in diagram 1 are tested on several gal⁻ mutant.

The allele carried by the various bacteria are U 112 = 105.1; U 135 = 33.2; U 186 = 1; U 190 = 6; U 201 = 4; U 212 = 7; U 162 = 2; U 34.6 = 34.6; U 34.2 = 34.2.

The ability of a given lysate to transduce a given mutant is indicated as papillae number per 0.05 of lysate. The sign + indicates a number of papillae not countable, usually above 100.

Table I gives the results of one experiment carried out according to the outlined scheme. The number of papillae per 0.5 lysate are given. The sign + indicates a strong reaction with confluent papillae usually over one hundred.

The five lysates here presented are compatible with deletion homozygotes; however, it is premature to say more than that, since many controls are still to be performed.

In conclusion: the first requisite of our experiment was the finding of a deletion in the gal region; such deletions were found never before in spite of an extensive if not deliberate search [8]; the few data collected seem to prove that deletions in gal region are obtainable.

The next question to be answered is whether these deletions have a modified density.

REFERENCES

[1] M. Morse, E. Lederberg and J. Lederberg: *Genetics*, **41**, 758 (1956).
[2] J. Weigle, M. Meselson and K. Paigen: *Brookhaven Symposia in Biology*, no. 12 (1959), p. 125.
[3] W. Arber, G. Kellenberger and J. Weigle: *Schweiz. Zeits. Allg. Pathol. u. Bakteriol.*, **20**, 659 (1957).
[4] A. Campbell: *Virology*, **4**, 366 (1957).
[5] A. D. Kaiser: *Virology*, **1**, 424 (1955).
[6] H. M. Kalckar, K. Kurahashi and E. Jordan: *Proc. Natl. Acad. Sci.*, **45**, 1776 (1959).
[7] E. Calef and G. Licciardello: *Virology*, **12**, 81 (1960).
[8] E. Lederberg: *Microbial Genetics. 1-th Symp. Soc. Gen. Microbiol.* (Cambridge 1960), p. 115.

SUPPLEMENTO AL VOLUME XVIII, SERIE X
DEL NUOVO CIMENTO

N. 2, 1960
4° Trimestre

A Study of Ribosomes from a Thermophilic Micro-Organism.

G. Tecce and G. Toschi

Istituto di Fisiologia Generale dell'Università e Istituto Superiore di Sanità - Roma

The ability to grow at high temperature, such as is shown by some thermophilic micro-organisms, has been attributed mainly to a particular thermal stability of certain cell constituents, namely the proteins [1]. This hypothesis however has been supported with only little experimental evidence and basic information on the properties of the pure protein constituents of these organisms is still lacking.

We have planned to study the mechanism of thermophilia by examining the molecular characteristics of certain cell constituents, well defined both as to their structural, physico-chemical and physiological properties. Such constituents are represented by ribosomes, *i.e.* the submicroscopic particles which are the main structural component of the cytoplasm in a number of bacteria. They are macromolecules of ribonucleoprotein and are an essential element in the synthesis of protein [2]. The present study is actually a preliminary survey of the main characteristics of the ribosomes in a strain of *Bacillus stearothermophilus* grown at 70 °C. This information moreover is an essential prerequisite for further investigation on protein synthesis in this organism.

In our laboratories, the actual presence and structural aspects of cytoplasmic particles of this type have been investigated by electron microscopy. Ultra-thin sections of intact cells as well as sections of protoplasts and of purified particles obtained from cell-free preparations have been studied. To our knowledge, no similar examination of any thermophilic micro-organism has hitherto been reported.

The bacterial cells were harvested from cultures in the logarithmic phase growing on a synthetic medium at 70 °C. Protoplasts were obtained by lysozyme treatment, in the presence of 0.32 M sucrose, 0.01 M phosphate buffer pH 7 and 0.001 M Mg acetate; cell-free extracts were obtained by osmotic shock of the protoplasts suspended in the same solution minus the sucrose.

The above ionic composition has proved effective in preserving the particles, which is in agreement with the findings of other workers [3]. After removal of other cell constituents by centrifugation at $18\,000 \times g$ for 20 min, ribosomes were collected by centrifugation at $105\,000 \times g$, and purified by repeated cycles of low- and high-speed centrifugation.

For electron microscopic examination, the cells were fixed with buffered isotonic osmium tetroxide and stained with uranyl acetate according to RYTER *et al.* [4], they were then embedded in butyl metacrylate and sectioned with a Porter-Blum microtome. Protoplasts and cell-free preparations of ribosomes were fixed and processed in the same way. Examinations were made at an initial magnification of $20\,000\times$ or $40\,000\times$ with a Siemens Elmiskop in the Dept. of Physics of the Istituto Superiore di Sanità.

In the electron micrographs of sections from intact cells, besides the cytoplasmic constituents, the usual structures of bacterial cells can be identified (Fig. 1). A thick cell wall (CW) and a thin plasma membrane (PM) are distinctly delimited. A « nucleoplasm » is frequently observed as a central zone of diffuse material forming a fine network and/or clumps. The cytoplasm shows a granular structure, consisting of small particles which are heavily stained, tightly packed and therefore not well demarcated. Their diameter is estimated as ranging from 100 to 200 Å. In addition to the particles, peculiar structures are frequently observed in the cytoplasm (Fig. 2), in the form of small oval bodies (M) which are formed by repeated folding of a thin membrane similar to the plasma membrane and apparently continuous with it. They are usually found in a peripheral or polar position, namely in the zone of cell division. Because of all these features, these bodies resemble very closely the membrane structures in the cytoplasm of a number of bacteria described by other workers [5].

The protoplasts are round-shaped, markedly swollen and delimited only by a very thin membrane, there being no remnant of cell wall (Fig. 3). Their content is very diffuse and consists of particles closely resembling those seen in intact cells, though they are more dispersed and therefore more sharply outlined. A few dense clumps also are frequently seen.

When the purified ribosome preparations were examined under the electron microscope, very similar particles proved to be their characteristic constituent (Fig. 4). The same preparations were also examined directly, unfixed, after « negative staining » with phosphotungstic acid, at an initial magnification of $80\,000\times$ [6]. With this technique the particles are particularly well defined (Fig. 5). They appear for the most part as single particles, round but irregularly shaped, with diameters (measured on 200 particles) distributed around two average values, respectively 130 and 160 Å. This suggests the presence of two classes of particles.

A parallel study of these same preparations of isolated ribosomes was done

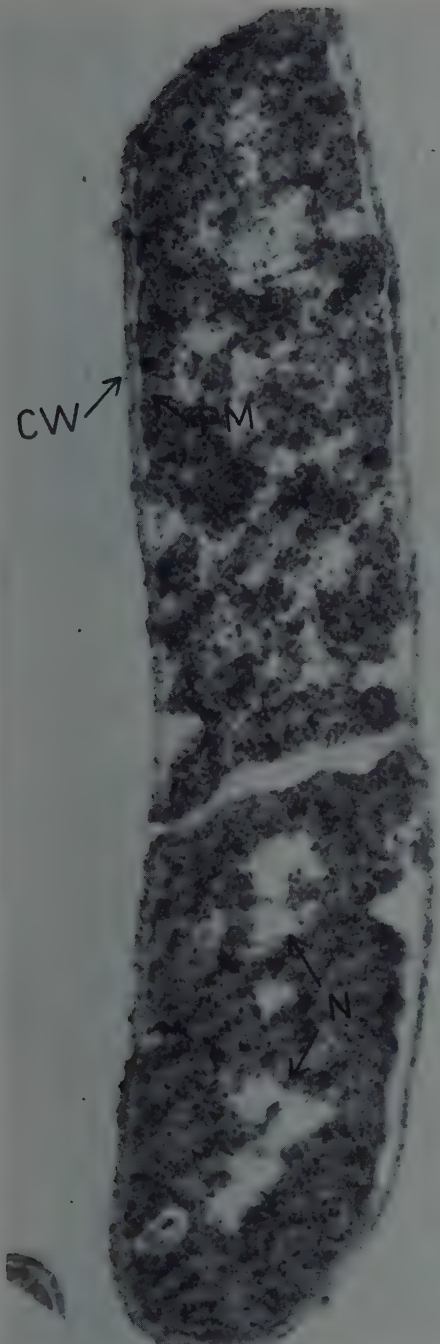

Fig. 1. – *Bacillus stearothermophilus*, intact cells. Cell wall (CW) plasma membrane (PM), and nucleoplasm (N) can be identified, as well as the cytoplasm consisting of evident particles. Magnification 68000×.

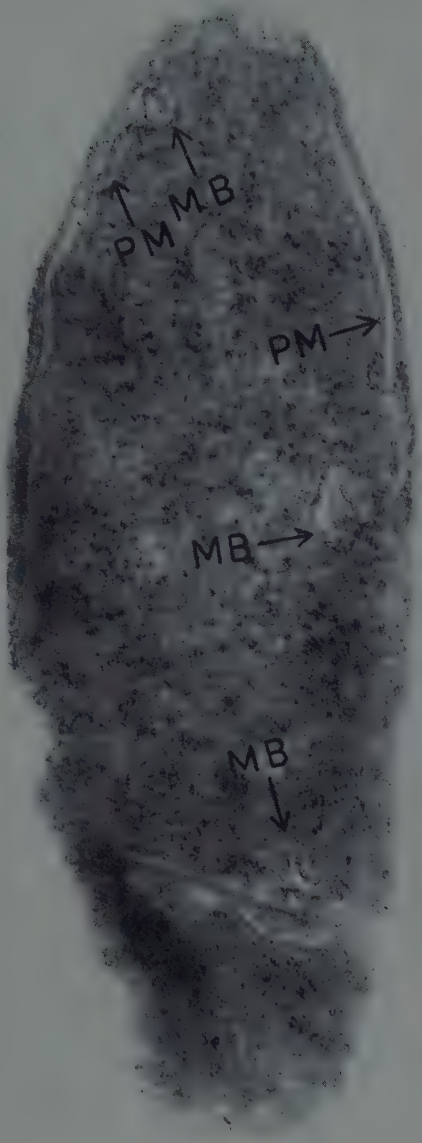

Fig. 2. – Detail of the membrane bodies (MB) in continuity with the plasma membrane (PM). Magnification 115 000×.

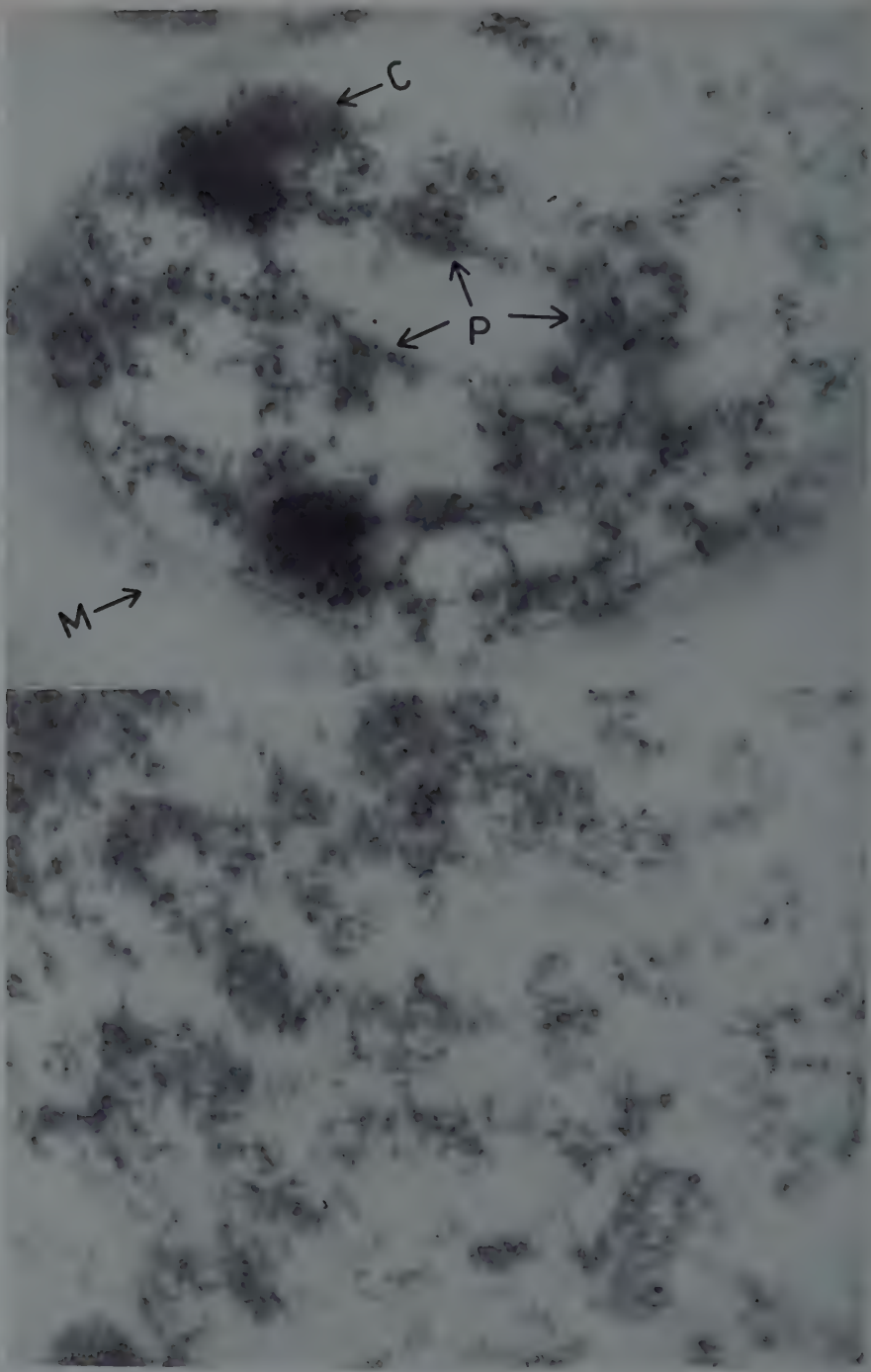

Fig. 3.

Fig. 4.

Fig. 3. Lysozyme-produced protoplast, delimited by a thin membrane (M) and containing particles (P). Magnification 120 000 ×.

Fig. 4. Purified preparation of cytoplasmic particles (ribosomes). Magnification 125 000 ×.

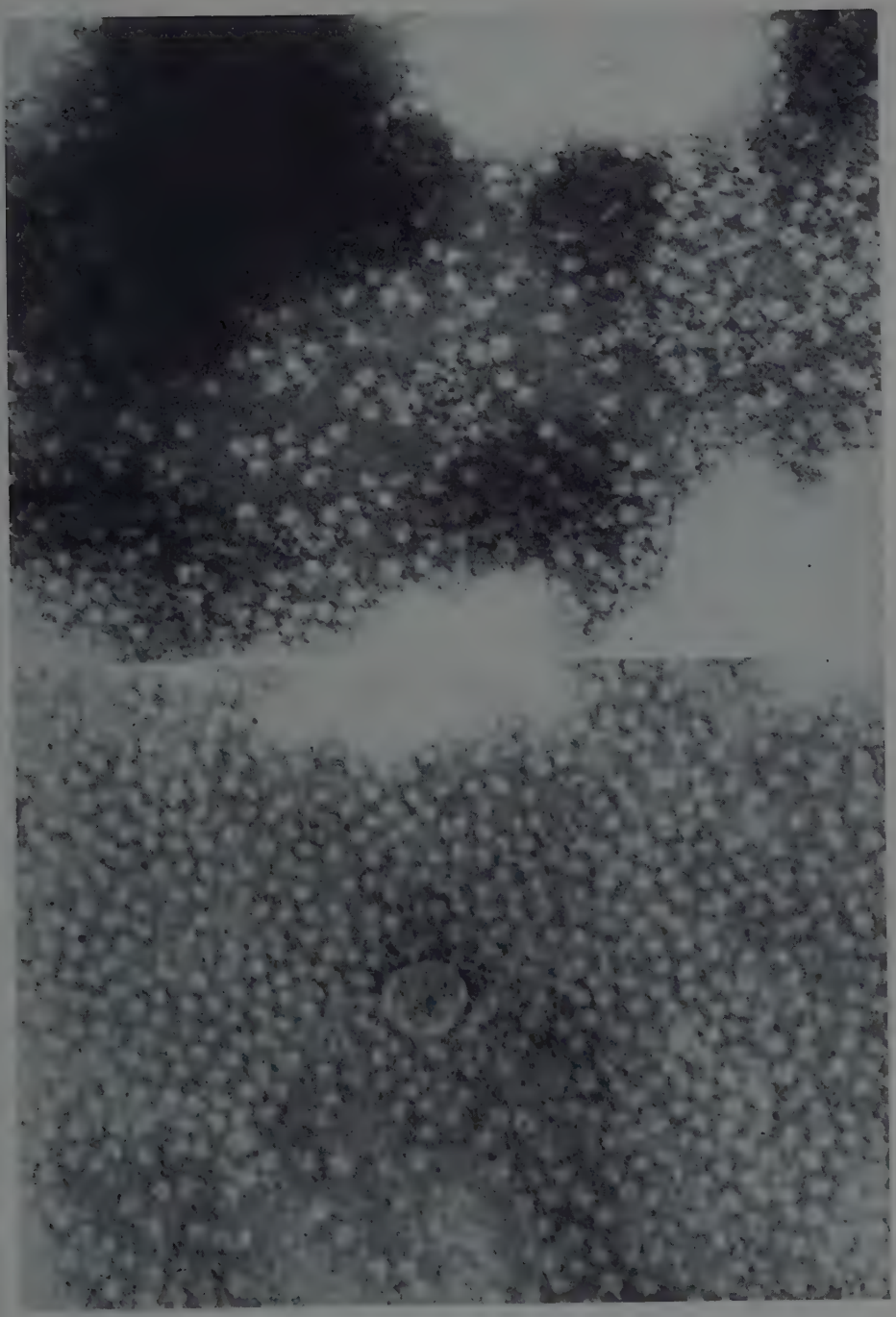

Fig. 5. – Purified preparations of ribosomes (49 and 34 S), negatively stained with phosphotungstic acid. Magnification 170000×.

by means of the analytical ultracentrifuge, both immediately after the extraction (« crude ribosomes ») and after repeated differential centrifugation (« purified ribosomes »). The effects of the variation in the ionic composition of the medium on the sedimentation characteristics of these ribosomes were also investigated. as well as their chemical composition in protein and ribonucleic acid (RNA)

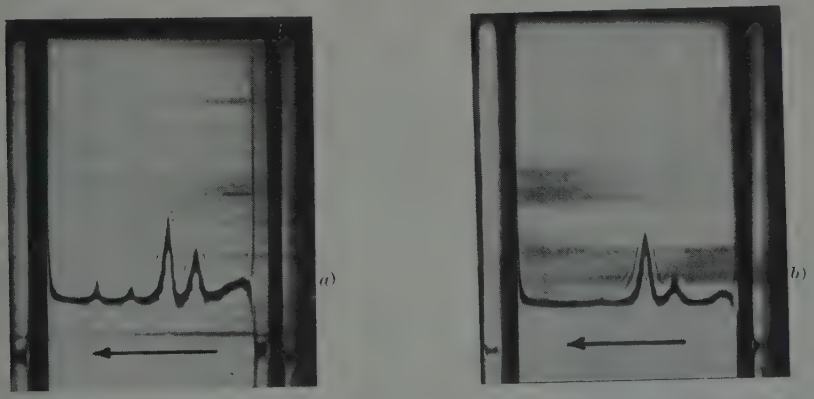

Fig. 6. – Ribosomes from *B. stearothermophilus*, prepared in 0.01 M phosphate buffer ph 7 and 0.001 M Mg acetate. *A*) « Crude preparation ». Chemical analysis: RNA mg 0.58 per mg of protein. Ultracentrifugal analysis: photograph after 18 min at 37020 rpm; the sedimentation coefficients of the four macromolecular components are respectively 86, 69, 48 and 33 S. Arrow indicates direction of sedimentation. *B*) « Purified preparation ». Chemical analysis: RNA mg 0.79 per mg of protein. Ultracentrifugal analysis: (the same conditions as in *A*); the sedimentation coefficients of the two main components are 49 S and 34 S.

and the nucleotide composition of this RNA. Fig. 6*A* shows that the « crude ribosomes » consist of a group of four distinct macromolecular components with sedimentation coefficients of 86, 69, 48 and 33 Svedberg units (S) respectively. The « purified ribosomes » (Fig. 6*B*) contain two macromolecular components, a principal one with 49 S and a minor one with 34 S. Characteristic changes in this composition have been observed on changing the ionic composition of the medium; when the concentration of the Mg ions is increased, these ribosomes consist mainly of components with higher sedimentation coefficients (Fig. 7). Chemical analyses have shown that these ribosomes have the characteristic composition of a ribonucleoprotein which contains about 40 per cent of RNA in the purified preparations. The nucleotide composition of this RNA has been examined by determining spectrophotometrically the percentage of the four main ribonucleotides, separated by paper electrophoresis of an alkaline hydrolysate [7]. These results are given in Table I, and a comparison with the composition of RNA in ribosomes from *E. coli* shows obvious differences in the percentage of guanylic and uridylic acid. The presence of

TABLE I. – *Nucleotide composition of the* RNA *in the ribosomes from B. stearothermophilus*

		B. stearothermophilus	*E. coli* [8]
Adenylic a.,	Moles percent	25.7	25.0
Guanylic a.,	Moles percent	34.5	31.5
Cytydylic a.,	Moles percent	22.0	22.1
Urydilic a.,	Moles percent	17.8	21.4

minor constituents has also been investigated by further chromatographic analysis; the « fifth nucleotide » (or pseudouridylic acid) was not detected. A preliminary evaluation of the molecular weight of these ribosomal particles (in a purified preparation as that illustrated by Fig. 5 and 6*B*) can be attempted on the basis of their volume, evaluated from the electron micrographs, assuming the particles to be practically spherical; and of their density, as resulting from their composition in protein and RNA, that is, 1.5. A value of about 1 000 000 is thus obtained for the smaller particles, with an average diameter 130 Å, and about 1 900 000 for the larger ones, with an average diameter of 160 Å. In order to evaluate these molecular weights on the basis of the sedimentation coefficients, the frictional coefficients of the particles are at present being determined by viscosimetric techniques.

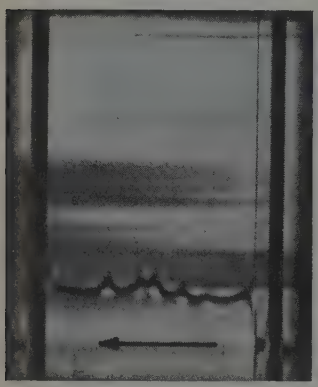

Fig. 7. – Ribosomes from *B. stearothermophilus*, prepared in 0.01 M tris-HCl buffer pH 7.4 and 0.005 M Mg acetate. « Crude preparation ». Ultracentrifugal analysis: photograph after 16 min at 37 020 rpm; the sedimentation coefficients of the 5 main components are 103, 84, 73, 52 and 45 S respectively.

On the basis of all the above reported findings, the cell structure of B. *stearothermophilus*, examined at a submicroscopic level, is seen to resemble that of a variety of mesophilic species. It does not show any particularity obviously related to the thermophilia. The similarity extends to the observed presence and to the main structural, chemical and physico-chemical characteristics of the ribosomes, as results from a comparison with the ribosomes of *E. coli* [3]. These observations provide us with a suitable background for a closer and more detailed investigation of the molecular characteristics of the ribosomes of *B. stearothermophilus*, which may possibly show some peculiar and significant relationship with the thermal stability of these cell constituents.

* * *

We wish to thank Prof. M. AGENO, Chief of the Physics Laboratory, for his stimulating interest in this work, as well as the Staff of the Electron Microscopy Section of the same Laboratory: Prof. D. STEVE BOCCIARELLI with Mssrs. A. CHIOZZOTTO, F. PICCIRILLI, N. TOMASSINI and F. VALENTE.

REFERENCES

[1] J. KOFLER: *Bacter. Rev.*, **21**, 227 (1957).
[2] K. MCQUILLEN, B. ROBERTS and R. J. BRITTEN: *Proc. Nat. Acad. Sci.*, **45**, 1477 (1959).
[3] A. TISSIÈRES, J. D. WATSON, D. SCHLESSINGER and B. R. HOLLINGWORTH: *Journ. Mol. Biol.*, **1**, 221 (1959).
[4] A. RYTER, E. KELLEMBERGER, A. BIRCH-ANDERSEN and O. MAALOE: *Zeits. Naturfor.*, **13**, 597 (1958).
[5] A. M. GLAUERT and D. A. HOPWOOD: *Journ. Biophys. Biochem. Cytol.*, **6**, 515 (1959).
[6] H. E. HUXLEY and C. ZUBAY: *Journ. Mol. Biol.*, **2**, 10 (1960).
[7] J. D. SMITH: *The Nucleic Acids*, vol. **1**, ed. by E. CHARGAFF and J. N. DAVIDSON (New York, 1955), p. 267.
[8] P. F. SPAHR and A. TISSIÈRES: *Journ. Mol. Biol.*, **1**, 237 (1959).

SUPPLEMENTO AL VOLUME XVIII, SERIE X
DEL NUOVO CIMENTO

N. 2, 1960
4° Trimestre

Further Research on the Fine Structure of Leptospirae.

B. Babudieri and D. Steve Bocciarelli

Istituto Superiore di Sanità - Roma

1. – Introduction.

Previous papers [1-3] have described the morphology of leptospirae as seen with the electron microscope. It was possible to show that no obvious structural differences existed between the various serological types of this spirochaete or between pathogenic and saprophytic leptospirae. It was shown that the leptospira consists of a fairly homogeneous cytoplasmic cylinder, wound around a central filament: the axostyle. This is probably contractile and involved in the motility of the leptospira. A fine surface membrane encloses the organism (Fig. 1). After certain initial discrepancies, this description has now been accepted by all later workers.

Certain features, however, of the structure of the leptospira, particularly concerning the surface membrane and the axostyle, have not been completely clarified. An attempt has now been made to settle these points using new techniques introduced into electron microscopy in the last years.

First ultra-thin sections were studied, which had been obtained from masses of spirochaetes from cultures in liquid media subjected to either the action of a specific antiserum or to high speed centrifugation. Fairly compact masses of spirochaetes were thus obtained, which were able to withstand fixation with 2% osmic acid, passage through the alcohols and embedding in acrylic resin. Sections were observed both directly and after staining with phosphotungstic acid.

Observations were also made on leptospirae after subjecting them to treatment with 2% sodium taurocholate or penicillin, or to trypsic digestion. It was possible to obtain a partial lysis of the organisms which facilitated the observation of certain structural features. After such a treatment the leptospirae were fixed in 2% osmic acid an then repeatedly washed in the centri-

fuge with doubly-distilled water. Observations were made both directly and after staining with phosphotungstic acid.

These techniques made possible a more thorough study of the structure of this spirochaete, with the following results.

2. – Enveloping membrane.

This fine membrane is perfectly homogeneous. It encloses the entire body of the spirochaete and there is a narrow space, which is transparent to electrons, between it and the cytoplasmic cylinder. The space is absent only where the membrane adheres to the underlying axostyle. It is not to be considered as an artefact since it is visible not only in sections but also when using the replicas technique [3] (Fig. 2).

The membrane is highly elastic which allows it to swell without breaking in hypertonic solutions of sodium chloride (Fig. 3). The membrane still does not show any structure even when so distended.

3. – Protoplasmic cylinder.

The cytoplasm appears to be homogeneous and opaque to electrons in the majority of leptospirae observed either whole or in section. Neither filaments, granules, nor the transparent areas—so characteristic of some treponema and the spirilli—are visible. In some cases, particularly with certain cultures of leptospirae of the « australis » serotype, the cytoplasm is less opaque and shows the presence of a series of dark granules which are rounded and of equal or even larger diameter than that of the leptospirae. These granules give the leptospirae the appearance of pods (Fig. 4, 5). However this special appearance, which is accompanied by changes in the motility and growth of the leptospirae, is thought to be pathological. The granules cannot be spores because those cultures which have granules do not show any greater resistance than those which do not have them.

It is probable that the cytoplasmic cylinder is bounded by a second membrane as in the schizomycetes. In fact when the external membrane is destroyed with sodium desoxycholate or trypsin, the spirochaete does not at once dissolve but retains its shape, at least for some time. However this second membrane can not be clearly distinguished in the preparations and it possibly consists merely of a denser peripheral zone of the cytoplasm.

4. – Axostyle.

The axostyle has been described by the present authors, as a slender filament running the length of the spirochaete body (Fig. 1, 6). In reality it has a rather more complicated structure which has been revealed, in particular, by the study of ultra-thin sections in both the longitudinal and transverse directions (Fig. 7-10). A transparent space exists about the fine central filament, which represents a slender canal enclosing the filament itself. This canal through the cytoplasm probably has its own membrane although this is difficult to distinguish. It could be seen from transverse sections that the axostyle has a peripheral position within the canal and probably adheres to its wall, through which it comes into close contact with the enveloping membrane of the leptospira.

The existence of this canal was confirmed in partially lysed but unsectioned leptospirae. Treatment with sodium desoxycholate, trypsin or penicillin dissolves, usually entirely, the enveloping membrane; the cytoplasm is lysed and the axostyle liberated (Fig. 11, 12). The latter retains its structure. It can be deduced that the axostyle is particularly firmly attached at the end of the leptospira and is inserted subterminally into the cytoplasma with two small disc shaped plates which recall the kineto-nuclei of some protozoa. The axostyle filament starts from the center of such a disc (Fig. 14). When the axostyle is liberated completely from the body of the spirochaete, by its dissolution, it always has the small disc at one end and terminates at the other in a long fine point. Axostyles which are partially detached from leptospirae never appear to be attached at both ends to the leptospirae: they are attached only at the end having the disc, whilst the pointed end remains free. Moreover the length of the axostyle—which is virtually constant for every strain and culture—does not corrispond to the average length of the respective spirochaetes but is only about one third of this. For example, axostyles of the *Bindjei* strain measure (3.2 ± 0.1) μm, those of the *Ballico* strain (2.9 ± 0.08) μm and those of the *AR* 18 strain (2.9 ± 0.06) μm (on 28 measurements) but the average length of leptospirae of the last two strains is 9.4 μm (on 43 measurements).

To explain these observations it is necessary to assume that the axostyle is not a single continuous filament but consists of two segments, each one inserted at one end by its disc, at opposite ends of the leptospirae and with the other end pointed. The two pointed ends of the segments meet in the centre of the leptospira, possibly fusing together or simply lying side by side for a short distance. However this does not explain why each individual free filament corresponds to a third rather than a half of the length of the leptospira. It must, however, be remembered that the axostyle is elastic, as can also be seen from the manner in which the free axostyles fall into coil. It is probable

1200

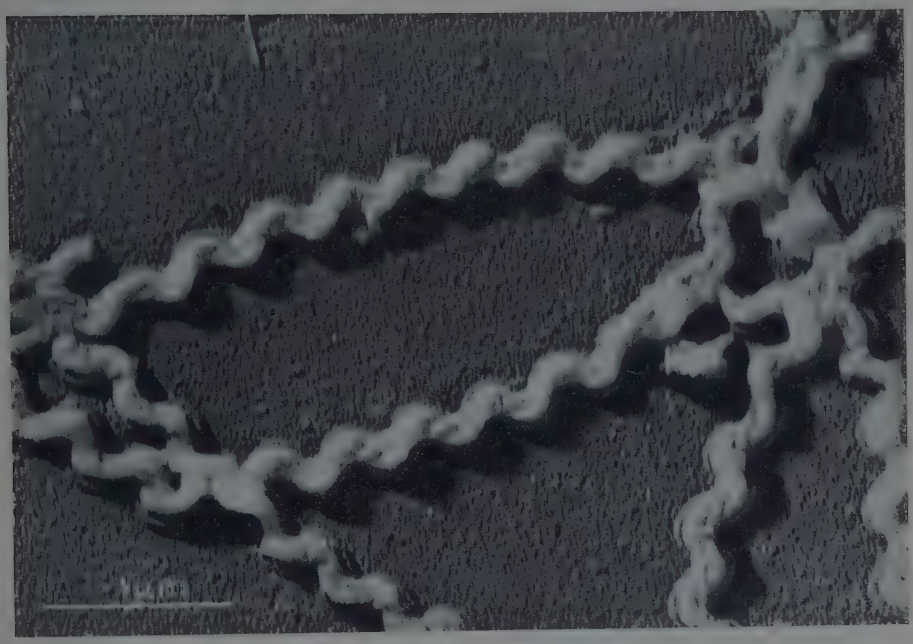

Fig. 1. – *Leptospira ictero-haemorrhagiae* shadowed with cromium.

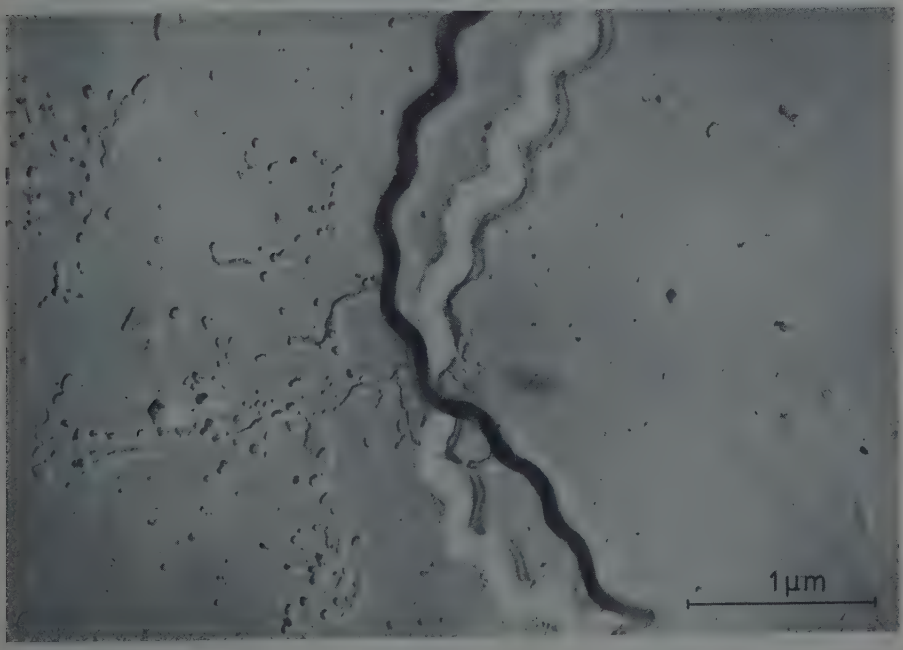

Fig. 2. – *Leptospira ictero-haemorrhagiae* and its replica.

Fig. 3. – *Leptospira ictero-haemorrhagiae* in hypertonic solution of NaCl, shadowed with cromium.

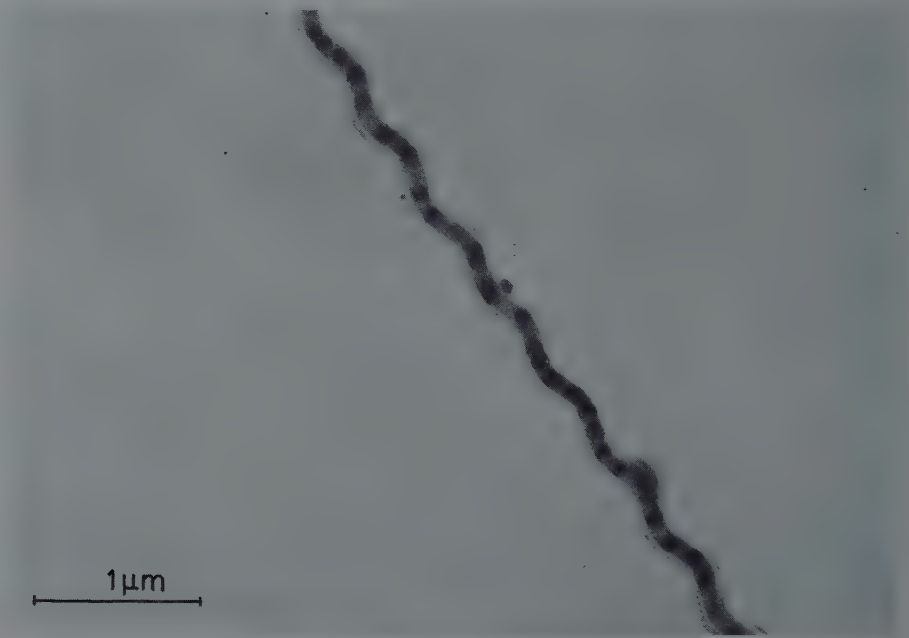

Fig. 4. – Dark granules in *Leptospira australis*, strain « Ballico ».

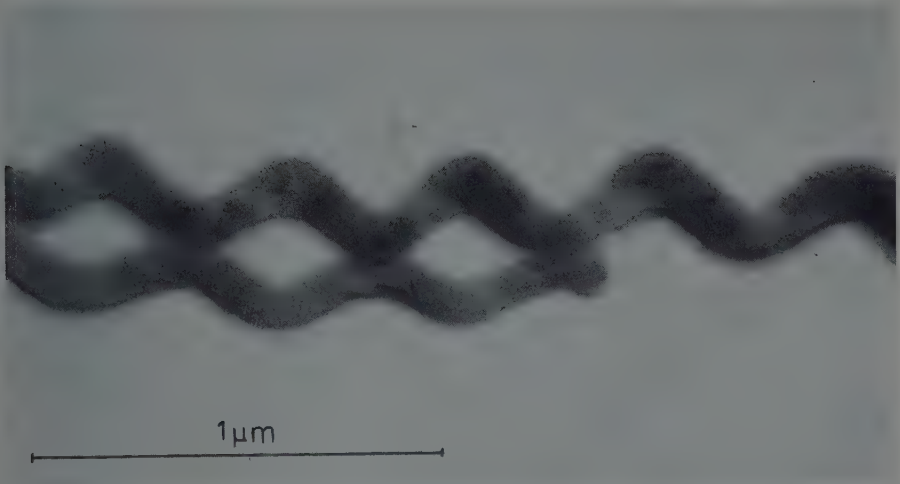

Fig. 5. – *Leptospira australis*, strain « Ballico ».

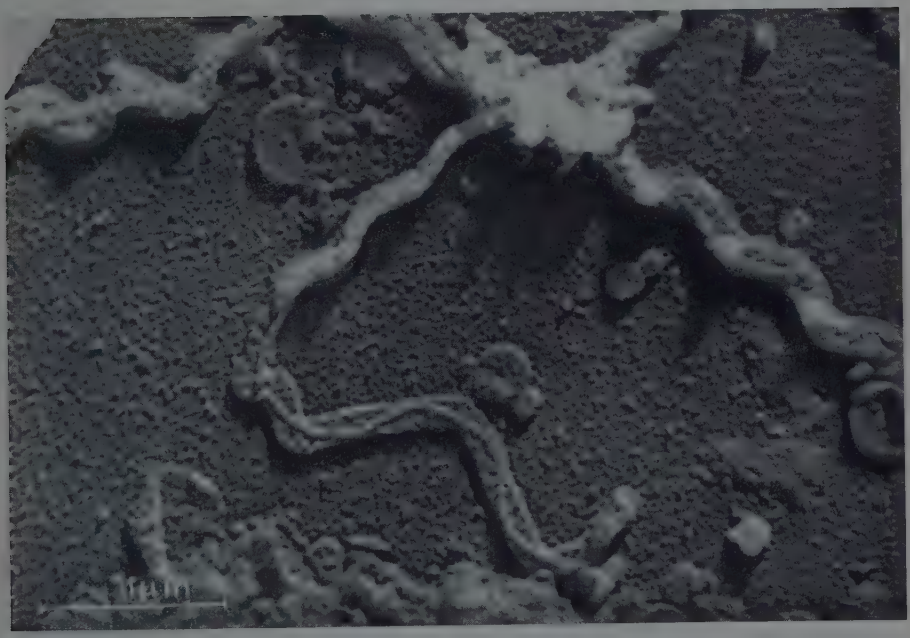

Fig. 6. – *Leptospira biflexa* partially lysed, shadowed with chromium. The axostyle is contained in the enveloping membrane.

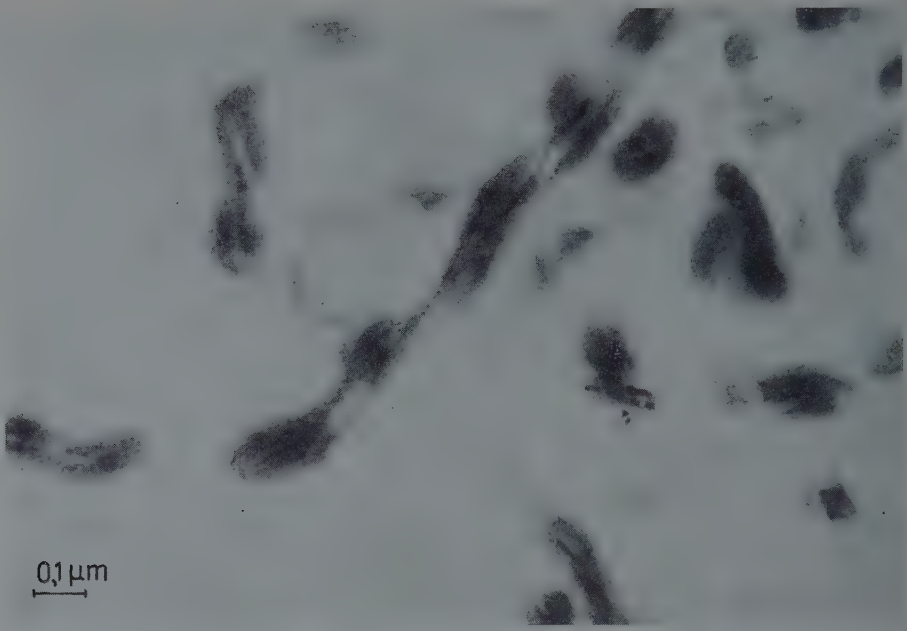

Fig. 7. – Section of *Leptospira australis* fixed in OsO_4 and embedded in methacrylate.

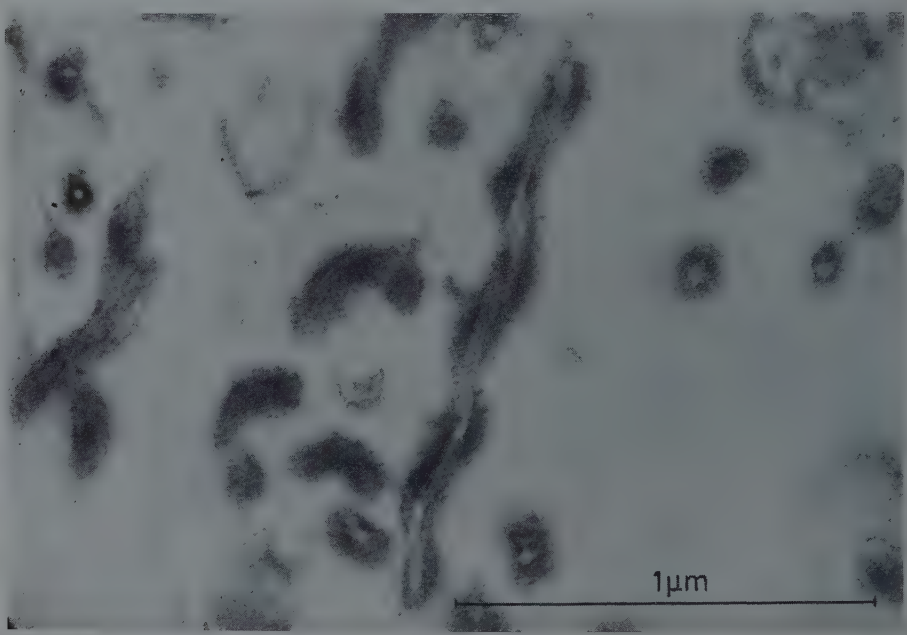

Fig. 8. – Section of *Leptospira australis* fixed in OsO_4 and embedded in methacrylate.

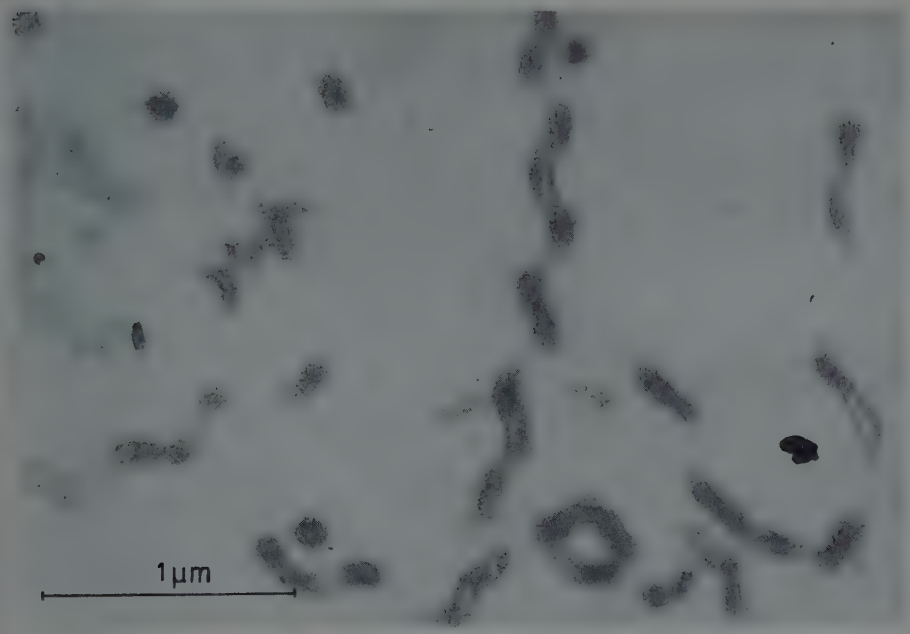

Fig. 9. – *Leptospira erinacei europaei* fixed in OsO_4 and embedded in methacrylate.

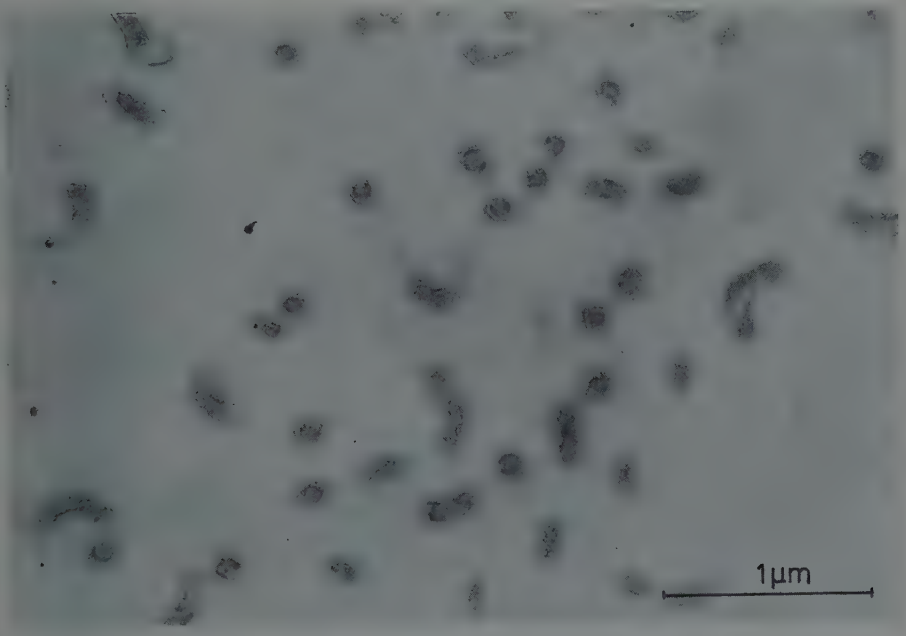

Fig. 10. – *Leptospira erinacei europaei* fixed in OsO_4 and embedded in methacrylate.

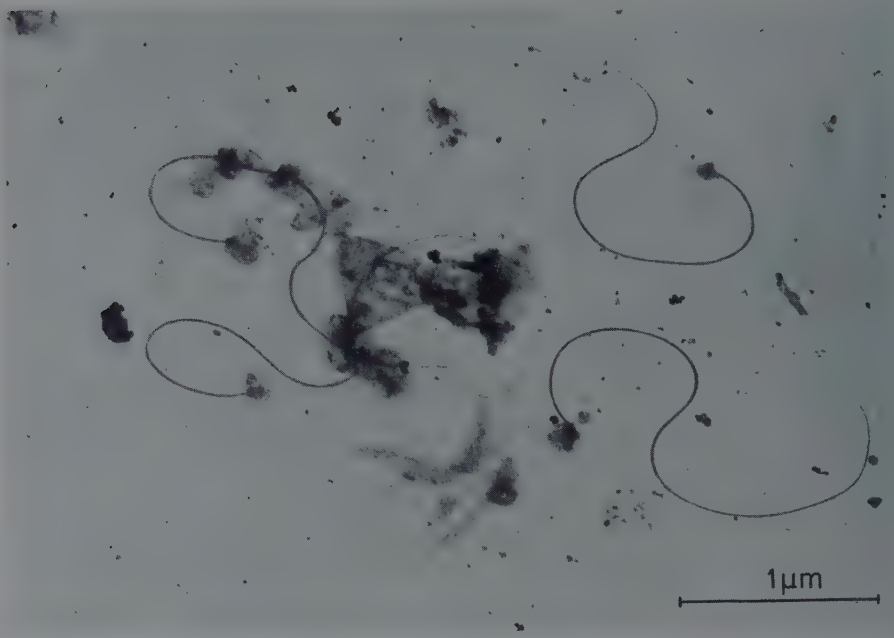

Fig. 11. – Axostyles from *Leptospira* lysed by Na desoxycholate.

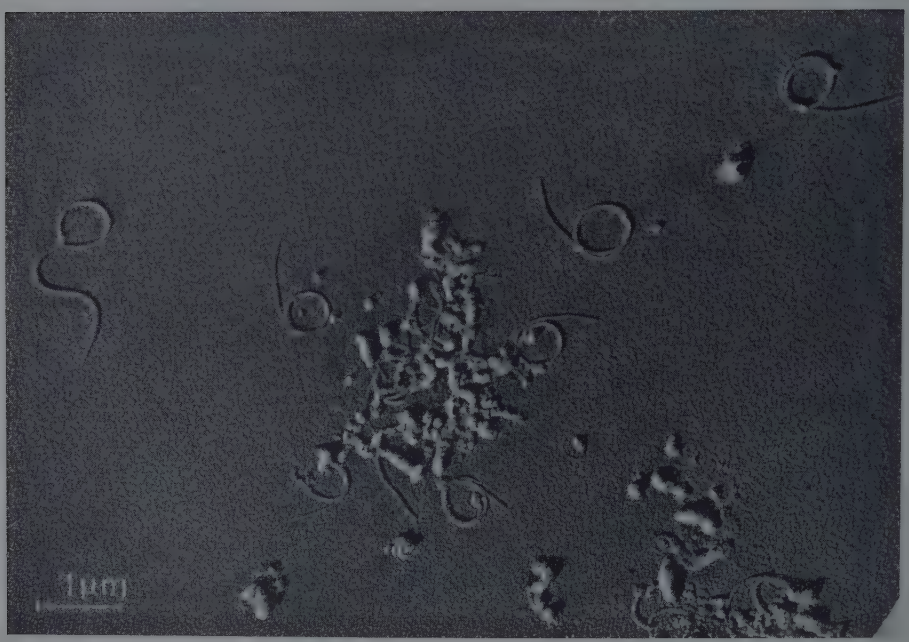

Fig. 12. – Axostyles from *Leptospira* lysed by Na desoxycholate, shadowed with cromium.

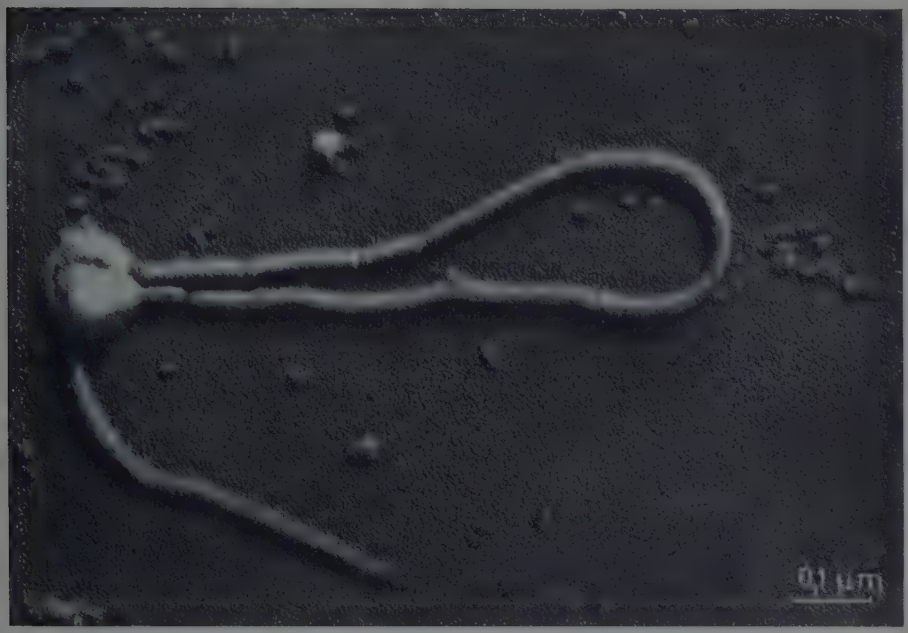

Fig. 13. – Axostyle at high magnification.

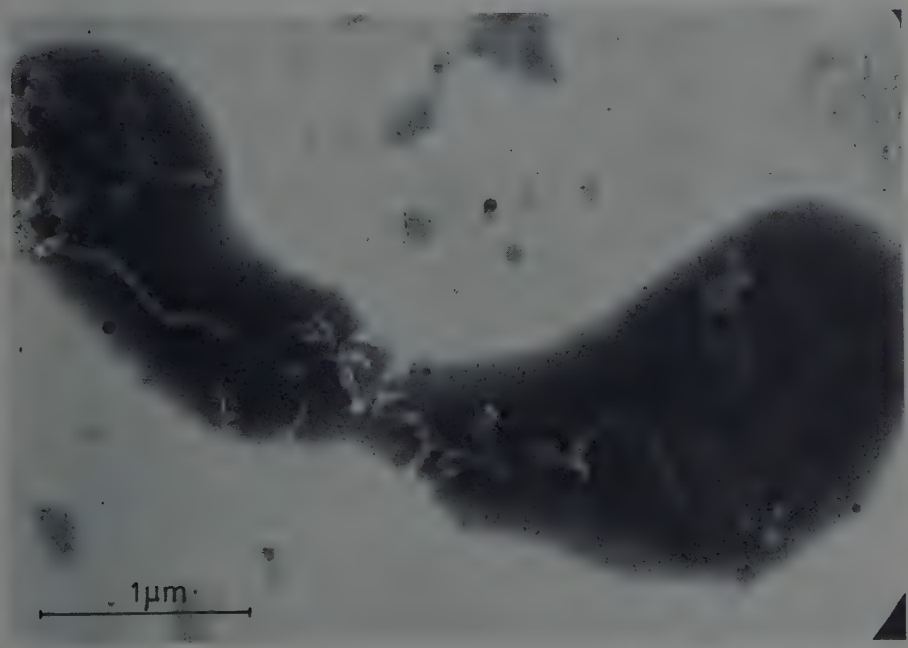

Fig. 14. – *Leptospira* negatively stained with phosphotungstic acid.

that the axostyle within the leptospira is normally under tension and that on liberation it contracts and becomes shorter.

Two other explanations are possible of the difference in length of the filament and the spirochaete. Firstly, the filament might be absent from the central part of the organism or secondly, a third central segment of the filament might exist. Of these explanations the first is not tenable because it is possible to see in the intact spirochaete that the axostyle runs right through the whole body of the organism; the second is also not tenable since lysis of the organisms never reveals any intermediary segments.

It may be supposed that, like other contractile structures, the axostyle would have a periodic organization; but observations at high magnification (up to 80 000 ×) (Fig. 13), even after phosphotungstic acid treatment (Fig. 14), showed it to be perfectly homogeneous without any periodicity.

The axostyle is certainly the most interesting structure possessed by the leptospirae and is certainly their locomotive organ. They move in liquid media with a characteristic screwing motion. They have no polarity, moving indifferently with either end foremost. It is believed that the axostyle filament adhering to the canal wall and through this to the enveloping membrane of the leptospira, produces by its successive contractions and relaxations a winding and unwinding of the micro-organism's spiral. This in turn leads to the movement of the organism through the medium. It is also possible that the contraction of the filament also lead to a flattening of the leptospira or its membrane which, by increasing its resistance to the medium in which it is immersed, facilitates its movement.

* * *

It is a pleasure to indicate the technical assistance of A. Chiozzotto, F. Piccirilli, F. Tangucci, N. Tomassini and F. Valente.

REFERENCES

[1] B. Babudieri: *Rend. Ist. Sup. Sanità*, **11**, 1046 (1948).
[2] B. Babudieri: *Erg. Mikrobiol., Immf. u. exp. Ther.*, **33**, 259 (1960).
[3] B. Babudieri and D. Steve Bocciarelli: *Rend. Ist. Sup. Sanità*, **17**, 456 (1960).

found experimentally in the bone could be higher (up to 2.26 [2]) than the molar Ca/P ratio corresponding to the above formula (2.15).

The ideal procedure for elementary analysis with X-rays is to use a monochromatic source emitting only rays of the same energy as the K line of the absorbing elements [3]. Elements of biological specimens, however, have their characteristic absorption lines in the very soft X-ray spectrum, that is they need a low energy source. To obtain good resolution in the primary image of the specimen produced with X-rays, it is necessary to use a point source. A monochromatic point source of very low energy (a few thousand volts) would be of such a low intensity that exposures would become extremely long. To avoid this difficulty an interesting method was used by ROWLAND, JOWESY and MARSHALL [4] for the quantitative analysis of Ca in bone. The same method has been used with better resolution in the present work and some preliminary results are given here.

The principle is to use a polychromatic source able to give parallel absorption curves for Ca, P and a standard element Al (Fig. 1). This condition is satisfied for X-rays produced by a tungsten target tube operated at 10 kV and filtered by 1 mm of beryllium.

If we neglect the X-ray absorption due to O, H, and the trace elements present in bone, whose amount is less than 1% of the total absorption, it is possible to determine the contribution of P with respect to Ca on the basis of the Ca/P ratio in the bone salt and the ratio of the mass absorption coefficients of these elements. The absorption by Ca may then be deduced from a comparison with the absorption by a reference system of aluminium sheets.

The following procedure was used.

Sections of ox femur diaphisis, (30÷40) μm thick, were exposed to X-rays together with a step wedge of aluminium foils, each step being 6.9 μm thick. In the experimental apparatus used [7] the osseous tissue and the reference system are pressed under vacuum against a fine-grained photographic emulsion (Kodak 649) having 1 μm resolving power. A 40 fold photographic enlargement of the microradiographic image of the section and of the reference system was made, and on this the microphotometric determinations were made. Fig. 2 gives an example of such an image, whose characteristic features are well known after the researches of AMPRINO and ENGSTRÖM [5] and VINCENT [6].

The light beam of the spectrophotometer was reduced to a useful circular section of 0.1 mm diameter. Using the enlargement of 40×, a resolving power of 2.5 μm is obtained on the bone section and it is possible to choose, in this manner, sufficiently uniform regions avoiding the presence of osteocytes. These regions were carefully identified on the microphotograph and in the section of the bone, and on the latter the measurements of thickness were made with the technique suggested by ROWLAND, JOWSEY and MARSHALL [4], by

which it is possible to limit the measured spot to 40 μm [5] with an error of 2%.

With the same sensitivity of the apparatus, microphotometric readings of the selected zone and of the step wedge system were made (Fig. 3 and 4). In Fig. 5 the ratios area/base of the photometric patterns are plotted against the corresponding Al thickness. The transparency of the photographic plate background was taken as 100. The ratios area/base found on the selected zones were recorded in the same units and the corresponding thickness of Al was found.

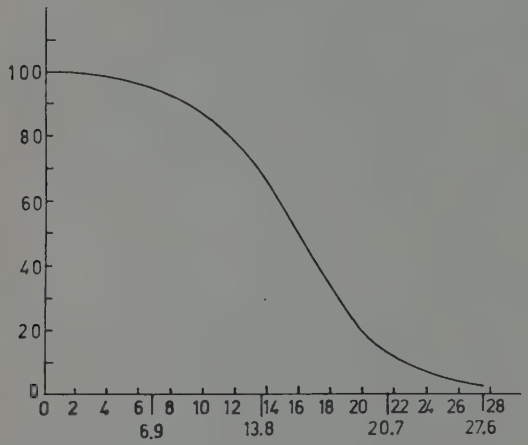

Fig. 5. – Ratios area/base of photometric patterns plotted against the corresponding Al thickness.

It is, of course, necessary to make rigorous controls for every operation in order to obtain significant results — uniform illumination for the microphotographs and the photographic enlargements, and constant sensitivity of the microphotometric apparatus.

In order to check the precision of the delimitation of the zones explored and of the reference system, four photometric determinations were made of the same zone, and of the corresponding step wedge, on the same plate, giving

TABLE I. – *Calcium density values from osteons marked in the cross section of ox bone.*

old osteons		young osteons	
zone	Ca (g/cm³)	zone	Ca (g/cm³)
1 sup.	0.540	8	0.451
1 inf.	0.535	9	0.455
2	0.533	10	0.382
3	0.560	11	0.360
4	0.564	12	0.428
5	0.583	13	0.397
6	0.558	14	0.391
7	0.560	15	0.387
—	—	16	0.381
—	—	17	0.363
—	—	18	0.374
—	—	19	0.417
mean value	0.55 ± 0.01	mean value	0.40 ± 0.01

the result: 0.392 ± 0.002. Moreover, six microradiographic images of the same two zones and the corresponding enlargements and microphotometric measurements gave the results: 0.50 ± 0.02 and 0.39 ± 0.02.

On a cross-section of bone from about 30 to 38 μm thick a series of measurements was performed whose results are summarized in the Table I.

On a longitudinal section, from about 35 to 50 μm thick, we had the results of Table II, that may be considered consistent with those of the former series, according to the estimate of the standard deviation of means.

TABLE II. – *Calcium density values from osteons of a longitudinal section of ox bone.*

old osteons		young osteons		interstitial lamellae	
zone	Ca (g/cm³)	zone	Ca (g/cm³)	zone	Ca (g/cm³)
23	0.420	20	0.320	37	0.575
24	0.470	21	0.340	38	0.501
26	0.374	22	0.273	39	0.530
28	0.547	25	0.363	40	0.505
32	0.542	27	0.385	43	0.534
33	0.510	29	0.440	44	0.520
34	0.547	30	0.550	45	0.552
35	0.602	31	0.447	—	—
36	0.575	—	—	—	—
41	0.484	—	—	—	—
42	0.515	—	—	—	—
mean value	0.51 ± 0.03	mean value	0.39 ± 0.03	mean value	0.53 ± 0.02

On the contrary, it is difficult to say if our results really depart from the values found by ROWLAND, JOWSEY and MARSHALL in cow, in spite of the fact they give higher values both for the low density (0.444 g/cm³) and the high density osteons (0.600 g/cm³). In fact their results lack an estimate of the reliability of their measurements data.

Our determinations were made on the hypothesis that the Ca/P ratio in the bone was that given from the hydroxyapatite formula; that is 2.15. If the highest value found experimentally, 2.26, is used, the density calculated has about an 1% higher value; which difference is clearly within the measurement errors.

* * *

The authors wish to express their grateful thanks to G. BUONVINO and N. MORTARA for their valuable technical assistance.

REFERENCES

[1] R. KLEMENT: *Zeits. Physiol. Chem.*, **184**, 132 (1929).
[2] M. J. DALLEMAGNE and C. FABRY: *Structure of bone salts, A Ciba Found. Symp. on Bone Structure and Metabolism* (London, 1956).
[3] A. ENGSTRÖM: *Acta Radiol. Suppl.*, **63**, 63 (1946).
[4] R. E. ROWLAND, J. JOWSEY and J. H. MARSHALL: *Radiation Res.*, **10**, 234 (1959).
[5] R. AMPRINO and A. ENGSTRÖM: *Acta Anat.*, **15**, 1 (1952).
[6] J. VINCENT: *Recherches sur la constitution de l'os adulte (Thèse de l'Université de Louvain)* (Bruxelles, 1955).
[7] A. ASCENZI, V. MARINOZZI and D. STEVE BOCCIARELLI: *Rend. Ist. Sup. Sanità*, **21**, 843 (1958).

1206

SUPPLEMENTO AL VOLUME XVIII, SERIE X
DEL NUOVO CIMENTO

N. 2, 1960
4° Trimestre

The Problem of Evaluating the Biological Significance of Sigmoidal X-Ray Inactivation Curves in Yeasts (*).

G. E. MAGNI

Istituto di Genetica dell'Università - Pavia

Introduction.

The analysis of dose-effect relationships in the killing action of ionizing radiations has offered very substantial data for the interpretation of the structure of genetic material and of the mechanisms of radiation lethal action in very simple organisms such as phages.

For more complex type of cells and namely for organisms of ploidy higher than 1, however, the inactivation curves are often sigmoidal and therefore not very easy to be correctly interpreted. Practically, very few criteria are available for their interpretation such as the shape of the curve and multiplicity, all of them still endowed with very doubtful significance.

Some speculations have been recently made on these types of curves and the theory applied to a few particular cases. ATWOOD and NORMAN [1] for example, discussed the distinction between a « multi-hit, single hit per unit hypothesis » and a « multi hit per unit hypothesis » and preferred the first one for the U.V. inactivation of *Neurospora crassa* conidia. TOBIAS [2] interpreted the X-ray sigmoidal inactivation curves of diploid yeast cells on the basis of a « recessive lethal defect theory » and calculated the possible number of sensitive sites per cell.

But, in spite of these useful trials there still is a general feeling among radiation biologists that sigmoidal curves are too complex for any reliable formal analysis.

(*) This work was supported by a grant of the Comitato Nazionale per l'Energia Nucleare, Rome.

As a matter of fact, however, deeper understanding of the biological elementary effects of radiations achieved by means of classical genetical techniques can help in resolving the complexity of the experimental curves into different well defined components. Only after such knowledge is reached it can be integrated into mathematical expressions which could eventually account for all the parameters of the complex experimental curves.

Some few example will illustrate this point of view.

1. – Haploid-diploid inactivation curves.

Since the first findings by LATARJET and EPHRUSSI [3] it was noticed that the exponential inactivation curve of haploid strains of *Saccharomyces cerevisiae* show a slope different from the exponential fraction of sigmoidal killing curve of diploid strains of the same species. Fig. 1 shows a typical example of this result.

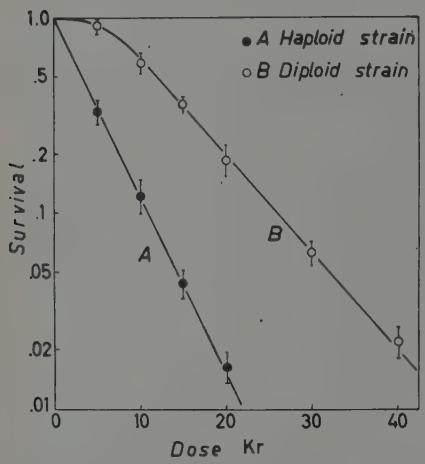

Fig. 1. – X-ray inactivation curves of haploid and diploid *Saccharomyces cerevisiae*.

TOBIAS [2] gave the first formal interpretation of the two types of inactivation curves assuming that the damage could be equivalent to recessive lethals and therefore one single event would be lethal for haploid cells while two independent events in homologous sensitive sites should be necessary for killing diploid cells. This interpretation, however, did not account for the different slopes found experimentally.

To-day, on the basis of genetic data available, we can give, a new interpretation which can account for the observed differences in slope. It has been demonstrated rather clearly (OWEN and MORTIMER [4]) that X-ray induced lethality in yeast is due to two main types of damage: recessive and dominant. In addition the same Author has demonstrated that recessive lethality accounts for a higher proportion of the killing action in haploid cells than in diploid cells. If it is assumed that the efficiency per ionization in inducing recessive lethals is higher than for dominant lethals, the difference in slope can be easily justified.

2. – Relationship between ploidy and radiosensitivity.

MORTIMER [5] has proved that radiosensitivity increases constantly from diploidy to higher ploidies. Some features of the inactivation curves of strains of different ploidy can help in suggesting a tentative interpretation on the basic lethal mechanism in these organisms. The multiplicity (*) of the sigmoidal curves for different ploidies seems to be rather constant as shown in Table I.

TABLE I. – *Multiplicity of sigmoidal X-ray inactivation curves in yeast strains of different ploidy.*

Ploidy	Multiplicity		
	Partial data	Reference	Average
Diploid	2.9 (*); 2.0 (*); 2.1 (*)	MORTIMER [5]	2.13
	2.0; 1.7; 2.1	MAGNI (unpublished)	
Triploid	2.1 (*); 2.2 (*); 1.8 (*); 2.1	MORTIMER [5]	2.05
Tetraploid	2.0 (*)	MORTIMER [5]	2.10
	2.2	MAGNI (unpublished)	
Pentaploid	1.5 (*)	MORTIMER [5]	1.50
Hexaploid	1.6 (*)	MORTIMER [5]	1.60
			$\bar{x}=1.87$

(*) Multiplicity data from MORTIMER [5] have been calculated graphically from very small figures and are therefore subject to a rather large error.

If these data will be confirmed on a larger scale one could conclude that multiplicity is not affected by ploidy, as for any chromosomal set it is not significantly different from 2.0 or if any, is affected in the wrong direction. This would allow an interpretation of the mechanism of killing action. It has been already mentioned that dominant lethals are more efficient than recessive ones in killing yeast cells of ploidy higher than 1. The constant multiplicity of 2.0 may be taken to mean that the basic phenomenon is a two hit damage, probably two breaks in a chromosome leading to large deficiencies or other aberrations, which behave as completely dominant lethals in any chromosomal set. The higher sensitivity of higher ploidy can be simply interpreted as due to an increased number of available targets (chromosomes).

(*) « Multiplicity » is here taken as the cutoff at the ordinate of the extrapolated linear portion of the curve.

3. – Inactivation of multispore asci.

The final result of meiosis in diploid yeasts is the formation of asci containing one to four haploid spores. When asci are transferred into complete media, spore germination takes place, the ascus wall is dissolved and spore either grow in haploid clones, or copulate pair-wise to reconstruct diploid chromosome sets. It was believed that yeasts asci could form a good material for testing the agreement with the theory of experimental survival curves.

One should expect 1-spore asci to give exponential survival (as proved true for haploid vegetative cells) and that 2-3-4 spored asci should give sigmoidal curves with predictable slope and multiplicity. Assuming the survival for 1-spore asci

$$N/N_0 = \exp[-kd] \tag{1}$$

the expected sigmoids should be

$$\text{for 2-spore asci } N/N_0 = 1 - (1 - \exp[-kd])^2 , \tag{2}$$

$$\text{for 3-spore asci } N/N_0 = 1 - (1 - \exp[-kd])^3 , \tag{3}$$

$$\text{for 4-spore asci } N/N_0 = 1 - (1 - \exp[-kd])^4 . \tag{4}$$

A sporulated culture of a diploid strain of *Saccharomyces cerevisiae* (157 *d*) was irradiated with different doses of soft X-rays (Gilardoni Neodermo Be, berillium window, 5.150 r/minute 0.1 Al filter at 70 kV 5 mA, water hemivalent layer 2.2 mm) and the four different types of asci isolated at the micro-manipulator, the formation of visible colonies from each ascus being scored after 72 hours.

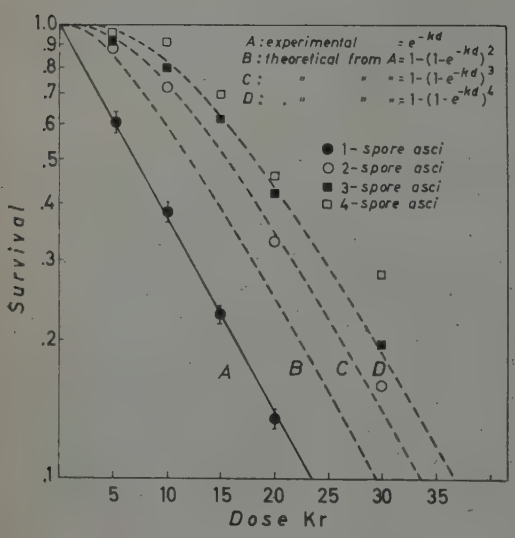

Fig. 2. – X-ray inactivation of single- and multispored asci of *Saccharomyces cerevisiae*. For the explanation see test.

Fig. 2 shows the results of such experiment. The continuous exponential line is the experimental survival of 1-spore asci, the dotted sigmoidals are the expected survival for 2, 3 and respectively 4-spore asci from the above expressions (2), (3), (4). As it can be easily seen there is practically no agreement between the experimental results and the theoretical expectation. The survival of 2-

spore asci fits rather well with the theoretical curve for 3-spore asci and the experimental survival of 3 and 4-spore asci fits respectively with the expectation of 4-spore and possibly 5-spore asci. This apparent shifting of one « grade » can not be justified in any way on the basis of theoretical expressions until a more careful analysis of survivors at different doses is performed.

Some of the survivors from multispore asci are diploid clones while, with no exception, all survivors from 1-spore asci are haploid. This proves that copulation takes place between spores at the time of germination in multispore asci as it is known (OWEN and MORTIMER [4]) that even « killed » haploid cells, *i.e.* cells which will not give rise to a visible colony, can still copulate with other cells of the opposite mating type. This observation can account for the discrepancy between expected and observed survival, from multispore asci. In fact, let us assume, as an example, that in all the 4 spores of an ascus a lethal damage has been induced. The four spores will not survive if separated each other, but in natural conditions, such as those of our experiment, the spores can copulate pair wise and give rise to a viable zygote if the damage induced in any one of the two partners is recessive. The consequence will be a survival higher than expected from the theoretical expression. Proper experiments were planned to check by the correctness of this interpretation. The surviving diploids were analysed for the presence of recessive lethals. A zygote of the type described above would yield $\frac{1}{2}$ asci showing two viable spores after dissecting and $\frac{1}{2}$ showing no survival among the four spores, because of the expected random distribution of chromosome carrying the lethals. The frequency of these type of zygotes among the diploid survivors from multispore asci was experimentally estimated for some doses and the results are reported in Fig. 3, where the experimental points are the same of Fig. 2 corrected for the presence of *double unpaired lethals*.

The agreement between the experimental finding and the theoretical expectation is now substantially impro-

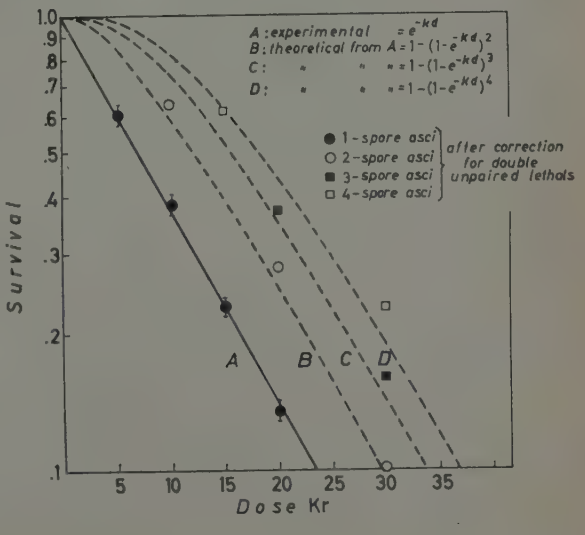

Fig. 3. – X-ray inactivation of single- and multi-spored asci of *Saccharomyces cerevisiae*. For the explanation see text.

ved. Considering the fact that our estimate of the frequency of induced lethals is short of the true value because some lethals are lost due to reversion and some of the lethality induced in spores is not genetic (MAGNI [6]), the agreement with theory should be perfectly acceptable.

From these few instances it seems that sigmoidal inactivation curves do not represent a serious obstacle for the study of the effects of ionizing radiations provided a discrimination between different components of lethality can be carried out on genetical or cytological bases. PUCK [7] has recently given a proof of the validity of an approach of this type for mammalian cells culture in vitro. Some features of this types of cells differ from what is known for yeasts as, for instance, the increasing radioresistance with increasing ploidy. The general conclusions reached by the author, however, based on the integration of biophysical and cytological data in theoretical expressions, are basically identical to the one mentioned above for yeast.

REFERENCES

[1] K. C. ATWOOD and A. NORMAN: *Proc. Nat. Acad. Sci., Wash.*, **35**, 696 (1949).
[2] C. A. TOBIAS: in *Symposium on Radiobiology* (J. J. NICKSON, ed.) (New York, 1952), p. 357.
[3] R. LATARJET and B. EPHRUSSI: *Compt. Rend.*, **229**, 306 (1949).
[4] M. E. OWEN and R. K. MORTIMER: *Nature*, **177**, 625 (1956).
[5] R. K. MORTIMER: *Radiation Res.*, **9**, 312 (1958).
[6] G. E. MAGNI: *Radiation Res., Suppl.*, **1**, 347 (1959).
[7] T. T. PUCK: *Amer. Nat.*, **94**, 95 (1960).

SUPPLEMENTO AL VOLUME XVIII, SERIE X
DEL NUOVO CIMENTO

N. 2, 1960
4° Trimestre

Analisi di alcuni fattori sperimentali che influenzano le curve di sopravvivenza ai raggi X di cellule umane coltivate in vitro.

G. Marin, F. Nuzzo e L. De Carli

Istituto di Genetica dell'Università - Pavia

1. – Introduzione.

L'azione elementare delle radiazioni può esser oggi studiata su ceppi cellulari di mammiferi coltivati *in vitro*, grazie ai recenti sviluppi delle tecniche di coltura. L'adattamento alle condizioni di coltura comporta nelle cellule modificazioni fisiologiche che non permettono di estrapolare direttamente dai risultati ottenuti *in vitro* dati validi per gli organismi pluricellulari da cui le cellule coltivate provengono; tuttavia questo inconveniente è largamente compensato dal vantaggio di ottenere risultati quantitativi, con una precisione prossima a quella offerta dalla tecnica microbiologica.

Attualmente si dispone di terreni nutritivi semi-sintetici che consentono per la maggioranza dei ceppi cellulari stabilizzati *in vitro* un'alta efficienza di piastramento, indipendentemente dall'ammontare dell'inoculo, fino alle concentrazioni cellulari più basse. L'esser riusciti ad ottenere colonie cellulari distinte dalla moltiplicazione di singole cellule isolate, permise a Puck e Marcus [1] e Puck *et al.* [2] di costruire curve di inattivazione ai raggi X di cellule umane (ceppo HeLa e cellule normali) con tecnica analoga a quella in uso per i microorganismi: per inattivazione era intesa la perdita della capacità riproduttiva e la sopravvivenza era valutata in base al numero di colonie sviluppatesi dal piastramento di sospensioni cellulari a titolo noto, irradiate con dosi crescenti.

I dati di Puck e Marcus [1] si adattano ad una curva teorica espressa dall'equazione di Atwood e Norman [3]:

$$N/N_0 = 1 - (1 - \exp[-kd])^n , \tag{1}$$

con un valore di n che sta fra 2 e 3.

L'equazione (1) esprime la sopravvivenza ad una dose d di una popolazione di N_0 individui ognuno dei quali presenta n ambiti sensibili, che devono tutti venir indipendentemente inattivati per portare a morte l'organismo; l'uccisione avverrebbe per un solo meccanismo, cioè per inattivazione di n ambiti aventi tutti la stessa sensibilità: l'inattivazione di ciascuno di essi dipenderebbe solo dalla probabilità, uguale per tutti, di essere interessato da una o più ionizzazioni. Essendo tale probabilità espressa dalla serie di Poisson, ne deriva la relazione esponenziale che lega la sopravvivenza alla « sezione d'urto » di questi ambiti sensibili e al numero di eventi ionizzanti, espressi dalla dose di radiazione. Per $n = 1$ l'equazione descrive una curva esponenziale semplice: l'inattivazione di molti organismi elementari segue questo andamento (per esempio, virus, lieviti aploidi, ecc.). Coll'aumentare di n la curva finisce per non distinguersi più da una sigmoide, quale si avrebbe se la sensibilità all'azione letale delle radiazioni fosse un carattere variabile avente una distribuzione normale nell'ambito della popolazione. Questa seconda interpretazione tuttavia non tien conto dell'aspetto fisico del danno e non spiega da cosa dipenda la sensibilità alla radiazione, ma si basa solo sulla constatazione che nelle popolazioni omogenee i caratteri a variabilità continua sono distribuiti normalmente. In realtà, se si tien conto del fatto che la radiazione X cede energia in modo tipicamente discontinuo (ionizzazione), e che organismi unicellulari vengono uccisi da dosi a cui l'energia apportata globalmente per cellula è estremamente bassa, si deve ammettere che il danno si esplichi là dove l'energia si libera per interazione primaria fra radiazione e substrato, e inoltre che nella cellula vi siano delle strutture gerarchicamente più importanti, di dimensioni tali da poter esser inattivate con una o poche ionizzazioni, e dalla cui attività dipendono le funzioni vitali della cellula.

In pratica, solo in pochi casi è possibile avere la conferma diretta di un modello costruito in base alla forma di una curva di sopravvivenza, ma anche la sola interpretazione formale secondo equazioni del tipo della (1) ha il vantaggio di fornire due misure della sensibilità di un determinato organismo, teoricamente indipendenti: n (molteplicità) e k (sezione d'urto). Secondo l'interpretazione corrente il valore di n dipenderebbe da caratteristiche genetiche della cellula e sarebbe quindi relativamente stabile, a differenza di k, o sensibilità dei singoli ambiti, soggetto a variare con le condizioni ambientali.

Nel presente lavoro vengono discusse, secondo l'interpretazione formale suesposta, curve di sopravvivenza ottenute da un ceppo di cellule a carattere epitelioide di embrione umano normale (EUE), stabilizzato *in vitro* da Terni e Lo Monaco [4]. In particolare vengono analizzate alcune fra le possibilità e i limiti tecnici inerenti al metodo di stima della sopravvivenza per conteggio di colonie sviluppatesi su piastra.

2. – Materiale e Metodi.

Il ceppo EUE, a carattere epitelioide, coltivato in terreno di Eagle (Eagle [5]) con 10% di siero umano, presenta un periodo di raddoppiamento di circa 33 ore.

Le curve di sopravvivenza furono costruite in base alla capacità di cellule singole a formar colonie macroscopiche dopo irradiazione, secondo la tecnica descritta da Puck *et al.* [2, 6].

Sospensioni cellulari monodisperse furono ottenute incubando per 15 minuti a 38 °C colture massive di cellule con tripsina (Difco 1:250) al 0.5% in soluzione di Hanks priva di ioni Ca e Mg. Le cellule, dopo centrifugazione a 800 rpm, venivano risospese in terreno completo e contate in contaglobuli di Bürker.

L'irradiazione veniva effettuata secondo due modalità: nella maggioranza degli esperimenti, dopo le opportune diluizioni, le sospensioni cellulari venivano piastrate in capsule Petri di 6 o 9 cm di diametro con terreno arricchito (15% di siero umano e 15% di siero di vitello) e incubate a 37 °C in atmosfera di CO_2 al 5% umidificata, per un tempo variabile da 5 a 9 ore. (Entro tale periodo le cellule aderiscono al vetro, ma non cominciano ancora a moltiplicarsi.) L'irradiazione era effettuata a temperatura ambiente, ponendo le capsule scoperte a 38 cm di distanza dal catodo di un apparecchio Gilardoni operante a 230 kV e 12 mA, filtrato con 0.5 mm di Cu e 1 mm di Al. In queste condizioni l'intensità di esposizione era di 75 r/min. In un singolo caso le cellule furono irradiate in sospensione, sottoponendo alle stesse condizioni di esposizione gocce di terreno contenenti titoli noti di cellule; queste venivano poi immediatamente diluite e piastrate secondo le modalità suddette.

Dopo irradiazione le capsule venivano riposte in termostato a 37 °C in atmosfera di CO_2 al 5% umidificata, per 8-10 giorni, così da permettere lo sviluppo di colonie chiaramente visibili; il conteggio era eseguito dopo fissazione e colorazione delle colonie con violetto di genziana acetico.

3. – Definizioni.

Efficienza di piastramento: rapporto fra numero di colonie contate e numero di cellule piastrate.

D_0: dose di radiazione in *röntgen* (r) necessaria per ridurre la sopravvivenza del 37%, nella regione in cui la sopravvivenza, espressa in scala logaritmica, è funzione lineare della dose. Essa fornisce una misura di k o pendenza della curva.

4. – Risultati.

Nella Tabella I sono raccolti i dati relativi a un singolo esperimento: un numero uguale di cellule fu seminato in diverse piastre, e queste irradiate con dosi crescenti di raggi X. Per ogni dose furono usate cinque replicazioni; le medie dei conteggi sono espresse come percentuali della media dei controlli,

TABELLA I.

Dosi in r	0	20	37	75	112	150	187	225	300
No. cellule seminate	600	600	600	600	600	600	600	600	600
No. colonie sviluppate	350 378 387 361 321 386	337 323 344 320 286	224 236 240 266 250	200 194 166 228 190	153 151 120 150 118	72 59 82 56 78	31 46 34 30 30	15 19 17 22 10	2 5 3 2 4
Medie	364	322	243	196	138	69	34	17	3
Dev. St.	25.5	22.4	15.8	22.2	17.8	11.5	6.8	4.5	1.3
% Sopravv.	100	88.5	66.7	53.8	37.9	18.9	9.3	4.6	0.9

Nel grafico della Fig. 1 sono riportati i logaritmi delle percentuali di sopravvivenza in funzione della dose. La curva a tratto continuo rappresenta l'equazione teorica (1) con parametri ricavati statisticamente dalla porzione lineare della curva sperimentale (KIMBALL [7]).

L'efficienza di piastramento, sempre inferiore ad uno per il ceppo EUE e variabile da un esperimento all'altro, richiede la presenza di controlli su cui stimare la sopravvivenza; inoltre per sperimentare uno spettro di dosi sufficientemente ampio si dovette usare un inoculo

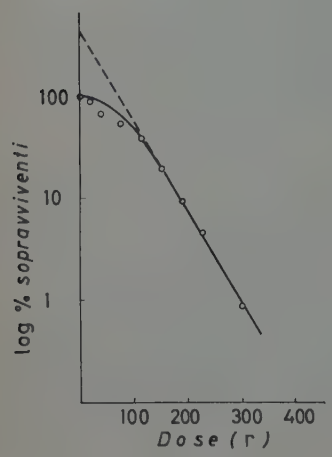

Fig. 1. – Curva di sopravvivenza ottenuta irradiando con ogni dose un ugual numero di cellule. La curva mostra un numero di urti (n) uguale a 4.29 e un valore di D_0 pari a 49 r.

che fosse il più alto possibile, compatibilmente con la possibilità di conteggio dei controlli. Parve perciò necessario verificare sperimentalmente i limiti entro cui il conteggio varia linearmente con la concentrazione dell'inoculo. Nella Tabella II-*A* e *B* e nella Fig. 2 sono illustrati due esperimenti distinti, ma condotti nelle stesse condizioni, in cui una sospensione cellulare venne piastrata a diluizioni diverse.

Mentre nell'esperimento *A* l'efficienza di piastramento si mantiene costante per tutto l'ambito di concentrazione, nell'esperimento *B* la linearità si conserva solo agli inoculi più bassi, mentre all'aumentare della concentrazione cellulare l'efficienza di piastramento diminuisce.

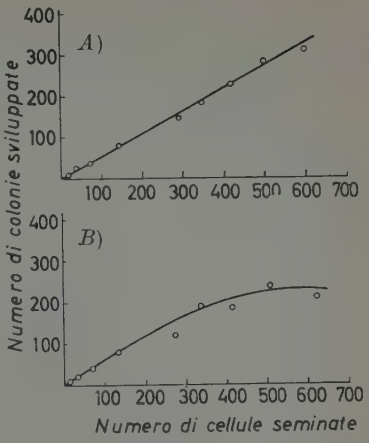

Fig. 2. – Le due curve mostrano l'efficienza di piastramento verificata in due esperimenti distinti, *A* e *B*.

Tabella II-*A*.

No. cellule seminate	600	500	417	347	289	144	72	36	18
No. colonie sviluppate	305	296	247	170	134	89	37	23	11
	293	248	224	186	145	75	26	18	13
	329	266	215	178	147	79	41	33	8
	—	314	216	202	160	80	45	21	8
Medie	309	281	225	184	146	81	37	24	10
Dev. st.	18.3	29.6	14.9	13.7	10.7	5.9	8.2	6.2	2.4

Tabella II-*B*.

No. cellule seminate	627	510	415	337	274	137	68	34	17
No. colonie sviluppate	218	229	138	198	139	76	45	19	14
	200	228	188	184	103	74	34	17	12
	202	246	222	200	—	73	46	23	15
	199	241	194	187	—	89	45	25	12
	—	248	—	187	—	82	42	26	10
Medie	205	238	185	191	121	79	40	22	13
Dev. st. —	8.9	9.4	35	7.3	25.5	6.7	5.6	3.9	1.9

La differenza tra cellule piastrate e colonie che si sviluppano dipende dal numero di:

1) cellule morte nell'inoculo;
2) cellule che non aderiscono al vetro;
3) cellule che si raggruppano prima d'iniziare la moltiplicazione;
4) colonie indipendenti che si fondono nel corso del loro accrescimento.

Le componenti 1) e 2) dipendono dallo stato della coltura di partenza, dal trattamento a cui vengono sottoposte le cellule per ottenere la sospensione mono-dispersa e dalle condizioni del vetro e del terreno; esse sono comunque presumibilmente indipendenti dalla concentrazione cellulare. Le componenti 3) e 4) invece, legate ai movimenti attivi compiuti dalle cellule (ABERCROMBIE *et al.* [8]) ed all'influenza che le condizioni del terreno possono avere sulla morfologia delle colonie (PUCK *et al.* [6]), potranno variare da un esperimento all'altro, ma in ogni caso è prevedibile che aumentino di importanza con la concentrazione.

Una curva di sopravvivenza ottenuta usando un inoculo troppo alto potrà esser perciò alterata per effetto di una minor efficienza di piastramento alle

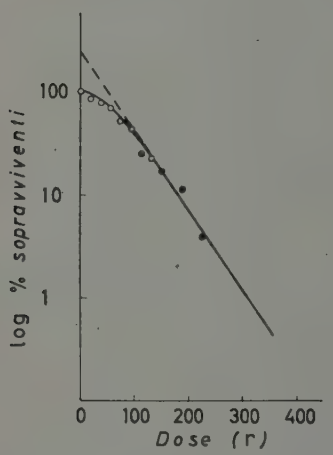

Fig. 3. – Curva di sopravvivenza ottenuta irradiando due diverse concentrazioni cellulari: 250 cellule per piastra furono irradiate con dosi da 20 a 133 r, 425 cellule per piastra con dosi da 122 a 225 r. La curva mostra valori di $n=2.4$ e $D_0=56$ r.

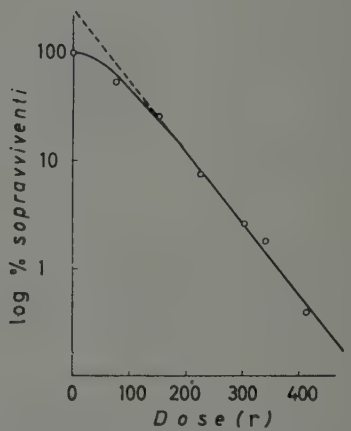

Fig. 4. – Curva di sopravvivenza ottenuta irradiando quattro diverse concentrazioni cellulari: 300 cellule per piastra furono irradiate con 75 r, 600 con 150 r, 2 500 con 225 e 337 r, 10 000 con 300 e 412 r. La curva mostra valori di $n=2.55$ e $D_0=65$ r.

dosi basse e nei controlli: le sopravvivenze calcolate come percentuali del controllo ne risulteranno sovrastimate. Per esempio è facile vedere, nell'esperimento 1, che se il conteggio delle colonie nei controlli fosse in difetto del 20%,

la stima della sopravvivenza alle dosi alte supererebbe circa del 25% il valore reale. La pendenza della curva non sarebbe modificata, ma il valore di n risulterebbe sovrastimato di circa un'unità.

Per evitare questo possibile errore conviene usare inoculi diversi alle diverse dosi, e calcolare la sopravvivenza solo sui controlli ottenuti con inoculi bassi: ne risulta pure avvantaggiato il valore statistico dei singoli punti, ricavati da conteggi più omogenei.

I dati della Tabella III e della Fig. 3 furono ottenuti da una stessa sospensione piastrata a due concentrazioni diverse: ogni concentrazione fu usata per un diverso ambito di dosi e le sopravvivenze calcolate sui rispettivi controlli.

Nell'esperimento di cui sono riportati i dati nella Tabella IV e nella Fig. 4, furono usate quattro diverse concentrazioni, calcolate in modo d'avere conteggi abbastanza omogenei dopo irradiazione con dosi crescenti: le due concentrazioni più alte furono pure irradiate con due dosi più alte. I primi due punti della curva furono calcolati sui rispettivi controlli; gli altri punti, i cui controlli non erano più contabili, furono calcolati per un'efficienza di piastramento intermedia a quella presentata dai controlli dei primi due punti.

Tabella III.

Dosi in r	0	20	37	56	75	94	133	0	122	150	187	225
No. cellule seminate	250	250	250	250	250	250	250	425	425	425	425	425
No. colonie sviluppate	85 117 123 109 120 88	90 95 96 98	75 98 84 —	65 74 77 83	69 49 51 55	50 33 59 —	22 29 24 24	252 263 282 —	78 75 52 62	40 48 — —	37 18 35 —	21 10 11 20
Medie	107	92	86	75	56	47	25	266	67	44	30	15
Dev. st.	16.6	8.3	11.6	7.5	9.0	13.2	3.0	15.2	12.4	5.7	10.4	5.8
% sopravv.	100	86.2	80.1	69.8	52.3	44.2	23.1	100	25.1	16.6	11.3	3.8

Da questi due ultimi esperimenti si ricavano valori di n molto simili tra di loro ed inferiori a quello ricavato dall'esperimento 1; sembra quindi probabile che l'esperimento 1 fosse realmente falsato per un eccessivo affollamento dei controlli.

La necessità di disporre di quantitativi di cellule irradiate da cui poter prelevare campioni per analisi cariologiche, biochimiche, ecc., ci ha indotto a

TABELLA IV.

Dosi in r	0	75	0	150	225	337	300	412
No. cell. seminate	300		600		2500		10000	
No. colonie sviluppate	215 217 239 236 210	119 116 103 93 —	384 361 381 336 398	87 90 89 93 105	174 95 126 — —	28 19 23 52 40 20 35 35 —	185 173 172 203 —	24 41 8 10 27 44 38 36 20
Medie	223	120	372	93	132	31	183	27
Dev. st.	13.2	32.3	24.1	7.2	39.8	11.3	14.4	13.2
% sopravv.	100	53.8	100	25	7.5(*)	1.8 (*)	2.6 (*)	0.4 (*)

(*) Calcolate per un'efficienza del 70 % nei controlli.

confrontare la sopravvivenza di cellule irradiate in sospensione a varia concentrazione e successivamente diluite e piastrate, con quella delle cellule irradiate dopo piastramento. Nella Tabella V sono raccolti i dati di un esperimento in cui singole gocce di sospensioni cellulari con 10^4, 10^5, 10^6 cellule per cm^3 furono irradiate con una sola dose di 150 r, e in seguito diluite e piastrate. I controlli, su cui valutare la sopravvivenza, consistevano in gocce delle stesse sospensioni sottoposte a trattamento parallelo, ad esclusione del-

TABELLA V.

Conc. cell. irradiate	$10^4/cm^3$		$10^5/cm^3$		$10^6/cm^3$	
Dosi in r	0	150	0	150	0	150
No. colonie sviluppate	217 245 296 202	167 156 147 96	279 276 277 319	83 100 133 107	225 263 230 239	101 140 148 85
Medie	240	141	288	106	239	118
Dev. st.	17.1	31.4	20.9	20.8	16.9	30.4

1220

l'irradiazione. Mentre la concentrazione cellulare all'atto dell'irradiazione non sembra influire sulla sopravvivenza, nei limiti di significatività dell'esperimento, è da notare che in tutti e tre i casi l'effetto della dose impiegata (circa 50% di inattivazione) è inferiore all'atteso in base ai dati precedenti. Per quanto preliminari questi dati suggeriscono l'esistenza di una componente indiretta nell'effetto dell'irradiazione, che si annulla quando la sospensione cellulare viene diluita dopo l'esposizione.

5. – Discussione.

Le cellule di metazoi coltivate *in vitro* hanno il vantaggio, rispetto ai microorganismi, di permettere un controllo diretto, cariologico ed istochimico, delle ipotesi sull'azione elementare delle radiazioni, formulate in base ad un'interpretazione formale delle curve di sopravvivenza. L'interpretazione più diffusa attribuisce l'effetto letale ad un danno nucleare, e il riscontro di valori di molteplicità relativamente bassi suggerisce un meccanismo di inattivazione semplice, quale l'induzione di mutazioni letali, geniche e cromosomiche.

In una discussione critica sulle cause del blocco mitotico da irradiazione, PUCK [9] considera più importante la produzione di anomalie cromosomiche che non l'induzione di letali recessivi, almeno per i ceppi iperploidi. L'adattamento dell'equazione di Atwood e Norman ai dati di sopravvivenza si basa appunto su una classificazione delle aberrazioni cromosomiche secondo il numero di « urti » che le avrebbe prodotte. In realtà dosi attive sulla moltiplicazione producono un sensibile aumento del tasso di aberrazioni cromosomiche; la frequenza di aberrazioni cresce all'aumentare della dose, con progressivo aumento percentuale di quelle del tipo a più « urti » (BENDER [10], PUCK [11]).

È chiaro che se l'inattivazione fosse principalmente dovuta all'induzione di letali recessivi si dovrebbe osservare una correlazione fra molteplicità della curva e ploidia del ceppo, mentre tale correlazione potrebbe mancare se l'inattivazione dipendesse da turbe meccaniche della mitosi conseguenti a danno cromosomico. D'altra parte anche in organismi ben noti dal punto di vista genetico, come i lieviti, la correlazione fra molteplicità e ploidia non è semplice (MORTIMER [12]).

PUCK trova valori di molteplicità prossimi a due con tutti i ceppi da lui sperimentati, sia iperploidi (ceppo HeLa, PUCK e MARCUS [1], confermato da BASES [13]), sia diploidi (cellule umane normali, PUCK *et al.* [2]; cellule normali di *Cricetulus*, PUCK [14]). Altri autori invece trovano valori di molteplicità più elevati, fino a 6-7 (ceppi stabilizzati di *Cricetulus*, ELKIND e SUTTON [15]).

Dai dati di sopravvivenza da noi ottenuti sul ceppo umano EUE, si ricava un valore di n compreso fra 2 e 3, e una D_0 di $(50 \div 70)$ r; la distribuzione del numero di cromosomi è simile a quella degli altri ceppi umani stabilizzati

in vitro, con una moda di 59 e un intervallo di variazione da 53 a 67 (De Carli e Chiarelli [16]). I parametri ricavati nei diversi esperimenti presentano però delle differenze importanti e si è visto come questa variabilità possa dipendere da condizioni sperimentali non sempre facilmente controllabili e tali da falsare l'interpretazione dei risultati. In particolare, la densità dell'inoculo può alterare i dati di sopravvivenza non per un effetto diretto sul trattamento, ma attraverso una modificazione dell'efficienza di piastramento.

Si deve pure tener conto del fatto che i parametri delle curve di inattivazione hanno intervalli fiduciali sempre molto ampi (Kimball [7]), per cui l'adattabilità dei dati ad equazioni del tipo della (1) ha sempre un ampio margine di incertezza: è anche possibile che l'inattivazione dipenda dall'interazione di più effetti aventi volumi d'urto diversi, come la forma stessa delle curve di sopravvivenza in alcuni casi suggerisce.

In conclusione, sembra prematuro formulare delle ipotesi sul meccanismo d'azione delle radiazioni nel produrre il blocco mitotico in base all'analisi formale delle curve di sopravvivenza, finchè questo dato non potrà essere integrato da un maggior numero di osservazioni dirette, a livello citologico e citochimico.

BIBLIOGRAFIA

[1] T. T. Puck e P. J. Marcus: *Journ. Exp. Med.*, **103**, 653 (1956).
[2] T. T. Puck, D. Morkovin, P. J. Marcus e S. J. Cieciura: *Journ. Exp. Med.*, **106**, 485 (1957).
[3] K. C. Atwood e A. Norman: *Proc. Nat. Acad. Sci.*, **35**, 696 (1949).
[4] M. Terni e G. B. Lo Monaco: *Lo Sperimentale*, **108**, 177 (1958).
[5] H. Eagle: *Science*, **122**, 501 (1955).
[6] T. T. Puck, P. J. Marcus e S. J. Cieciura: *Journ. Exp. Med.*, **103**, 273 (1956).
[7] A. W. Kimball: *Biometrics*, **9**, 201 (1953).
[8] M. Abercrombie, J. E. M. Heaysman e H. M. Karthauser: *Exp. Cell. Res.*, **13**, 276 (1957).
[9] T. T. Puck: *Amer. Nat.*, **874**, 95 (1960).
[10] M. A. Bender: *Science*, **126**, 974 (1957).
[11] T. T. Puck: *Proc. Nat. Acad. Sci.*, **44**, 772 (1958).
[12] R. K. Mortimer: Rep. UCRL-3902 of the U. S. Atomic Energy Commission (1957).
[13] R. E. Bases: *Cancer Res.*, **19**, 311 (1959).
[14] T. T. Puck: *Progr. in Biophys.*, **10**, 1 (1959).
[15] M. M. Elkind e H. Sutton: *Nature*, **184**, 1293 (1959).
[16] L. De Carli e B. Chiarelli: *Atti della V Riunione dell'A.G.I.* (Ott. 1959), p. 265.

SUPPLEMENTO AL VOLUME XVIII, SERIE X
DEL NUOVO CIMENTO

N. 2, 1960
4° Trimestre

Impiego delle radiazioni ultraviolette per lo studio dei gruppi attivi degli enzimi (*).

A. Vescia, E. Boeri (†) e S. Traniello

Istituto di Fisiologia Umana dell'Università - Ferrara

1. – Introduzione.

Lo studio dei gruppi attivi degli enzimi costituisce un problema molto interessante della chimica fisica delle molecole proteiche.

Gli enzimi idrolitici sono stati i primi ad essere studiati da questo punto di vista e la teoria di Michaelis-Menten [1] della formazione del complesso enzima-substrato è stata formulata per la prima volta su enzimi idrolitici.

La formulazione originaria della teoria di Michaelis e Menten è stata ulteriormente sviluppata da vari autori [2-5] ed estesa anche a reazioni enzimatiche non idrolitiche. Per quanto riguarda queste ultime, dopo le prime ricerche di Bergman e Fraenkel-Conrat [6] si è visto che numerose reazioni d'idrolisi sono in realtà reazioni di trasporto di gruppi. L'enzima, in questo tipo di reazione, non solo deve legarsi al substrato, ma anche all'accettore del substrato stesso o di una parte di esso secondo questo schema generale:

$$E + S_1 \leftrightarrow ES_1$$

$$E + S_2 \leftrightarrow ES_2$$

$$ES_1 + S_2 \leftrightarrow ES_1S_2$$

$$ES_2 + S_1 \leftrightarrow ES_1S_2$$

$$ES_1S_2 \longrightarrow E + P_i$$

dove S_1 è il substrato, S_2 è l'accettore e P_i i prodotti della reazione.

(*) Lavoro eseguito con fondi del C.N.E.N., Roma.

(†) Deceduto il 28 Ottobre 1960.

In una reazione idrolitica semplice l'accettore (S_2) è costituito dall'H_2O.

Tra gli enzimi idrolitici le fosfatasi, sia alcalina che acida, mostrano una netta attività transferasica in cui il gruppo fosforico del substrato viene trasportato su una sostanza diversa dall'acqua [7-9].

Da quanto detto appare evidente che il centro « attivo » di una molecola enzimatica, cioè la parte dove si lega il substrato, è notevolmente complessa, e, probabilmente, vi sono due o più punti della molecola che sono interessati nella reazione catalitica.

Nel presente lavoro viene affrontato lo studio del numero dei gruppi attivi presenti in una molecola di fosfatasi acida di prostata umana.

Quest'enzima oltre ad avere attività idrolitica su numerosi esteri monofosforici organici, ha anche una specifica attività fosfotransferasica se, nel mezzo di reazione, è presente un accettore adeguato.

Secondo MORTON [10] il meccanismo di attività di questo enzima consisterebbe essenzialmente di tre fasi: in una prima fase il substrato (donatore) verrebbe adsorbito sull'enzima con conseguente rottura del legame di estere e formazione di un legame tra fosforo ed enzima; successivamente il fosforo del donatore, legato all'enzima, verrebbe trasferito su una molecola di H_2O (=idrolisi) o di un altro accettore (glucosio, glicerolo, ecc.), specificamente legate sulla superficie dell'enzima (= transfer).

Se il punto dove si lega l'acqua è identico a quello dove si lega un altro accettore è un problema ancora non ben chiarito [11]. In una precedente ricerca [12] sono stati riportati alcuni dati che confortavano l'ipotesi che i due punti fossero diversi.

Il presupposto del presente lavoro si basa sull'ipotesi che il problema dell'esistenza di un unico punto o di due punti diversi sulla superficie dell'enzima per l'attacco dell'acqua o dell'accettore poteva essere risolto studiando l'effetto dell'irradiazione ultravioletta sulle due attività, idrolitica e transferasica.

Se il punto di attacco dell'acqua fosse stato lo stesso di quello dell'accettore, l'effetto dell'irradiazione ultravioletta avrebbe dovuto essere lo stesso per entrambe le attività; nel caso invece che esistessero due punti di attacco diversi, l'effetto dell'irradiazione avrebbe potuto essere diverso per le due attività.

2. – Metodi.

L'enzima usato nel presente lavoro è stato preparato secondo il metodo descritto [13], ed ha un'attività superiore a quella delle precedenti preparazioni (14 moli di substrato scisso per ora e per litro da 1 mg di proteina).

L'attività idrolitica era misurata spettrofotometricamente usando come substrato il monofenilfosfato di sodio (Merck) in una concentrazione finale di $1 \cdot 10^{-3}$ M, in una soluzione tampone di acetato 0.01 M.

L'attività transferasica era eseguita usando come accettore il glucosio (3 M), e determinando enzimaticamente la formazione di glucoso-6-fosfato con il metodo di Slater [15].

Per l'irradiazione U.V. l'enzima, diluito fino ad una concentrazione di 0.026 mg per ml, veniva posto in una cuvetta di quarzo dello spettrofotometro Beckman da 1 cm di percorso ottico e 3 ml di capacità, irradiato da una lampada Hanau con generatore NN 15/44 con luce monocromatica di 2 537 Å. La superficie della cuvetta esposta all'irradiazione era di 3 cm^2; l'energia totale incidente su detta superficie di $15.5 \cdot 10^3$ erg$\times s^{-1}$.

Per le prove di attività veniva prelevata a tempi determinati una aliquota di enzima pari a mg 0.001 di N. Le misure di pH erano eseguite con potenziometro Beckman.

3. – Risultati.

Nelle Fig. 1 e 2 sono riportati i dati relativi alla cinetica dell'inattivazione, per azione dell'irradiazione U.V., delle due attività enzimatiche idrolitica e transferasica a pH 5 e pH 3.7.

Dall'esame dei dati e dai valori delle costanti di reazione risulta chiaramente che la velocità d'inattivazione è nettamente maggiore per l'attività idrolitica che per quella transferasica ad entrambi i valori di pH.

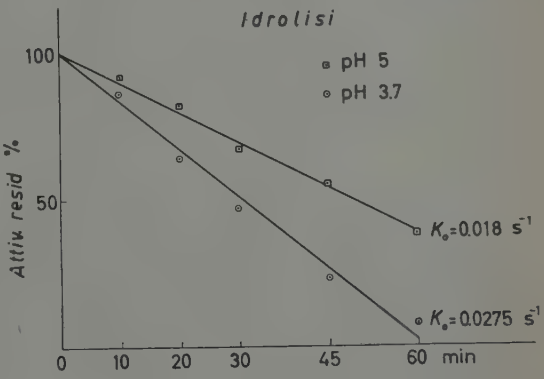

Fig. 1. – Azione dell'irradiazione U.V. sull'attività idrolitica. La concentrazione dell'enzima, nelle prove di attività, è di mg 0.001 N/ml. La misura dell'attività idrolitica era seguita per 60 s con la tecnica descritta in *Metodi*. L'enzima era diluito in buffer di acetato 0.01 M a pH indicato. Temperatura 20 °C.

Inoltre è di particolare interesse notare che la cinetica di inattivazione è di ordine zero sia per l'idrolisi che per il transfer; questo fatto ci sembra di particolare interesse dato che la cinetica di inattivazione per azione di qualsiasi tipo d'irradiazione è sempre di primo ordine [16].

Un'altra notevole differenza nel processo d'inattivazione delle due attività enzimatiche è evidente dall'esame delle curve riportate nella Fig. 3, dove l'effetto dell'inattivazione per azione dell'irradiazione U.V. è studiato in funzione del pH.

Dato che i vari anioni hanno di per sè una notevole importanza sia sul-

l'attività idrolitica sia su quella transferasica [17], le prove sono state eseguite sia in assenza di ioni (H_2O) sia in presenza di acetato.

Dalla Fig. 3 appare che l'attività idrolitica in entrambe le condizioni sperimentali è molto più sensibile all'azione dell'irradiazione U.V. di quella transferasica a tutti i valori di pH studiati.

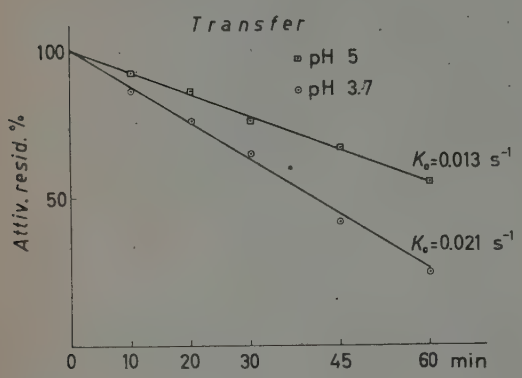

Fig. 2. – Azione dell'irradiazione U.V. sull'attività transferasica. La concentrazione dell'enzima, nelle prove di attività, è di mg 0.001 N/ml. La misura dell'attività transferasica era eseguita come descritto; la durata dell'incubazione (37 °C) con l'enzima era di 5 min. Buffer di acetato come Fig. 1.

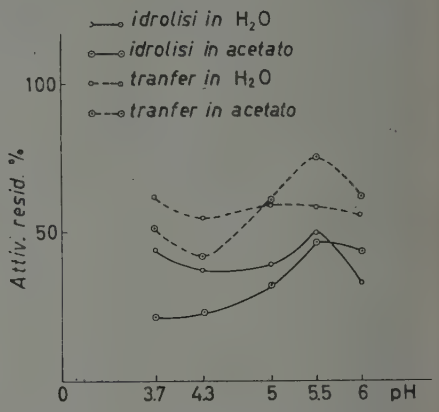

Fig. 3. – Influenza del pH sull'azione dell'irradiazione U.V. sull'attività idrolitica e transferasica. Condizioni sperimentali come Figg. 1 e 2. Nelle prove in H_2O (senza ioni) la soluzione di enzima era portata al pH desiderato con aggiunta di HCl o NaOH diluiti. Tempo di irradiazione = 45 min.

Inoltre, sempre dall'esame della Fig. 3, risulta che al valore di pH 3.7 ed in presenza di acetato, la differenza quantitativa della inattivazione tra idrolisi e transfer raggiunge il valore più alto.

Infine, supponendo che il glucosio, quale accettore del gruppo fosforico nella reazione transferasica, si legasse specificamente sul punto attivo dell'enzima responsabile dell'attività transferasica,

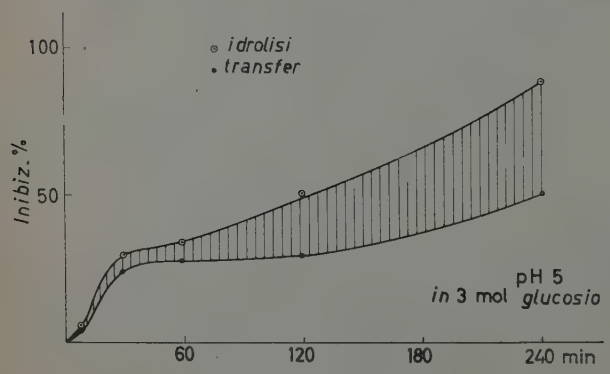

Fig. 4. – Influenza del glucosio sull'azione dell'irradiazione U.V. sull'attività idrolitica e transferasica. Per le condizioni sperimentali vedi testo e Figg. 1 e 2.

1226

proteggendo in tal modo questa attività enzimatica dall'inattivazione per azione dell'irradiazione U.V., abbiamo eseguito un esperimento nel quale la fosfatasi veniva sciolta in una soluzione 3 M di glucosio portata a pH 5.5 per aggiunta di buffer di acetato 0.01 M, e sottoposta all'irradiazione.

Dalla Fig. 4 appare, in effetti, chiaramente che il glucosio 3 M protegge notevolmente sia l'attività idrolitica che transferasica (occorre prolungare notevolmente il tempo d'irradiazione per ottenere la stessa percentuale d'inattivazione ottenuta nelle esperienze precedenti) ma che l'attività transferasica viene protetta in una misura notevolmente maggiore di quella idrolitica.

4. – Discussione.

Il meccanismo d'azione della fosfatasi acida nella sua duplice azione idrolitica e transferasica, è stato discusso da vari autori [18-20].

Numerosi esperimenti fanno supporre, come si è detto, che sia l'acqua (nel caso che si abbia idrolisi) sia l'accettore (nel caso che si abbia transfer) siano *fissati* sulle molecole dell'enzima.

In precedenti lavori [12, 21] mediante l'uso di diversi inibitori della fosfatasi acida si era fatta l'ipotesi che il punto della molecola enzimatica dove si lega l'acqua sia diverso da quello dove si lega l'accettore, anche se i due punti sono probabilmente vicini tra loro.

I dati presentati in questo lavoro sembrano dare un'ulteriore riconferma a tale ipotesi, dato che le due attività legate alla fosfatasi acida sono molto diversamente influenzate dall'azione dell'irradiazione U.V.

In realtà se il punto della molecola proteica fosse lo stesso sia per il legame dell'H_2O sia per quello dell'accettore, ci si sarebbe dovuto aspettare che un'alterazione di detto punto per effetto dell'U.V. avrebbe dovuto produrre un eguale effetto su entrambe le attività enzimatiche.

Invece sia lo studio della cinetica dell'inattivazione (Fig. 1 e 2) sia l'andamento dell'inattivazione a differenti valori di pH, e in presenza o assenza di ioni, mostrano chiaramente che le due attività enzimatiche vengono influenzate in modo molto diverso.

Anche il fatto che la presenza di glucosio (accettore del gruppo fosforico del substrato in questi esperimenti) protegge molto più l'attività transferasica di quella idrolitica, rafforza maggiormente l'ipotesi che l'acqua e l'accettore si leghino in due punti diversi della superficie enzimatica.

È da notare che un analogo risultato hanno ottenuto Aronson e coll. [22] per la chimotripsina; infatti questi autori hanno visto che il rendimento quantico per l'attività esterasica è tre volte maggiore di quello per l'attività proteolitica. Noi abbiamo osservato che a pH 5 il rendimento quantico per l'attività transferasica è circa due volte maggiore di quello per l'attività idrolitica.

In realtà si potrebbe, però, anche supporre che esista un unico punto sull'enzima su cui si lega sia l'acqua che il glucosio e che la modificazione subita per azione dell'irradiazione U.V. sia tale da rendere più difficile il legame del l'acqua che non quello del glucosio. Tale ipotesi, però, sembra molto poco verosimile sia perchè la concentrazione dell'acqua è molto maggiore di quella del glucosio, sia perchè il glucosio è una molecola più complessa dell'acqua e quindi ci si aspetterebbe il contrario, cioè che il legame del glucosio sul punto attivo dell'enzima venisse reso più difficile di quello dell'acqua.

Ulteriori esperimenti sono in corso per poter ancora maggiormente confermare l'ipotesi su esposta.

Un punto che risulta molto interessante e che richiede una più approfondita indagine sperimentale, riguarda, infine, il fatto che la cinetica dell'inattivazione, sia per l'idrolisi che per il transfer, segue una reazione di ordine zero.

Non sembra facile poter interpretare questo risultato che è contrario a tutti i dati esistenti in letteratura.

A noi sembra, comunque, che essenzialmente due ipotesi possano essere fatte per spiegare questo dato sperimentale.

La prima ipotesi è che usando noi un enzima molto purificato ma non cristallino, possono esservi delle sostanze che accompagnano l'enzima stesso che interferiscono, in modo imprecisato, sull'azione denaturante dell'irradiazione ultravioletta in modo da modificarne sostanzialmente l'ordine della reazione.

L'altra ipotesi, che ci sembra più probabile, prevede che l'enzima, per azione dell'irradiazione, passi per uno stato di particolare sensibilità, prima di essere denaturato, secondo questo schema:

$$E \leftrightarrow E' \rightarrow E_{in} .$$

L'equilibrio del primo stato $E \leftrightarrow E'$ dovrebbe essere spostato molto verso sinistra per cui la concentrazione di E' rimane praticamente costante fino al quasi completo esaurimento di E.

Tale ipotesi per poter essere confermata, richiede ulteriori indagini che sono in corso in questo laboratorio; d'altra parte che la cinetica dell'inattivazione, nel caso studiato, è particolare lo dimostrano anche le curve della Fig. 4, dove l'enzima è irradiato in presenza di glucosio.

BIBLIOGRAFIA

[1] L. Michaelis e M. L. Menten: *Biochem. Zeits.*, **49**, 333 (1913).
[2] H. Lineweaver e D. Burk: *Journ. Am. Chem. Soc.*, **56**, 658 (1934).
[3] O. H. Staus e H. Goldstein: *Journ. Gen. Physiol.*, **26**, 559 (1943).

[4] H. GOLDSTEIN: *Journ. Gen. Physiol.*, **27**, 259 (1944).
[5] A. HUNTER e C. E. DOWNS: *Journ. Biol. Chem.*, **157**, 427 (1944).
[6] M. BERGMAN e H. FRAENKEL-CONRAT: *Journ. Biol. Chem.*, **119**, 707 (1937).
[7] H. APPLEYARD: *Biochem. Journ.*, **42**, 596 (1948).
[8] B. AXELROD: *Journ. Biol. Chem.*, **172**, 1 (1948).
[9] R. K. MORTON: *Biochem. Journ.*, **70**, 134 (1958).
[10] R. K. MORTON: *Discussions of Farad. Soc.*, **20** 149 (1955).
[11] E. D. KOSHLAND jr.: *Discussions Farad. Soc.*, **20**, 271 (1955).
[12] A. VESCIA: *La Ricerca Scientifica*, **29**, 2427 (1959).
[13] A. VESCIA e C. TESTI: *Giornale di Biochimica*, **7**, 115 (1958).
[14] A. VESCIA: *Boll. Soc. Ital. Biol. Sper.*, **33**, 1737 (1957).
[15] E. C. SLATER: *Bioch. Journ.*, **53**, 157 (1953).
[16] A. D. MCLAREN: *Adv. in Enzymol.*, **9**, 75 (1949).
[17] A. VESCIA: *Boll. Soc. Ital. Biol. Sper.*, **35**, 162 (1958).
[18] H. S. STEIN e E. D. KOSHLAND: *Arch. Biochem. Biophys.*, **39**, 229 (1952).
[19] O. MAYERHOL e D. E. GREEN: *Journ. Biol. Chem.*, **197**, 347 (1952).
[20] R. K. MORTON: *Nature*, **172**, 65 (1953).
[21] A. VESCIA e E. K. CHANCE: *Bioch. Biophys. Acta*, **30**, 446 (1958).
[22] D. ARONSON, L. NEC e C. L. SMITH: citato da M. W. DALE in *Ciba Symp. on Ionizing Radiations* (London, 1956), p. 25.

INDICE DEL SUPPLEMENTO

AL VOLUME XVIII, SERIE X, DEL

NUOVO CIMENTO

Anno 1960

E. Eriksen and M. Kolsrud – Canonical transformations of Dirac's equation to even forms. Expansion in terms of the external fields . . . . . pag. 1

J. Shapiro – Statistical weights in multiple particle production . . . . . » 40

P. G. Bordoni, M. Nuovo and L. Verdini – Dislocation relaxation in silver, gold, palladium and platinum . . . . . » 55

J.-P. Amiet – Modèle semi-phénoménologique du noyau basé sur l'interaction nucléons-mésons π . . . . . » 89

Rendiconti dei Lavori Scientifici presentati alla Sezione di Biofisica del XLVI Congresso Nazionale della Società Italiana di Fisica (Napoli, 4 Ottobre 1960) . . . . . » 135

1231

Fine del *Supplemento* al Vol. XVIII, Serie X
del *Nuovo Cimento*, 1960

PROPRIETÀ LETTERARIA RISERVATA

Direttore responsabile: G. POLVANI Tipografia Compositori - Bologna

Questo fascicolo è stato licenziato dai torchi il 31-XII-1960

1252